[redacted]

(NASA-CR-180575) TECTONIC EVALUATION OF THE NUBIAN SHIELD OF NORTHEASTERN SUDAN USING THEMATIC MAPPER IMAGERY Final Report (Bechtel National) 255 p Avail: Issuing Activity

N87-22319

Unclas
CSCL 08B 00/46 0069646

ORIGINAL CONTAINS
COLOR ILLUSTRATIONS

Bechtel

NATIONAL AERONAUTIC AND SPACE ADMINISTRATION

TECTONIC EVALUATION OF THE NUBIAN SHIELD OF NORTHEASTERN SUDAN USING THEMATIC MAPPER IMAGERY

FINAL REPORT

PRINCIPAL INVESTIGATOR: Dr. Carol Tosaya

CO-INVESTIGATORS: Mr. David Harnish
Mr. Richard Day

APRIL 1987

Bechtel

TECTONIC EVALUATION OF THE NUBIAN SHIELD OF NORTHEASTERN SUDAN USING THEMATIC MAPPER IMAGERY

FINAL REPORT

CONTENTS

Section		Page
1	EXECUTIVE SUMMARY	1-1
2	INTRODUCTION	2-1
	2.1 GENERAL	2-1
	2.2 PREVIOUS WORK WITH LANDSAT IN ARABIAN-NUBIAN SHIELD	2-2
	2.3 LANDSAT THEMATIC MAPPER DATA	2-3
	2.4 REPORT ORGANIZATION	2-4
	2.5 IDENTIFICATION OF SCENES	2-4
	2.6 TERRAIN vs. TERRANE	2-5
3	GENERAL GEOLOGY	3-1
	3.1 THE SUDAN	3-1
	3.1.1 Precambrian Continental Shield	3-1
	3.1.2 Phanerozoic Cover	3-2
	3.2 RED SEA HILLS	3-3
4	METHODS	4-1
	4.1 DIGITAL IMAGE PROCESSING FOR BASE MAP	4-1
	4.2 DIGITAL IMAGE ENHANCEMENT METHODS FOR DETAILED LITHOLOGIC DISCRIMINATION	4-8
	4.3 GEOLOGIC MAPPING	4-11
	4.3.1 Ophiolitic Rocks	4-11
	4.3.2 Nafirdeib Volcanics	4-12
	4.3.3 Nafirdeib Sediments	4-12
	4.3.4 Altered Nafirdeib Series	4-13
	4.3.5 Batholithic Granites	4-13
	4.3.6 Hybridized Units: Ba/Namp, B/Namp	4-14
	4.3.7 Young Granites	4-15
	4.3.8 Nubian Sandstone	4-15
	4.3.9 Gneisses and Amphibolites	4-15
	4.3.10 Alluvium	4-16
	4.3.11 Recognizing Structural Features	4-16

TECTONIC EVALUATION OF THE NUBIAN SHIELD
OF NORTHEASTERN SUDAN USING THEMATIC MAPPER IMAGERY

FINAL REPORT

CONTENTS
(Continued)

Section			Page
5	STRATIGRAPHY		5-1
	5.1 GENERAL		5-1
	5.2 OPHIOLITES (O)		5-2
	5.3 NAFIRDEIB SERIES (Ncv)		5-2
		5.3.1 Volcanics (Nv)	5-4
		5.3.2 Metasediments (Nc)	5-4
	5.4 SYNOROGENIC GRANITES		5-5
	5.5 ANOROGENIC "YOUNG" GRANITIE SERIES		5-6
	5.6 PHANEROZOIC COVER SEDIMENTS		5-7
	5.7 DIKES		5-7
	5.8 YOUNG MAFIC INTRUSIVES		5-8
	5.9 ALTERATION AND METAMORPHISM		5-8
6	RESULTS AND DISCUSSION		6-1
	6.1 STRATIGRAPHY		6-1
		6.1.1 Ophiolites and Serpentinites	6-1
		6.1.2 Nafirdeib Series	6-3
		6.1.3 Syntectonic Granites	6-4
		6.1.4 Young Granites	6-5
	6.2 ALTERATION AND METAMORPHISM		6-7
		6.2.1 Localized Contact Metamorphism	6-7
		6.2.2 Regional Metamorphism	6-7
	6.3 PROTEROZOIC TECTONICS IN THE RED SEA HILLS		6-9
		6.3.1 Structural Style	6-9
		6.3.2 The Sol Hamed Suture	6-10
		6.3.3 The Alaqui Suture	6-11
		6.3.4 The Port Sudan Suture	6-12
		6.3.5 Late Pan-African Shear Zones	6-14
		6.3.5.1 Deraheib Shear	6-15
		6.3.6 Odib Terrane	6-16
		6.3.7 Mohammed Qol Terrane	6-17
		6.3.8 Western Terrane (?)	6-18

CONTENTS
(Continued)

Section			Page
	6.3.9	Post-Pan-African Faulting	6-20
		6.3.9.1 Northwesterly Faults	6-20
		6.3.9.2 Red Sea Rifting	6-20
6.4	PLATE TECTONIC MODEL		6-21
	6.4.1	Tectonic Development of the Northern Red Sea Hills	6-21
	6.4.2	Phanerozoic Models Which Fit Proterozoic Observations	6-22
	6.4.3	Tectonic Models for the Nubian-Arabian Shield	6-23
7	FIGURES		7-1
8	REFERENCES		8-1
9	BIBLIOGRAPHY		9-1

TECTONIC EVALUATION OF THE NUBIAN SHIELD
OF NORTHEASTERN SUDAN USING THEMATIC MAPPER IMAGERY

FINAL REPORT

LIST OF ILLUSTRATIONS

Figure

Figure 1 Map Overlay and 7,4,2 Photo Mosaic: Tectonic Map of the Northern Red Sea Hills (1:4,000,000)

Figure 2 Location Map, TM-LANDSAT Scenes

Figure 3 Location of Previous Field Studies

Figure 4 Generalized Geologic Map of Northeastern Sudan

Figure 5 Distribution of Pan-African Age Orogenic Rocks and Older Cratons

Figure 6 Summary of Pan-African Geochronology

Figure 7 Sample Digital Number Plots of Various Lithologies

Figure 8 Sample 7/5 Values from Identically Enhanced Single Ratio Images

Figure 9 Locations of Figures 12, 15, 18, and 19

Figure 10 Geologic Map Overlay and 7,4,2 Image: Odib Terrane, the Eastern Edge of the Batholith through the Marginal Basin, Scene 172,45 Q4 (1:500,000)

Figure 11 Lithotectonic Belts of the Odib Terrane, Scene 172,45

Figure 12 Geologic Map of the Wadi Onib Ophiolite Area, Intersection of Sol Hamed Suture and Deraheib Shear (1:100,000)

Figure 13 Geologic Map and 7,4,2 Image: the Alaqui Suture on the North Margin of the Western Terrane, 173,45 Q1 (1:500,000)

Figure 14 Geologic Scene Map and 7,4,2 Image: the Port Sudan and Nakasir Fault Zones in the Mohammed Qol Terrane, Scene 171,46 Q3

Figure 15 Geologic Map of Fold and Thrust Structure in the Odib Terrane (1:50,000)

Figure 16 Geologic Map and 7,4,2 Image: Southern Portion of the Deraheib Shear and a Prominent Young Granite in the Western Terrane, Scene 173,46 Q2 (1:500,000)

LIST OF ILLUSTRATIONS
(Continued)

Figure 17 Plate Tectonic Model of Pan-African Arc Accretion

Figure 18 Geologic Map of a Portion of the North Branch of the Sol Hamed Suture (1:50,000).

Figure 19 Red Sea Transform Faults Transsecting a Pan-African Suture (1:100,000)

Plate

1 Geologic Map of TM Landsat Scene 173,45, Northern Red Sea Hills, Sudan

2 Geologic Map of TM Landsat Scene 173,46, Northern Red Sea Hills, Sudan

3 Geologic Map of TM Landsat Scene 172,45, Northern Red Sea Hills, Sudan

4 Geologic Map of TM Landsat Scene 172,46, Northern Red Sea Hills, Sudan

5 Geologic Map of TM Landsat Scene 171,46, Northern Red Sea Hills, Sudan

6 Tectonic Map of the Northern Red Sea Hills, Sudan

TECTONIC EVALUATION OF THE NUBIAN SHIELD
OF NORTHEASTERN SUDAN USING THEMATIC MAPPER IMAGERY

FINAL REPORT

TABLES

Table		Page
2-1	Identification of TM Scenes	2-4
4-1	Interband Statistics of Subscene 173,45 Q2	4-2
4-2A	General Interband Statistics, 1024 x 1024 Subscene of 173,45 Q2	4-4
4-2B	Correlation Matrix for 1024 x 1024 Subscene, Derived from Covariance Matrix	4-5
4-3	Graded RGB Band Combinations for Base Map	4-7
4-4	Final Ranking of RGB Band Combinations for Base Map	4-8
4-5	Band-Combination Ranking Based on Method of Sheffield (1985)	4-10
5-1	Radiometric Dates	5-9

Section 1

EXECUTIVE SUMMARY

This final report presents results of a study that uses digitally enhanced Landsat Thematic Mapper (TM) data in conjunction with published and unpublished geologic information to compile the first comprehensive regional tectonic map of the Proterozoic Nubian Shield exposed in the northern Red Sea Hills of northeastern Sudan (Figure 1). Previous interpretations were based on isolated geologic studies and on extrapolations of tectonic events recorded on the Arabian Shield of southwestern Saudi Arabia (e.g., Vail, 1985 and 1983; Gass, 1982; Greenwood, et al., 1980). The improved understanding of the geologic setting and distribution of structural and lithologic provinces in the Red Sea Hills that resulted from this research was used to test, verify, and expand existing tectonic models.

Owing to the size, inaccessibility, and harsh, arid climate of the Red Sea Hills, remotely sensed satellite imagery is well suited for analysis of the region. Previously, geologic maps of limited detail and coverage were available for less than half of the area. Thus, the primary objective of this study was to define and delineate regional structural and lithotectonic provinces. The current program used the improved spatial and spectral resolutions offered by TM compared to MSS imagery to map structural and lithologic provinces and to extend this mapping throughout the northern Red Sea Hills of Sudan.

The Proterozoic Shield of the Red Sea Hills is exposed over an area of nearly 350,000 square kilometers. Of this region, we selected an area of approximately 125,000 square kilometers of the northernmost Red Sea Hills which contains the greatest amount of published geologic data for the preliminary study using Landsat TM imagery. This region borders Egypt, where the Proterozoic basement is better mapped and known ophiolites and geologic structures extend southward into northern Sudan.

Significant accomplishments of this study were as follows:

- o Review of pertinent published and unpublished geologic literature and maps of the northern Red Sea Hills to evaluate the geologic framework of the region.
- o Processing of TM imagery for optimal base-map enhancements; preparation of photo mosaics of enhanced images to serve as base maps for compilation of geologic information.
- o Interpretation of TM imagery from photos and on-screen images to define and delineate structural and lithologic provinces.
- o Compilation of geologic information (petrologic, geochemical, and radiometric data) from the literature onto base-map overlays.
- o Evaluation of the tectonic evolution of the Nubian Shield based on the image interpretation and the compiled tectonic maps.

With regard to structure and to lithologic delineation, this area is complicated. We see good evidence for Proterozoic accretion of oceanic island-arc terranes along significant crustal sutures. Extensions of major tectonic features across the Red Sea rift from the Arabian Shield are readily delineated. It is an excellent region for demonstrating that TM data can yield vast improvements in the understanding of crustal evolution over what is available in the literature. Specifically, improvements have been made in more precise delineation of lithologic contacts, faults locations and extents, the regional distribution of specific rock types including metamorphic grades, and the resulting definition and regionalization of major lithotectonic elements.

Section 2

INTRODUCTION

2.1 GENERAL

This study was designed to use TM imagery in conjunction with previously published field studies to define continental processes and the evolution of the northeastern Nubian Shield. We recognize that new findings that result from this study will be expanded and modified as new, field-verified data become available. However, we believe that this study demonstrates that TM-image interpretation can greatly aid geologic mapping. A principal product of the study is a set of tectonically consistent geological maps covering the northern Red Sea Hills (Plates 1-5). From the structure and geology as interpreted from TM imagery, we have derived the first comprehensive regional tectonic map of the Proterozoic Nubian Shield exposed in the northern Red Sea Hills of northeastern Sudan (Figure 1, Plate 6). The improved understanding of the geologic setting and distribution of structural and lithologic provinces in the Red Sea Hills which resulted from this study enhance our knowledge of the evolutionary growth of the Sudanese Nubian Shield.

The Proterozoic Shield of the Red Sea Hills is exposed over an area of approximately 350,000 square kilometers. Of this region, we selected an area of approximately 125,000 square kilometers of the northernmost Red Sea Hills which contains the greatest amount of published geologic data and unpublished theses (Figure 2). This region borders Egypt, where the Proterozoic basement is relatively well mapped.

The size, inaccessibility, and harsh, arid climate of the Red Sea Hills have severely limited the number of ground-based geologic studies that have been completed in this region. Previously published geologic maps of limited detail, coverage, and verification were available for about one third of the area (Figure 3). Extensive investigation of digital image processing techniques was required to define and delineate regional structure and lithology. The excellent, widespread rock exposure makes the region ideally suited to geologic analysis using TM imagery.

Recent Landsat Multispectral Scanner (MSS) investigations in the region by Ahmed (1982); Blodget and Brown (1982); and Bechtel (1983 a,b) documented the usefulness of digitally processed satellite imagery in delineating large Proterozoic shear zones, probable tectonic sutures, ophiolitic assemblages, and multiple periods of orogenesis marked by intrusive activity and fold deformation. As an extension of the earlier MSS work, this program uses the improved spatial and spectral resolution offered by TM to refine the structural and lithologic provinces and to extend known, mapped occurrences of identified lithologies throughout the northern Red Sea Hills of Sudan. The improved spatial resolution greatly facilitated the mapping of surface textures including lineaments, lithologic contacts, folds, and faults. The improved spectral resolution allowed greater discrimination of bedrock lithologies, particularly in the separation of carbonate from volcaniclastic sediments; the separation of ultramafic, mafic, and ophiolitic complexes; the separation of amphibolite-grade from low-grade metamorphic rocks; and the identification of multiple-phase felsic intrusions accompanied by contact metamorphism, hydrothermal alteration, and emplacement of dikes.

2.2 PREVIOUS WORK WITH LANDSAT IMAGERY IN ARABIAN-NUBIAN SHIELD

Several preliminary MSS investigations have been conducted over parts of the Arabian and Nubian Proterozoic Shields. Blodget and Brown (1982) used digitally processed winter and summer MSS imagery to aid geologic mapping of regional structure and lithology over portions of the Arabian Shield of southwestern Saudi Arabia. Ahmed (1982) used digitally processed single-band black and white MSS imagery to map lineaments over 400,000 square kilometers of northeastern Sudan. He subsequently explored the correlation of known occurrences of mineralization in the Proterozoic basement with major lineaments and intersecting lineaments. Almond (1982) used MSS imagery to study lineaments in the Red Sea Hills.

More recently, Bechtel (1983a,b) used digitally processed winter and summer MSS imagery to map Proterozoic lithology and structure in the Red Sea Hills of Sudan and in the Arabian peninsula. Enhanced images were used to

supplement and refine existing geologic maps as well as to produce new maps in areas of sparse geologic information. The improved geologic maps were used to locate favorable targets of potential mineralization and to assist in developing an exploration strategy for the region. Winter imagery with low sun-angle illumination provided the greatest amount of structural information, while the summer imagery with high sun-angle illumination was most useful for determining the spectral characteristics of lithologies.

Each of these studies demonstrated that satellite-acquired imagery can be a valuable mapping tool in the arid, sparsely vegetated areas of northeastern Sudan and southwestern Saudi Arabia. Landsat studies in the Red Sea Hills by Bechtel (1983a) concluded that MSS imagery could be used to: (1) discriminate, in places, basement rocks of different metamorphic grade (i.e., amphibolite-granulite grade from greenschist grade from relatively unmetamorphosed rocks); (2) discriminate ultramafic and mafic complexes and metamorphosed basement; (3) detect major Proterozoic shear zones, faults, lineaments, and fold belts; (4) discriminate felsic plutons of different ages and separate them from surrounding basement; (5) separate basalt flows for different periods of extrusion based on their iron content or degree of surface weathering; and (6) identify large areas of gossan and laterite. TM findings were verified using published geologic reports and maps. The spectral and spatial resolutions of MSS, however, were not adequate to map accurately the lithologic contacts, to differentiate specific lithologies of felsic and ultramafic rocks, to recognize non-limonitic hydrothermal alteration, or to differentiate carbonate from volcaniclastic basement lithologies reliably.

2.3 LANDSAT THEMATIC MAPPER DATA

Major limitations of Landsat MSS imagery for geologic applications result from the coarse spatial resolution and limited spectral coverage (0.5 -1.1 microns) of this sensor which does not extend to wavelengths that are most useful for characterizing the spectral properties of geologic surface materials. The Landsat TM overcomes many of the limitations of the MSS sensor with its improved spatial resolution and extended spectral coverage

(primarily band 5 at 1.55 - 1.75 microns and band 7 at 2.08 - 2.35 microns). Prior to the availability of TM data, geologic studies using MSS spectral bands found that limonitic hydrothermally altered rocks were not separable from limonitic unaltered rocks. Furthermore, non-limonitic hydrothermally altered rocks commonly were not detectable in arid regions (Abrams et al., 1977, 1983; Podwysocki et al., 1983).

2.4 REPORT ORGANIZATION

This report is organized to illustrate the specific advances that TM imagery has made in the interpretation of the geology of the northern Red Sea Hills. The General Geology and Stratigraphy sections are syntheses from literature and previous geologic studies of the region. The Methods section discusses the criteria that we used to enhance and recognize geologic structures and units on the imagery and to extrapolate geology into previously unmapped areas. The Results and Discussion section places the lithologic units within the regional tectonic context that evolved during the course of this investigation.

2.5 IDENTIFICATION OF SCENES

The study area is covered by five TM scenes, as illustrated in Figure 2. We refer to scenes by their World Reference System locations in all ensuing sections. Table 2-1 lists pertinent identifiers.

Table 2-1

Identification of TM Scenes

Scene Number	Path, Row	Date	Plate
Y5026207373X0	173,45	18 Nov 84	1
Y5026207375X0	173,46	18 Nov 84	2
Y5012707300X0	172,45	06 July 84	3
Y5012707302X0	172,46	06 July 84	4
Y5010407240X0	171,46	13 June 84	5

2.6 TERRAIN vs. TERRANE

Following the convention of current tectonic literature, the word terrain is used in reference to a geographic province or a geomorphic feature, with no tectonic implication. Terrane, however, is used in describing a distinct lithotectonic unit that is isolated from its surroundings by structural discontinuities. Use of terrane implies allogenic emplacement by transport along plate-margin faults.

Section 3
GENERAL GEOLOGY

3.1 THE SUDAN

The Republic of the Sudan is the largest country in Africa, occupying nearly one million square miles. Owing to its vastness and inaccessibility, detailed geologic mapping is difficult, and reconnaissance surveys have been the primary source of geologic information. Digital image processing of Landsat imagery can greatly contribute to geologic mapping by providing regional lithologic and structural information in those areas where access is difficult and existing information is sparse. Rocks in the Sudan are divided into the Archean and Proterozoic igneous and metamorphic rocks of the Nubian Shield, and younger Phanerozoic cover series (Vail, 1978; Whiteman, 1971). Figure 4 presents a generalized lithologic map (Almond, 1978).

3.1.1 Precambrian Continental Shield

Archean (more than 2000 million years) and Proterozoic (2000-600 million years) rocks of the Nubian continental shield underlie nearly all of Africa, as shown in Figure 4 (Vail, 1978A; Garson and Shalaby, 1976; Neary, 1978). These rocks are exposed over 49 percent of the Sudan (Ahmed, 1983). They are divided into the stable Archean to early Proterozoic Nile Craton in the southwest and the Proterozoic, or Pan-African, continental margin complex in the northeast (Figure 4). The Nile Craton consists primarily of granites and amphibolite-granulite gneisses (Vail, 1978; Hepworth, 1979). Radiometric ages were reset during a late Proterozoic orogenic event (or events) that produced extensive deformation over much of Africa; this broadly is referred to as the Pan-African event. The Red Sea Hills are part of the Pan-African continental margin complex. The continental margin complex consists of deformed greenschist to amphibolite facies metavolcanics and metasediments intruded by granitic plutons. Scattered ultramafic

complexes, representing the basal Proterozoic oceanic crust, also are present along deep crustal sutures. The continental margin complex in Sudan consists of accreted arc terranes and may be the northern extension of the Mozambique mobile belt, which represents the Proterozoic plate margin in southern and eastern Africa (Almond, 1978; Dawoud, 1982; Hepworth, 1979)(Figure 5). Calc-alkaline island arc plutonism and volcanism during the Nubian orogeny (900 to 820 million years ago) and the Pan-African orogeny (Ca. 780 to 530 million years ago) were widespread along Africa's continental margins (Gass, 1982; Greiling, et al., 1984; Almond, 1982; Fleck, et al., 1976; Kroner, 1979; Sillitoe, 1979). Post-orogenic intrusives, including ring complexes, became increasingly alkaline in composition as the Proterozoic continental margin became "cratonized", or converted to continental crust (Harris, 1982; Bentor, 1985). Gass (1979) shows that the evolution of niobium fractionation in granites is also compatible with the crust evolving to a more continental composition with in-plate magmatic activity.

3.1.2 Phanerozoic Cover

Half of the Sudan is covered by Phanerozoic (less than 600 million years old) sedimentary and volcanic rocks which rest unconformably on the Proterozoic Arabian-Nubian continental shield (Figure 4). The most extensive cover rocks are the Cretaceous (140 to 65 million years ago) Nubian sandstone in northwestern Sudan and the Quaternary (less than 2 million years old) alluvial deposits in central and southeastern Sudan. The Nubian sandstone consists of red quartzose sandstone, mudstone and conglomerate which accumulated in fresh-water lakes and alluvial fans (Vail, 1978; Whiteman, 1971; Tudor Engineering, 1959). Cenozoic (less than 65 million years old) marine sediments are present in a strip bordering the Red Sea. Cenozoic volcanic rocks are present in several areas and consist primarily of flood basalts and intrusive plugs. The Phanerozoic sedimentary and volcanic units have not been extensively deformed or metamorphosed (Vail, 1978).

3.2 RED SEA HILLS

The Red Sea Hills are an uplifted and eroded exposure of the Proterozoic continental margin complex in northeastern Sudan (Figure 4). The age, lithology and probable tectonic setting of the principal stratigraphic units are described in Section 5.

Geologic maps of portions of the northern Red Sea Hills have been published by various authors and agencies (Figure 3). These include work performed by Sudanese, American, Egyptian, German, English and French geologists. Although stratigraphic nomenclature varies greatly from region to region, gross similarity in basic map units is present. The regional perspective offered by the TM has, where appropriate, permitted stratigraphic and structural correlation between maps generated by these various investigators.

Section 4
METHODS

4.1 DIGITAL IMAGE-PROCESSING FOR BASE MAP

Statistical techniques for principal-components analysis in remote sensing are well documented (e.g., Merembeck et al., 1976; Sheffield, 1985; Hord, 1982; Chavez et al., 1984; Taylor, 1974; Podwysocki et al., 1977; Blodget et al., 1978). Our base map color combination, while not intended to bring out all the details of each image, was selected to distinguish among major lithologic units and structural features that are significant to a tectonic study. From published geologic maps of the Nubian-Arabian shield, previous related Landsat MSS studies (Blodget et al., 1978; Bechtel, 1983 A and B), and recent insights into the tectonic development of the region (e.g. Vail, 1985, 1983; Shackleton, 1986; Kroner, 1985; Almond, 1978, 1979, 1982; El Nadi, 1984; Al-Shanti and Roobol, 1979), the lithologic units and structural features that required discrimination were:

(1) Paleozoic and younger sediments
(2) ophiolites
(3) metasediments
(4) metavolcanics
(5) limestones
(6) intrusives rocks of different ages and compositions
(7) folds and faults, with particular emphasis on zones defining major sutures and distinguishing offset along faults

Using scene 173,45, which was the first tape received from NASA, we examined the entirety of the structurally interesting Quad 2. A general statistics study demonstrated that data in the spectral bands of TM were highly correlated, as shown in Table 4-1.

Table 4-1: Interband Statistics, Subscene 173,45 Q2

Band 1	Band 2	Band 3	Band 4	Band 5	Band 7
Lower Triangle Cov. Matrix					
1					
1273.798					
2					
784.597	500.350				
3					
1176.571	754.985	1153.580			
4					
909.839	585.449	896.292	704.951		
5					
1581.228	1011.041	1551.547	1228.510	2276.723	
6					
1023.014	653.513	1002.807	795.009	1473.827	976.054
Mean Vector:					
107.996	52.806	73.422	57.135	115.436	74.305
Min. Vector:					
.000	.000	.000	.000	.000	.000
Max. Vector:					
251.000	149.000	224.000	174.000	255.000	185.000
Std. Dev:					
35.690	22.368	33.964	26.550	47.715	31.241
Eigen Values:					
.967	.024	.005	.002	.000	.000
Eigen Vectors:					
1					
-.424	-.269	-.411	-.322	-.577	-.374
2					
-.587	-.275	-.294	-.099	.552	.420
3					
.655	-.151	-.544	-.450	.103	.192
4					
.043	-.045	-.075	-.038	.586	-.803
5					
.166	-.467	-.348	.790	-.078	-.027
7					
.125	-.779	.565	-.237	-.003	.077
E_1	E_2	E_3	E_4	E_5	E_7

Table 4-1, continued

Correlation Matrix

	1	2	3	4	5	7
1	-					
2	.983	-				
3	.971	.994	-			
4	.960	.986	.994	-		
5	.929	.947	.957	.969	-	
7	.917	.935	.944	.958	.958	-

Eigen Matrix Expressed as % of Contribution

1	2	3	Band
17.97	7.24	16.89	1
34.46	7.56	8.64	2
42.90	2.28	29.59	3
0.18	0.20	0.56	4
2.75	21.81	12.11	5
1.56	60.68	31.92	7

A 1024 x 1024 pixel subscene was chosen for detailed analysis of optimal color combinations for the base map. The selected subscene included some available ground truth in the form of geologic mapping that encompassed most of the features that we wished to delineate, including an ophiolite. We recognized that different scaling adjustments would be required for scenes of different dates and observed features. Table 4-2A shows the general interband statistics for this area. Table 4-2B presents the correlation matrix derived from the covariance matrix. A number of bands are highly correlated, but, overall, a lower degree of correlation exists for combinations of bands 7, 4, 2 and 1 than for other combinations in scene 173,45 Q2 as shown in Table 4-1. An eigen analysis for principal components (Table 4-2B) shows the relative contribution of each band to an eigen vector. Note that the first eigen vector has 93.9% of the total variance and that E_1 and E_2 have 97.6% of the total variance.

Table 4-2A: General Interband
Statistics, 1024 x 1024 Subscene of 172,45 Q2

Band 1	Band 2	Band 3	Band 4	Band 5	Band 7
Lower Triangle Cov. Matrix					
1					
366.927					
2					
256.023	201.866				
3					
422.919	315.881	534.732			
4					
322.294	246.550	410.804	338.441		
5					
610.834	457.089	768.869	619.643	1310.643	
7					
406.358	309.522	524.111	426.943	880.673	636.231
Mean Vector:					
113.492	56.298	78.524	61.076	122.698	80.236
Min. Vector:					
61.000	18.000	17.000	8.000	9.000	2.000
Max. Vector:					
205.000	129.000	200.000	156.999	255.000	183.000
Std. Dev:					
19.155	14.207	23.124	18.396	36.202	25.223
Eigen Values:					
.939	.037	.010	.006	.003	.003
Eigen Vectors:					
1					
-.316	-.237	-.396	-.316	-.631	-.432
2					
-.512	-.323	-.447	-.190	.461	.427
3					
-.398	.084	.205	.397	-.552	.573
4					
.579	-.134	-.123	-.504	-.282	.544
5					
.099	-.895	.384	.187	-.002	-.068
7					
-.363	.109	.661	-.644	.053	-.006
E_1	E_2	E_3	E_4	E_5	E_7

Table 4-2B: Correlation Matrix

for 1024 x 1024 Subscene, Derived from Covariance Matrix

Correlation Matrix

$$\text{Corr} = \frac{\text{Cov}[XY]}{\sigma_x \sigma_y}$$

	1	2	3	4	5	7
1	-					
2	94.08	-				
3	95.48	96.15	-			
4	91.46	94.36	96.57	-		
5	88.09	88.87	91.84	93.04	-	
7	84.11	86.38	89.86	92.01	96.45	-

Expressed as % of Contribution

	1	2	3	4	5	7
1	9.98	5.61	15.68	9.98	39.81	18.66
2	26.21	10.43	19.98	3.60	21.25	18.23
3	15.84	0.70	4.20	15.76	30.47	32.83
4	33.52	1.80	1.51	25.40	7.95	29.59
5	0.98	80.10	14.74	3.49	0	0.46
7	13.17	1.88	43.69	41.47	0.28	0

The statistical processing demonstrated that color combinations of bands 1,4,7 and 2,4,7 have lower correlation than other band combinations. Eigen vector bands also were analyzed in the color-combination testing.

To corroborate the statistical band selections and to familiarize ourselves with the potential of certain color combinations to distinguish specific lithologies or structural features, we examined all possible combinations of the raw spectral bands in red, green, and blue (RGB). Each color combination was linearly contrast stretched for maximum color separation, and each received the same edge enhancement to improve details of linear structural features. Logarithmic and exponential contrast stretching at different histogram peak offsets were evaluated but judged to be inferior in image clarity to the linear contrast stretch. Combinations were ranked with a letter grade. We sought the maximum color separation of image features regardless of the colors produced by a particular three-band combination. Hence, the same three bands in different combinations of RGB frequently received different grades (Table 4-3).

The top-ranking combinations were re-evaluated. The final ranking is listed in Table 4-4. The top selection for the base map was 7,4,2 (RGB). This color combination with an edge enhancement was used to generate the base quad maps. Scaling for all quads was adjusted for sun azimuth and elevation and for differences in atmospheric scattering.

Eleven color-ratio combinations were evaluated; all were judged less superior to 7,4,2.

Color combinations of the eigen vector bands (Sheffield, 1985) did not provide a useful selection for the base enhancement. However, these band combinations were valuable for distinguishing finely detailed features and for identifying lithologies that appeared similar in 7,4,2.

Table 4-3: Graded RGB Band Combinations for Base Map

	1	2	3	4	5	7
1		123 D 124 D 125 D 127 D	132 B- 134 C 135 C- 137 B-	142 C- 143 C- 145 B 147 B	152 D 153 C- 154 B 157 B	172 C- 173 C- 174 C 175 C+
2	213 D 214 D 215 D 217 D		231 C 234 D 235 C- 237 D	241 C 243 C 245 C+ 247 C	251 C 253 C 254 B- 257 B	271 D 273 D 274 C- 275 B
3	312 C- 314 D 315 C+ 317 C	321 B- 324 E 325 D 327 D		341 D 342 E 345 C 347 C-	351 D 352 D 354 D 357 C+	371 C- 372 B- 374 C 375 B-
4	412 C- 413 C 415 B- 417 C+	421 B- 423 C- 425 C- 427 C-	431 B- 432 B+ 435 C- 437 C		451 C- 452 C- 453 C- 457 B-	471 C- 472 C- 473 C- 475 B-
5	512 C- 513 C- 514 B- 517 C-	521 B+ 523 B- 524 B- 527 C-	531 A- 532 B- 534 C 537 C	541 A- 542 A- 543 B+ 547 C+		571 C- 572 C 573 C 574 B-
7	712 C 713 C- 714 C 715 C-	721 B- 723 C- 724 C 725 C-	731 A 732 B+ 734 C+ 735 C+	741 A 742 A+ 743 A- 745 B-	751 B 752 B+ 753 B 754 B+	

Table 4-4: Final Ranking of RGB Band Combinations for Base Map

Rank	R	G	B	
1	7	4	2	Final Selection
2	7	4	3	
3	7	4	1	
4	7	3	2	
5	5	3	1	
6	5	4	2	
7	7	3	1	
8	5	4	1	
9	5	2	1	
10	4	3	2	
11	5	4	3	
12	7	5	4	
13	7	5	2	

4.2 DIGITAL IMAGE ENHANCEMENT METHODS FOR DETAILED LITHOLOGIC DISCRIMINATION

On a quad-by-quad basis, the following information was used to aid in developing the geologic interpretation:

1. Published literature, including maps, whole-rock chemistry petrologic data, and age dates (Figure 6);
2. Spectral signature extension;
3. Full-resolution, CRT-monitor mapping with optimized eigen vector band combinations (Sheffield, 1985) and with band combinations selected by evaluating digital-number responses of known lithologies in different lithologic assemblages.

We first mapped the basic geology onto our 7,4,2 optimal base-map enhancement with constant, linear contrast stretching and edge enhancement. After a first pass through the whole area, we dealt with details of structurally and lithologically difficult areas.

Following the algorithm of Sheffield (1985) to select the optimal TM- band subset from the variance/covariance information generated in Table 4-1, we obtained the rankings shown in Table 4-5. Top-ranked band combinations proved valuable for discriminating lithologies in complicated geologic settings.

Three additional techniques were used to identify unknown lithologies. The first technique is commonly referred to as "Digital Number" or "DN" technique). This uses the characteristic signature of the linearly stretched digital modal or mean intensities across all bands. For instance, in subscene 172,45 Q2, digital numbers for ground-truthed lithologies within the Sol Hamed ophiolite complex and surrounding rocks were plotted, and then DN signatures of unknown lithologies in previously unidentified ophiolites were compared to the known DN signatures. This procedure was carried out also for regions of Nafirdeib volcanics, Asoteriba (calc-alkaline) volcanics, sedimentary lithologies, contact-metamorphic zones, and batholithic granite/younger granite bodies. Twenty-five regions of known lithology in scene 172, 45 and approximately 80 units of unknown lithology were identified by the DN technique. Graphs of key signatures are shown in Figure 7. These identifications not only helped to resolve problems in the geologic mapping but ultimately contributed greatly to the tectonic interpretation.

A scaled ratio of bands 7/5 provided excellent scene-specific highlighting of serpentinites (Figure 8). Within scenes containing the Wadi Onib and the Sol Hamed ophiolites, serpentinites appeared black. However, the reliability of this enhancement was greatly diminished beyond scenes with known occurrences of serpentinites to use for calibration. A third technique that simply used the weighted differences between 2 bands aided in highlighting alteration zones.

Table 4-5: Band-Combination Ranking
Based on Method of Sheffield (1985)

Rank	173,45 Q2	Determinant	1024 x 1024 Subscene of 173, 45 Q2	Determinant
1	531	16161722	753	4804541
2	541	9514956	751	4771848
3	731	8878091	531	3554187
4	751	8786194	541	3431861
5	741	5569835	754	2504626
6	521	5075912	752	2467124
7	753	4809682	521	2153708
8	721	2662933	731	2089930
9	752	2568368	543	2056927
10	754	2104181	741	1983089
11	532	1343434	532	1669968
12	542	1294364	721	1339116
13	543	1264883	542	1315990
14	742	760686	743	1181045
15	732	741200	732	1000257
16	743	740188	742	734766
17	431	707300	431	392621
18	432	399845	421	299418
19	421	285901	321	244318
20	321	60069	432	178448

4.3 GEOLOGIC MAPPING

Three working-map overlays were prepared for each quadrant. Interpreted geology was mapped onto the main working overlay. Literature "ground-truth" information was plotted onto the second. These data included lithologies that were described in the field by previous researchers and petrologies and geochronologies (Table 4-1) obtained from the literature. The third overlay was a lithotectonic map at a scale of 1:1,000,000 that emphasized the continuity of regional trends within and beyond the study area. Four subscenes were mapped at full resolution to generate two 1:50,000 and two 1:100,000 geologic maps in areas of special tectonic interest. Additionally, four 1:500,000 7,4,2 composite photographic images with geologic map overlays of selected quads are provided. The locations of these maps are shown in Figure 9.

Band combinations (RGB) 5,3,1 and 7,3,1 in addition to 7,4,2, with edge enhancement and linear contrast stretch that were examined at full resolution worked well for discriminating units within the ophiolites. The enhancements resolve structure within the units as well.

4.3.1 Ophiolitic Rocks

Sol Hamed ophiolite units could be discriminated quite well in 7,4,2, in 7,3,1, and in 5,3,1 band combinations. The Sol Hamed and Wadi Onib ophiolites were used as "type" ophiolites. Their spectral character, outcrop morphology, and structural setting were extrapolated to map other ophiolite complexes. Figure 7-D shows the digital-number response of Sol Hamed and Wadi Onib ultramafics. In 7,3,1 the ultramafic units (Ou) appear dark navy blue and are clearly discernible. The overlying sheeted dike and gabbro unit (Og) was previously described as being, in places, a true serpentine matrix "with disoriented gabbro blocks in a serpentinite matrix" (Fitches, et al., 1983). Melange development is clearly tectonic. Tectonic brecciation noted in the field by other workers can be seen in the gabbro complex on TM imagery. Dark navy blue serpentinite mixed as fault slices and as brecciated matrix is distinguishable on the imagery. Pillow basalts and marine sediments (Op) have been field mapped and are readily discernible as a separate unit in our "type" ophiolites.

Linearly contrast-stretched 7/5 ratio images aided discrimination of ophiolite units from Nafirdeib series rocks; ultramafic units and Nafirdeib clastics were consistently separated. The altered gabbros, sheeted dike complex, and pillow basalts could be distinguished from Nafirdeib volcanics as well. The enhanced images displayed variably serpentinized ultramafics as black, the Nafirdeib sediments and volcanics as intermediate shades of grey, and the altered pillow lavas and gabbros as very light grey. Intensities for known lithologies are plotted in Figure 8.

4.3.2 Nafirdeib Volcanics

The volcanics generally appear reddish-orange on the 7,4,2 (RGB) false-color composite base maps, but dacite, gabbro and andesite mapped by El Nadi (1984) appear dark grey, similar to the metasediments. The topographic expression generally reflects geologic structure. Apparent bedding on the scale of hundreds of meters usually is distinct and probably represents compositional variations, flow contacts, and variable amounts of intermixed sediments. Some units are more resistant to erosion and, thus, help define bedding. Wadis follow less resistant beds, joints, and faults. DN signature analysis and accompanying characterization of topographic expression were used to discriminate and identify these lithologic units.

4.3.3 Nafirdeib Sediments

A lens of conglomerate mapped in the field by Gass (1955) northwest of the Oyo mine (east-central 172,45 Q1) appears dark bluish grey on the base 7,4,2 composite. Gass (1955) and Hussein et al. (1982) also documented occurrences of pelitic rocks near the coast (southeast corner of 172,45 Q2) which appear dark grey on our base imagery. Flysch deposits mapped by El Nadi (1977) just northeast of the Sofaya ring complex in 172,45 Q4 (21°20'N, 36°17'E) are greyish brown and dark purplish grey. Kabesh (1962) mapped greywackes and reworked volcanics which generally appear dark bluish grey and greyish brown. The Nafirdeib metasediments usually are distinct from surrounding metavolcanics. The strong color contrast between the units aids delineation of structure since it is an easily mapped contact. Some of the

sediments are not discriminated easily from volcanics. In the fold and thrust area of 172,45 Q4, El Nadi (1984) has field-mapped volcanics and "molasse" which are indistinguishable in 7,4,2. The unit appears similarly colored to verified occurrences of Nafirdeib volcanics in 7,4,2 band combination and has a similar DN signature across all bands.

Sheet-silicate-rich rocks, mapped as Nc or Ncv, are poor reflectors in all TM bands and thus appear dark on our false color-composite base images. In contrast, sheet-silicate poor rocks appear reddish brown on the 7,4,2 base images.

The topographic expression of the metasediments is similar to that of the volcanics, but generally more subdued.

4.3.4 Altered Nafirdeib Series

Where Nafirdeib series metavolcanics and metasediments were recognizable but somewhat altered from their normal appearance, they were designated Na. If they were distinguishable as predominately altered volcanics they were designated Nv/Na. Predominately clastic altered Nafirdeib series rocks were designated Nc/Na.

The highest metamorphic grade Nafirdeib units were known from the work of other investigators to be amphibolite facies (Namp) rocks. Often these units had distinct spectral characters.

Nc/Namp, Nv/Namp, and N/Namp are designations for intermediately altered Nafirdeib series rocks. They are altered more than Na lithologies and are spectrally intermediate between Na and amphibolite gneiss terrains, Namp.

4.3.5 Batholithic Granites

The Batholithic Granites are the syntectonic granites which were intruded during Pan-African island-arc activity. They underlie large areas in the Red Sea Hills and are reported in field studies to form extensive areas of subdued sand-covered plains (El Nadi, 1984: Neary, 1976). Some syntectonic

granites also form areas of high, rugged relief. Both of these topographic expressions are encountered in this study, although large batholithic intrusives that form sandy plains with inselbergs protruding through the alluvium are more common (Almond, 1978; present study). Sandy plains are mapped here as alluvium. Distinguishable inselbergs are mapped separately. Drainage patterns form a medium-tight dendritic network and are shallow. In places, drainage is controlled by faults or prominent joints.

For intrusive units lacking radiometric dates, the prime discriminating factors are: the presence of Pan-African deformation and a spectral match to other batholithic granites (Figure 7A). The degree of deformation in batholithic granites varies from strongly jointed plutons that are elongated parallel to deformation, to plutons with vaguely deformed country-rock contacts. Plutons that are transected by all deformational events are included as batholithic granite.

The color of the batholithic granites on the 7,4,2 false-color composite photos varies from greyish tan to greyish brown to purplish brown. In the pluton that is faulted-out by the northern limb of the Sol Hamed suture in the northwest corner of 172,45 Q1, probable hydrothermal alteration is evident in the area of the thrust fault ($22^{o}10'N$, $35^{o}30'E$, Figure 4). Similar color changes are seen in other areas as well (eg., 172, 45 Q2, $21^{o}43'N$, $36^{o}30'E$ is in the center of one. These color variations may be a function of the degree of secondary hydrothermal alteration but also are influenced by variations in primary mineralogy of the pluton.

4.3.6 Hybridized Units: Ba/Namp, B/Namp

The digital-number signatures and morphological expression of these units are between batholithic granites and amphibolite-facies (or strongly altered) Nafirdeib series. These may be migmatitic amphibolites, syntectonic foliated granites, xenolithic granites, or "assimilation" granites which have been reported to be present by field investigators (Gass, 1955; Kabesh, 1962). Assimilation granites are amphibolites which have undergone anatectic melting.

4.3.7 Young Granites

Young granites are post-tectonic and cross-cut previously existing structures. The Young Granites usually form high, rugged terrain 1000-1500 meters above the surrounding country rock, but also form low, circular, sandy areas bounded by country rocks (El Nadi, 1984; Neary et al, 1976; Greenberg, 1981). The resistant plutons have coarse polygonal drainage patterns that follow the geometry of joints and dikes rather than dendritic patterns that typify batholithic granites. The low, flat, circular plutons occasionally are sand covered with dendritic drainage patterns similar to batholithic granites.

The color on the 7,4,2 false-color composite is variable from pinkish grey to brownish grey or grey to brown. Many of the intrusives are circular and show multiple episodes of igneous activity, often with discernible compositional differences on the TM imagery. Some young intrusives appear compositionally bimodal as gabbroic-granitoid. The gabbroic rocks are dark brown on the 7,4,2 composites.

4.3.8 Nubian Sandstone

The Cretaceous (Vail, 1978; Whiteman, 1971) Nubian sandstone overlies all other formations and, in the one large outcrop in the study area, is noticeably higher in relief. Very few drainage channels are developed in the outcrop, but it is textured with long narrow linear features which are brown in color. The color on the 7,4,2 base maps is tan to light reddish brown.

4.3.9 Gneisses and Amphibolites

We have dealt with each reported occurrence of Kashebib series rocks or high grade metamorphic rocks separately (Whiteman, 1971; Gabert et al, 1960; Gass, 1955). Each can be explained as either faulted high-grade metamorphic rocks from lower in the Nafirdeib island-arc pile or as contact-metamorphosed rock. The bulk of the potentially reported "paragneisses" mineral assemblages (Kabesh, 1962) are characteristic of greenschist facies. Some of the Kabesh "orthogneisses" may be syntectonic granites.

The gneissic terrains are low and hilly, in places covered with expanses of wind-blown sand (Kabesh, 1963). Drainage patterns are dendritic and form a dense, shallow network, often sand filled. Gneissic amphibolites occur extensively in one place in the study area, as a northeast belt of up-thrusted amphibolites and gneisses stretching from the northern part of subscene 171,46 Q1 to subscene 171,46 Q4 (Plates 4 and 5).

The color in 7,4,2 is light greyish brown in both areas. The spectral signatures across all seven bands differ from those of the Batholithic and Young Granites series.

We have designated the high-grade equivalents of Nafirdeib series rocks as Namp. These can be traced along several kilometers to less altered Nafirdeib rocks.

4.3.10 Alluvium

Wind-blown sands, colluvium, slope wash, wadi sands and gravels, and marine-deposited sands are all mapped together as Quaternary alluvium. Alluvium is mapped where it completely obscures bedrock geology. Extensive areas of windblown sand and alluvium cover batholithic granites and amphibolite gneisses, and can be mapped easily. Alluvium generally has a high albedo in all bands.

4.3.11 Recognizing Structural Features

El Nadi (1984) concluded, after his field work, that "the drainage system of the Red Sea Hills is generally structurally controlled, where most of the khors and wadis (wide khors) follow fault lines and structural joints, but their tributaries form dendritic patterns."

We mapped faults only where units were truncated or displaced in line with other truncations and displacements. We agree with El Nadi that faults often are marked topographically by saddles, wadis, and khors in the Red Sea Hills, as occurs in many other morphologically immature areas throughout the world.

We mapped persistent, linear, topographically expressed features without distinguishable displacement or truncation as lineaments/joints. Some of these may be reclassified as faults with measurable displacement in the field, but displacement is not discernible using TM imagery. In some places, interaction of the fault plane with topography allowed an approximate dip determination; these dip estimates are plotted on the map. Prominent joint sets were mapped wherever present. However, detectable joints are numerous and not all are mapped to prevent obscuring of other significant data.

Folds were mapped in the Nafirdeib series by mapping bedding trace lines. Where the "law of V's" allowed determination of dip on stratigraphic sequences, anticlines and synclines were discriminated. Dip symbols that were interpreted from imagery do not have numerical values; dip values are designated only for field measurements that were obtained from the literature.

Section 5
STRATIGRAPHY

5.1 GENERAL

The Methods section described our criteria for recognizing tectonically significant, mappable units using TM. The following discussion synthesizes available literature on the geology, petrology and geochemistry of these units to provide a tectonics-oriented description of the stratigraphy. Many of the ideas outlined here are refined and expanded in the Results and Discussions.

The Proterozoic basement has been divided stratigraphically by previous workers into the Kashebib, Nafirdeib, and Awat Series (Gass, 1955; Kabesh, 1962; Vail, 1978; Whiteman, 1971). The basal Kashebib Group is metamorphosed to amphibolite facies. In the Red Sea Hills, there is disagreement in the literature as to whether these rocks represent Nafirdeib series rocks with higher metamorphic grade or small pre-Nafirdeib cratonic blocks. The Nafirdeib and Awat series consist of greenschist to amphibolite facies island-arc volcanics and sediments.

Pan-African orogenesis is marked by intrusion of large plutons of the calc-alkaline Syntectonic or Batholithic Granite series into the Nafirdeib rocks, extensive deformation, and emplacement of ultramafic rocks along faults. Nafirdeib series calc-alkaline volcanic rocks are contemporaneous with the Batholitic Granites and, therefore, represent an essential element of the Pan-African continental margin complex. The ultramafic rocks include lithologies characteristic of ophiolite assemblages, and some of these ophiolite belts are believed to be the western continuation of those found in Saudi Arabia (Vail, 1983, 1985).

Mafic to felsic plutons and ring complexes of the Young Granite complex intruded the Proterozoic rocks during and after the Pan-African orogeny 630 to 400 million years ago, and in some regions of the Red Sea Hills

occupy over half of the exposed surface area. Older Young Granites are calc-alkaline and geochemically (El Nadi, 1984) similar to the Syntectonic Granites. Younger Young Granites are alkaline in composition, typical of intra-cratonic plutonism (Sillitoe, 1979). This is supported by radiometric age dates which range from 780 to 121 million years old. The Young Granites are commonly oval to circular; ring structures also are common.

5.2 OPHIOLITES (O)

Tectonically disrupted ophiolite complexes are likely the oldest rocks in the northern Red Sea Hills (Figure 6). Ophiolite suites represent Proterozoic oceanic crust that are now incorporated into the continent. In the Arabian Shield, major sutures that bound terranes have ophiolites and ultramafics distributed along them (Stoeser and Camp 1985; Greenwood, et al., 1980; Vail, 1985, 1984, 1983; Shackleton, 1986). In Egypt, flat-lying serpentinites have been interpreted as extensive ophiolite nappes which were emplaced over shelf metasediments (Ries et al., 1983).

Two ophiolites in the study area have been described in the literature. The Sol Hamed ophiolite (22°15'N, 36°08'E) has been studied in detail in the field by Fitches et al. (1983) and Hussein (1977). The Wadi Onib ophiolite (21°34'N, 35°17'E) (Figure 12) was described by Hussein et al. (1982) and Kroner (1985). Wadi Onib is the most complete ophiolite complex known in the Nubian Shield.

The ophiolites are all tectonically disrupted to varying degrees, and ophiolitic belts are associated with major tectonic shears and sutures.

5.3 NAFIRDEIB SERIES (Ncv)

Nafirdeib volcanics and associated sediments unconformably overlie ophiolites at Sol Hamed and Wadi Onib (Fitches et al. 1983). The Nafirdeib series is a greenschist-facies low-grade metamorphic complex of volcanics and associated sediments. The use of Nafirdeib series was first proposed by Ruxton (1956).

Workers in the Red Sea Hills have given rocks of the Nafirdeib series different names in different places, but most recent work has supported combining formations rather than splitting them.

The most recent geologic syntheses considered this family of rocks as a single group. Vail (1978) called the greenschist facies metavolcanics and metasediments the "Greenschist Assemblage". A regional geologic map of the Red Sea Hills prepared by the Sudanese Department of Geology and Mineral Resources (1:500,000) mapped all the low grade volcano-sedimentary metamorphics as the Nafirdeib series (El Nadi, 1984). That map was not available to our study.

All workers report that in some areas volcanics predominate and that in other areas sediments predominate. No investigators in this region have been able to develop a comprehensive stratigraphic column that is generally applicable. In fact, Shackleton et al. (1980) recommend that since most "stratigraphy" has been prepared lacking recognition of the widespread tectonic contacts, it must all be re-evaluated. Embleton, et at. (1982) emphasize the importance that recognition of ophiolite bearing sutures has on understanding Red Sea Hills stratigraphy. An understanding of the distribution of stratigraphic units requires that lithotectonic units be dealt with independently. Embleton et al. write: "Field evidence indicates that the volcano-sedimentary rocks and their intrusives are lithologically, environmentally, and morphologically somewhat similar throughout the Red Sea Hills. It is not surprising, therefore, that earlier workers endured much difficulty in constructing a stratigraphic sequence."

We have distinguished sediment-rich and volcanic-rich Nafirdeib series where possible. In this study, the Nafirdeib series includes the Oyo series of Gass (1955), Nafirdeib series of Ruxton (1956), the "schist-mudstone-greywacke series", Nafirdeib, and Awat series of Kabesh (1962), and the Nafirdeib series of Gabert et al (1960).

The Awat series is similar to the Nafirdeib series, but unconformably overlies it. It is deformed into open folds parallel to those of the

Nafirdeib, and is composed of acid volcanics, silty mudstones and conglomerates (Ruxton, 1956; Gabert et al. 1960; Kabesh, 1962). We consider the Awat series to be late Nafirdeib volcanics for two reasons. First, the two rock series are similar in structure and lithology, and indistinguishable on the TM imagery. Second, the dynamic regime of an island arc makes unconformities between episodes of magmatism and deposition expected. The unconformities that have been mapped between Nafirdeib and Awat series volcanics in places may simply represent localized episodes of uplift in late Nafirdeib arc time. Unconformaties may not be correlative. Thus, for the regional scope of this study, we have combined the Awat series of Kabesh (1962) with the Nafirdeib series.

The Nafirdeib volcanics and metasediments have been metamorphosed to greenschist facies field assemblages and are reported to have amphibolite facies assemblages in places (El Nadi, 1984; Vail 1978).

5.3.1 Volcanics (Nv)

The volcanics are basalts and andesites with volcaniclastics and agglomerates. Petrologically and geochemically they are distinctly calc-alkaline and have close affinities to island-arc volcanism in other parts of the world (El Nadi, 1984). They are intra-oceanic island-arc volcanics, with available dates in the Red Sea Hills ranging from 790 to 700 m.y. (Figure 6) and many at 720 to 710 m.y. Klemenic (1982, 1983) reported results of isotopic studies of Nafirdeib volcanics in the Red Sea Hills and found $^{87}Sr/^{86}Sr$ ratios of .7028 and .7034. This is similar to values reported for Egypt, and implies a primitive, mantle-derived source.

5.3.2 Metasediments (Nc)

The associated Nafirdeib sediments have been described as flysch and molasse (El Nadi, 1984) and include conglomerates, greywackes, pelites, calcareous shales, sandstones, and minor limestone. These terms

specifically imply a continental source for the clastics during convergence. Because field studies have defined no available continental source for these clastics, only a volcanic source, we consider the sediments to be reworked volcanics derived from the Nafirdeib intra-oceanic island arc. The clastic rocks are composed of variably reworked volcanics identical in composition and in spectral signature to the Nafirdeib volcanics.

Volcanics interbedded with metasediments east of the Gebeit Mine (21°08'N, 36°30'E) are distinctly different both geochemically and petrologically from the nearby predominantly volcanic Nafirdeib series. They are tholeiitic basalt flows with rare-earth chemistry that closely resembles marginal-basin volcanics (analogous to a back-arc basin) (El Nadi, 1984). Back-arc basin sediments and volcanics are interfingered with island-arc volcanics, suggesting a back-arc or marginal-basin setting.

Gass (1955) described the Oyo series sediments near the Oyo mine (approximately 21°54'N, 36°07'E). These rocks consist largely of pelites with resistant quartzites and marbles. Some pelites are largely reworked volcanics. Gass (1955) noted that the character of the sediments varies, and stressed that their depositional environment was in many small basins. Kabesh (1962) describes the Nafirdeib-type sediments as slates, greywackes, mudstones and minor marble.

5.4 SYNTECTONIC GRANITES

The Syntectonic Granites are the Batholithic Granites of previous investigators (e.g., Vail, 1978). They intrude deformed greenschist to amphibolite facies volcano-sedimentary rocks. They are foliated with varying degrees of intensity parallel to regional structure (e.g., Sillitoe, 1979; El Nadi, 1984). The granites coalesce to form extensive batholiths of diorite, monzonite, granodiorite and granite. Mafic intrusives such as gabbros are present but clearly subordinate (Vail, 1978; El Nadi, 1984). They are geochemically calc-alkaline.

Synorogenic granites in the Nubian-Arabian Shield range in age from 900 to 590 m.y., with many in the 820 to 720 m.y. range (Figure 6). No detailed systematic spatial variation in age is yet apparent. Defining individual orogenic cycles requires abundant radiometric and field geologic data. These are not available for the Nubian Shield. Available radiometric data for the northern Red Sea Hills fit this general time frame. Ages range from 770 to 545 m.y. (Figure 6, Table 5-1). Cavanaugh (1979) dated batholithic granites in the vicinity of Jebel Asoteriba (21°52', 36°30') at 686± 18 m.y. (Rb/Sr whole rock).

The synorogenic granites have been studied in the northern Red Sea Hills by Neary et al. (1976), El Nadi (1984), Cavanaugh (1979) and peripherally in several other studies. Enough ground information is available in the literature to allow us to map batholithic granites using TM imagery.

5.5 ANOROGENIC YOUNG GRANITE SERIES

The Young Granites are so named because they cross-cut deformation and are postorogenic (Almond, 1979; Greenberg, 1981). The Young Granite series includes a range of compositional types and a large range of ages. Ages in the Nubian-Arabian Shield range from 620 to 400 m.y. and available dates in the Red Sea Hills approximately fill this time span (Figure 6). Vail (1978) identified three intrusive episodes in Sudan at approximately 550 m.y., 230 m.y. and 100 to 50 m.y. No tectonic controls on the distribution are evident (Vail, 1978; Almond, 1979; Neary et al., 1976).

Compositionally, the granites are typically alkaline and aluminous although the oldest are calc-alkaline syenites, granites, and gabbros (Almond, 1979). Structurally, these intrusives are generally circular or oval in plan, sometimes occurring as ring dikes. They are found to be sub-volcanic, multi-stage, complex intrusives. The Sofaya ring complex (21°18', 36°08') is a multi-stage anorogenic granite that has been studied by several workers (e.g. Gass 1955; Cavanaugh, 1979; El Nadi, 1984). It has yielded seven K/Ar whole rock ages between 550 and 226 m.y., and two Rb/Sr dates of 465±9 and 384±9 m.y. (Vail, 1976).

The Young Granites of the Nubian-Arabian Shield are part of a continental east-west belt of anorogenic alkaline intrusives. This belt extends into west Africa, where the Young Granites host some of the largest tin and tungsten deposits in the world (Almond, 1979). Vein and disseminated mineralization is associated with less than 1% of the granites, generally in the late-stage, highly differentiated plutons (Sillitoe, 1979).

5.6 PHANEROZOIC COVER SEDIMENTS

Cretaceous and Cenozoic sedimentary and volcanic rocks locally cover the older basement and intrusive rocks. These include the eroded remnants of the Nubian sandstone, post-Nubian sandstone flood basalts and trachytes and the marine deposits along the Red Sea coast. Wind-blown sand, alluvium and colluvium are present along drainages and on slopes, and locally obscure large areas of bedrock.

5.7 DIKES

Numerous dikes of various ages cut the northern Red Sea Hills. Abundant E-W mafic dikes cut batholithic granites throughout the area. They are especially pronounced near the Red Sea coast (171,46 Q1), where they cut syntectonic diorites and Nafirdeib series rocks, but do not transect the amphibolites west of the NE trending suture. E-W dikes also cut batholithic granites in other areas (e.g., 21°35'N, 35°38'E). These E-W mafic dikes are syntectonic with dioritic intrusion and faulting.

Felsic or siliceous dikes intrude late-tectonic north trending shear zones, forming resistant parallel ridges along zones of shear (21°35'N; 36°53'E).

Late reddish orange dikes cut batholithic granites and Nafirdeib series rocks although these may be hydrothermally altered, iron-enriched areas.

5.8 YOUNG MAFIC INTRUSIVES

Late-occurring mafic intrusive rocks, possibly related to the young granites, are found throughout northeastern Sudan (Vail, 1978; Almond, 1979; Kabesh, 1962). They cross-cut all Pan-African structures and generally are circular in plan view.

5.9 ALTERATION AND METAMORPHISM

The field designation of greenschist facies generally has been assigned to the volcanics and country rocks of the Nafirdeib series (Vail, 1978). However, Vail (1978) also reports amphibolite-facies metamorphism in the Precambrian shield rocks of this area. This is a point of concern for discriminating rock types on TM imagery, since the formation of new mineral phases in a rock may change its reflectances. The greater the extent of metasomatism (the exchange of chemical constituents between the rock and hydrothermal fluid), the more likely it is that the spectral signature of the rocks has changed.

The significance of the high-grade Kashebib series metamorphic rocks is problematic, and previous investigators have defined it differently. Kashebib series rocks have been interpreted in the past as representing Archean or lower Proterozoic crust (Garson and Shalaby 1976; Vail, 1978), but recently this has been questioned (Kroner, 1985; Vail, 1985, 1983). Egypt's eastern desert also contains high-grade metamorphic rocks (i.e. Meatiq dome) which in the past have been interpreted as upwardly displaced sialic basement or exotic continental fragments. But isotopic studies have shown them to be isotopically primitive, and none has been found to be older than 800 m.y. (Kroner, 1985).

Table 5-1 Available Radiometric Dates in Study Area

	Rock	Date	Method	Location	Reference
1	Young Muscovite Granite	575 m y	Whole Rock K/Ar	21°08'30N, 36°10'E	Technoexport (1974)
2.	Young Granodiorite	543± 18 m y	Rb/Sr	22°N, 36°11'30'E	Vail (1978)
3	Young Alkali Granite	530± 2 m y.	Whole Rock K/Ar	21°14'N, 36°15'E	Vail (1978)
4	Granite Gneiss	580 m y.	Whole Rock K/Ar	21°00'N, 36N15'E	Technoexport (1974)
	Pegmatitic Granite	610 m.y.	Whole Rock K/Ar	21°00'N, 36N15'E	Technoexport (1974)
5.	Asoteriba Volcanics	649± 18 m y	Rb/Sr	21°50'N; 36°32'30"E	Cavanagh (1970)
6.	Nafirdeib Volcanics	712± 54 m.y.	Rb/Sr	Between Sol Hamed and Wadi Onib 21°50'N; 36°32'30"E	Fitches, et al (1983)
		543± 18 m y	Rb/Sr	22°N;36°11'30"E	Vail (1978)
7	Batholithic Granites	686± 18 m y.	Rb/Sr	N W of Jebel Asoteriba 22°N; 36°25'E	Cavanagh (1974)
8.	Batholithic Granodiorite, Small Stock	770 m y.	Whole Rock K/Ar	21°15'6"N, 36°20'6"E	Technoexport (1974)

Section 6

RESULTS AND DISCUSSION

A systematic integrated study using TM yields vast improvements in the understanding of structural and magmatic history and tectonic interpretation of the area studied over what is available in the literature. Specifically, improvements have been made in the more precise delineation of lithologic contacts, fault locations and extents, the regional distribution of specific rock types and the resulting regionalization of major lithotectonic elements. After synthesizing geologic maps and literature with our TM observations, we offer some new insights into Red Sea Hills stratigraphy and the tectonic significance of the units.

6.1 STRATIGRAPHY

6.1.1 Ophiolites and Serpentinites

Different types of tectonic models have been proposed to describe the occurrence of ophiolites in the Red Sea Hills, and all are similar in some respects. Most workers consider ophiolites to be found only near paleo-subduction trenches, emplaced tectonically during or after island - arc related convergence. Supporting this, we have found that the serpentinites and ophiolites in the northern Red Sea Hills of the Sudan are faulted-in along major fault zones that can be traced for hundreds of kilometers (Figure 1). The serpentinites and ophiolite suites along the Sol Hamed and Alaqui sutures were brought up along thrust faults. But not all serpentinites are associated with ophiolites; some are found apparently isolated with no gabbros, sheeted dikes or pillow basalts.

The ophiolite complexes along the Sol Hamed suture are soled by a thrust fault, and, spectrally and morphologically, appear to have a relatively consistent lithotectonic stratigraphy (Figures 11 and 12). Ultramafics and tectonized ophiolite occur at the base of the upper plate along

almost the entire length. The basal unit is ultramafic, variably serpentinized, with some interlayered gabbros(?). It is isoclinally folded in places, such as southwest of the Wadi Onib ophiolite, with some internal coherence. Overlying the ultramafic is a gabbro, a sheeted dike, and a serpentine melange that everywhere appears to be in fault contact with the basal unit. Flows and dikes are brecciated and cannot be followed over long distances. Serpentine forms a matrix to the breccia as stringers. Pillow basalts and breccias overlie the gabbros. Basaltic to andesitic Nafirdeib volcanics and sediments unconformably overlie the ophiolitic rocks. 7/5 band-ratio images allow us to separate the sheeted dike and pillow basalts from the Nafirdeib volcanics consistently (Figure 8). This separation may be due to differences in bulk composition, but may in part be due to the extensive sausseritization and uralitization reported in the ophiolite gabbros and basalts (Hussein, 1977).

Serpentinites along the Deraheib shear are not clearly associated with other ophiolitic type rocks. They may have been dragged from the Sol Hamed and Alaqui convergent boundaries during shear deformation, or forced up along them during late orogenic wrench faulting.

The Alaqui suture, which was identified for the first time in this study concurrently with the field work of Stern et al. (1986), contains interspersed serpentinites (Figure 13, Plate 1). Serpentinites occur along the main boundary faults of the Alaqui suture zone and generally are isolated from other ophiolitic rocks. The lithotectonic stratigraphy is poorly preserved compared to stratigraphy within the Sol Hamed suture.

Small, isolated serpentinites in the Mohammed Qol sheet area occur along the northeast-trending Port Sudan and Nakasir faults. The sausseritized gabbro is not a mappable unit using TM imagery, suggesting that these serpentinites represent ophiolites which have been tectonically dismembered (Figure 14). Field-identified distributions of ophiolitic rocks along the Sol Hamed and Alaqui sutures and the Deraheib shear by Stern et al. (1986) generally are in agreement with our interpretations.

6.1.2 Nafirdeib Series

The diverse Nafirdeib series is a mix of island-arc, arc-trench and back-arc-basin lithologies that typify sedimentation within an active plate margin. Some of the reported sediments are mature, including quartzites, and oolitic carbonates. But most of the reported sediments are greywackes, dirty silts, polymict conglomerates, and olistostromal conglomerates, all typical of immature, rapid sedimentation. Gass (1955) emphasized that areas of sediment deposition occurred in small, discrete basins. This implies a tectonically active area marked by abundant small marine basins that are common at active plate margins. The development of basins during deformation is often associated with convergent plate settings, both in foreland thrust belts (e.g., Ouachitas) and accretionary wedges (e.g., Lesser Antilles and the Makran Range, Pakistan).

Vail (1978) mapped the "greenschist assemblage" which includes the Nafirdeib series lithologies. However, detailed mapping of the distribution of Nafirdeib volcanics and pelitic sediments is first accomplished by this TM study. Structural control of the distribution also is identified for the first time in this study. The ability of TM processing to distinguish metapelitic rocks from Nafirdeib volcanics and carbonates permits us to identify and map relict sedimentary facies.

Some regions evidently were quiet basins during Nafirdeib time. The southern part of the Western terrane contains abundant pelitic rocks. In the Odib arc terrane, the Nafirdeib is also relatively rich in metapelites. In the Mohammed Qol terrane, few areas are recognizable as basinal metapelitic sediments. Higher grades of metamorphism that result in less hydrous mineral assemblages may also influence recognition of these rocks.

The Nafirdeib calc-alkaline volcanics in the northern Red Sea Hills erupted over a discrete period that coincides with similar volcanism reported throughout the Nubian-Arabian shield (Figure 6). Radiometric dates in the Red Sea Hills are 800 to 712 m.y. with most of the reported dates from 720 to 712 m.y. Nubian-Arabian shield dates range from 900 to 575 m.y., with most from 780 to 729 m.y. (Vail, 1983). Nafirdeib volcanism represents a discrete event in the evolution of the shield.

Geochemical studies of the volcanics show that back-arc tholeiites are interbedded with the thick section of Nafirdeib metasediments east of the Gebeit Mine at 21°00'-21°15'N, 36°20'-36°28'E, Plate 3) (El Nadi, 1984). Other reported occurrences of back-arc basin volcanics in the Nubian-Arabian Shield (Stern, 1981; Kroner, 1985) indicate that this is not unique. How many of the Nafirdeib sedimentary sections are back-arc basins? This is speculative, but data suggest that back-arc basins probably are caught up in other areas between juxtaposed arcs. Some of the sedimentary piles are likely from the arc-trench gap, or simply reworked volcanics from the arc axis.

6.1.3 Syntectonic Granites

Syntectonic granites that occur as extensive batholiths are called "batholithic granites" by previous investigators. Available ages for the batholithic granites in the study area range from 770 to 648 m.y., similar to the ages reported for occurrences in Egypt, 987 to 640 m.y. (Hashad, 1979). Like the volcanics, their intrusion represents a discrete event within a much longer period of calc-alkaline Pan-African intrusion throughout the Nubian Shield (Figure 6).

The granites are pre- and syntectonic and show various degrees of deformation. They are faulted by Pan-African reverse faults, but some deformed plutons cut these faults as well. We have reclassified some plutons as "young granites" and some young granites as "syntectonic granites" based on structural relations. Additionally, small plutons

that previously were unmapped are newly recognized in this study. The Western terrane of the Red Sea Hills has much less batholithic granite exposed than the Odib and Mohammed Qol terranes.

Syntectonic granites are found along the Alaqui suture (21°5'N, 33°52'E in Figure 13 and Plate 1) and the Sol Hamed suture (21°38'N,35°15'E) and are localized along other thrust faults as well (e.g., 36°12'E, 21°25'N). Syntectonic granites also occur as extensive batholiths.

The occurrence of anatectic granites that were produced by anatectic melting in zones of intense deformation has been noted in the northern Cordillera of Alaska and British Columbia (Hollister and Crawford, 1986). The pressure and temperature regimes that are sufficient to produce pervasive anatectic melting and ductile behavior are suggestive of mid-crustal deformation. The geometry of occurrences of syntectonic granites with major sutures in the northern Red Sea Hills suggests that granite genesis here, in some cases, may be similarly controlled.

El Nadi (1984) noted a westward increase in $K_2O/K_2O + Na_2O$ and Rb/Sr ratios in intrusives within his study area, and we believe that this demonstrates the differences in the compositions and levels of two exposed island arcs. El Nadi did not recognize two arcs. The eastern Mohammed Qol arc is associated with amphibolitic gneisses and is predominantly dioritic. The western Odib arc intrudes greenschists and is predominantly granitic. The compositional difference aids in explaining El Nadi's observations and illustrates the importance of recognizing terrane boundaries in the interpretation of these data.

6.1.4 Young Granites

Numerous young granites and ring complexes have been added to the inventory of known occurrences (Whiteman, 1970; Vail, 1978) as a result of this study. They range widely in topographic expression and spectral

signature, but all cut Pan-African structure. Many young granites show evidence of multiple stages of intrusion by compositionally distinct magma. Some are altered and form sandy plains; others evidently are fresher.

Full-resolution screen images of the Salala ring complex shown in Figure 10 (21°19'N, 36°9'E) allowed us to identify the large intrusive differentiates that were mapped by Cavanaugh (1979). Neither Cavanaugh nor Gass (1955) recognized the large-scale faulting around the ring complex. A NW-trending, steeply dipping fault truncates the northeastern edge of the complex and an ENE-trending fault separates the two main lobes of the ring complex (Figure 10, Plate 3).

Other young granites include the large, NW-trending tear-drop shaped intrusions near 21°55'N, 36°22'E. These intrude batholithic granites and Nafirdeib series. This area was mapped previously by Gass (1955), Neary et al. (1976), and Hussein (1977). The current interpretation shows considerable increase in structural detail over earlier maps (Plate 3). The use of TM imagery allows recognition of major faults that are associated with these units and the complex nature of the intrusives and their contacts.

As with previous workers (Almond, 1978, 1979; Vail, 1978; Serencsits et al., 1981), we see no pattern controlling the distribution of young granites, even with the regional overview offered by TM. They are multi-stage, show variable alteration, and cross-cut Pan-African structure. Other young granites that occur in areas of recent field work have been found by this study to cross-cut previously unmapped Pan-African structures, thereby confirming their age. For example, a granite at 36°23'E, 22°10'N cuts a NE-trending Pan-African fault. Also, a young granite that was mapped by Neary et al. (1976) cuts Pan-African structures near the Sol Hamed ophiolite at 22°17'N, 36°17'E.

Young granites are either lobate or circular in plan view. Lobate occurrences are always elongated N to NNW. The few available radiometric dates indicate that the older plutons (older than 550 m.y.) are lobate and younger ring complexes are circular. A young granite at 21°15'N, 36°15'E has a K/Ar age of 530 ± 2 m.y. (Vail, 1978) and is elongated NNW. The change from lobate to circular in plan view may reflect a relaxation in the horizontal compressive-stress difference between the two episodes of emplacement.

6.2 ALTERATION AND METAMORPHISM

6.2.1 Localized Contact Metamorphism

Alteration of the country rock surrounding plutons was reported by Vail (1978) and Neary et al. (1976). Metamorphic and hydrothermal halos conform to intrusive contacts, discoloring contiguous rocks while only minimally disrupting their structure. Kabesh and Afia (1959) report contact-metamorphic assemblages in the Nafirdeib series rocks at Dirbat Well, west of Port Sudan. Cordierite-biotite-quartz, andalusite-sillimanite-quartz, and wollastonite-diopside marbles are all high temperature, low-medium pressure assemblages. With special attention, TM spectral data prove excellent for mapping these contact aureoles. Gass (1955) and Neary et al. (1976) both reported "assimilation granites" that showed extensive contamination of the granitic batholiths by country rock. In the present study, the same region was independently identified as consisting of extensively metasomatized volcanics intruded by altered batholithic granites (172,45 Q2, north-central portion). Numerous similar areas of hydrothermal alteration can be identified by following structures from unaltered rocks into altered zones.

6.2.2 Regional Metamorphism

Areas mapped by Gabert (1960) as Kashebib series in 172,45 Q3 (Plate 3) are considered here to be metamorphosed and metasomatized amphibolite- facies Nafirdeib series rocks. We interpret these rocks as roof pendants and xenoliths in batholithic granite; thus, their metamorphic grade should be higher than elsewhere. One of these pendants includes metamorphic rocks in Jebel Kashebib, the type locality for the Kashebib series in northeastern Sudan. Since the amphibolite-grade Kashebib type locality can be interpreted as simple roof-pendant metamorphism, we do not believe that the Kashebib series represents a significant basal unit or a cratonic block.

A belt of amphibolite-facies Nafirdeib metasediments and meta-volcanics (the paragneisses of El Nadi, 1984) are faulted against greenschist-facies Nafirdeib metasediments at the eastern edge of 172,45 Q4 (Figures 10, 19, Plate 3). For this same area, Gabert et al. (1960) report a northeasterly trending belt of amphibolite Nafirdeib group rocks. The mineral assemblage reported to occur in these metasediments is cordierite + garnet + kyanite + occasional sillimanite (El Nadi, 1984). This is not a contact-metamorphic assemblage. Pressures greater than 4-6 kilobars and temperatures in excess of 500°C are required (Turner, 1981). This represents amphibolite-grade metamorphism at distinctly deeper crustal levels than that affecting the Nafirdeib series to the west of the faults. We interpret this juxtaposition as a diffuse fault boundary between the greenschist-facies Odib terrane on the north and the amphibolite-facies Mohammed Qol terrane on the south (Figures 1, 17, Plate 3).

El Nadi (1984) describes the original lithology of the Mohammed Qol terrane amphibolite gneisses as distinctly different from the Nafirdeib series, including quartzites which he describes as continental shelf-type deposits. But Kabesh (1962) reports quartzites in the Nafirdeib series in the Mohammed Qol area to the south and Gass (1955) reports that quartzites are common north and west of El Nadi's area. Gass specifically mentions the paucity of quartzites in the area of El Nadi's study; thus we believe that El Nadi simply was in a quartzite-poor area of the Nafirdeib.

We interpret the "paragneisses" of Kabesh and El Nadi in the Mohammed Qol terrane to be higher-grade metamorphic equivalents of rocks similar to the Nafirdeib series. The units are readily distinguished on the imagery, and are mapped as Namp. They are interpreted as either early Nafirdeib island-arc volcanics and sediments or older, pre-arc sediments. Kabesh (1962) describes several mineral assemblages in the "paragneisses", the bulk of which are chlorite-sericite schists with local garnet-actinolitic hornblende schists and biotite-schists. The mineral assemblages in the "paragneisses" represent greenschist to amphibolite-facies metamorphism.

6.3 PROTEROZOIC TECTONICS IN THE RED SEA HILLS

In the ensuing discussion, we use the term Pan-African to refer to the late-Proterozoic orogenic event of folding, faulting, and magmatic emplacement (Figure 5). In actuality, the regional Pan-African orogeny likely comprised several discrete arc and marginal-basin collisions and deformation. Pan-African radiometric ages are recorded in mobile-belt zones along the rim of the African continent (Figure 5, 6).

6.3.1 Structural Style

Pan-African deformation is multi-phase and pervasive. Major sutures comprise en echelon and parallel faults and mylonitic shear zones. The Sol Hamed and Alaqui sutures have wide zones of parallel deformation in their upper plates (Figures 13, 18). Throughout the study area, Nafirdeib metasediments are more deformed than the intercalated volcanics. Gass (1955) also noted this contrasting structural behavior in his extensive field work, and described the volcanics as "augens" in a more deformed sedimentary matrix.

The most striking features within the study area are major fault zones that encapsulate relatively undeformed blocks (Figure 1, Plate 6). The north-trending Deraheib shear cuts the Sol Hamed and Alaqui convergent sutures. Its structural style and apparent displacement are right

lateral strike slip. Parallel north-trending shear zones cut convergent-style boundaries in many areas. The presence of major strike-slip faults intermediate in orientation (e.g., a N20W-striking fault intersecting the Deraheib shear on east side (20°34'N, 34°51'E) suggests that this shift in deformational style and direction was not abrupt (Figure 16). Pan-African deformation in the northern Red Sea Hills changed its style from convergent deformation to shear faulting at 630 to 620 m.y. (Figure 6).

Multi-stage Pan-African deformation in east Africa just recently has been correlated with plate-tectonic events (Shackleton, 1986). Shackleton sees evidence of NW-SE directed motion followed by N-S post-collisional ductile shear. His model for East Africa, multi-stage subduction deformation followed by ductile and then brittle shear parallel to the plate boundary, fits our observations.

6.3.2 The Sol Hamed Suture

The deep-seated faults along which the Sol Hamed, Wadi Onib and other ophiolites were emplaced is called the Sol Hamed suture here, after Vail (1985). It dips steeply to the northwest in the north and shallowly southeast towards its southern termination by the younger, north-trending Deraheib shear zone (Figure 12). On the northeast it is terminated by Red Sea graben faults and covered by alluvium (Figure 1, Plate 6). It can be traced over approximately 225 km along strike. Our interpretation of the TM imagery shows that the ophiolites face up to the southeast and are faulted at their base. Ophiolitic rocks are thrust over Nafirdeib series rocks and batholithic granites. The suture represents westerly transport of the upper plate relative to the lower plate.

The Sol Hamed basal thrusts comprise parallel zones of intense deformation (Figure 18). The suture bifurcates and isolates some occurrences of very altered Nafirdeib rocks. The fault-bounded slivers are intruded by syntectonic batholithic granites. The main suture has been deformed by subsequent convergence, and its change in dip along strike is evident on the imagery.

This recognition of consistent lithotectonic stratigraphy in the ophiolites above the main thrust is new, as is recognition of age relations with the Deraheib shear. The Sol Hamed suture both cuts and is cut by batholithic granites.

The Sol Hamed Suture is younger than the 712 $\pm$ 54 m.y. Nafirdeib volcanics (Fitches et al., 1976) which it transects. This suture is currently being studied by Stern et al. (1986) who interpret its age as 740 to 710 m.y. based on new radiometric data. This is within the inferred range of convergent deformation for the northern Red Sea Hills implied by synthesizing previously available information (Figure 6).

Vail (1985) recognized the Sol Hamed suture but included the Deraheib shear as a part of it. Concurrent with our study, Stern et al. (1986) have recognized that the Deraheib shear cuts the Sol Hamed suture.

The Sol Hamed suture previously was considered to be the Nubian Shield equivalent of the Saudi Arabian Yanbu suture (Vail, 1985; Camp, 1984; Shackleton, 1986; Stern et al., 1986). Our characterization of the width of the suture, structural style, and nature of adjacent lithologies supports this interpretation.

6.3.3 The Alaqui Suture

The Alaqui suture previously was not identified or mapped. The general trend of the rocks was mapped by El Ramly (1972) but he did not recognize the fault zone that is present. The E-W trending suture has associated amphibolites, syntectonic granites, and serpentinites (El Ramly, 1972; this study). It is truncated in the east by the Deraheib shear; it continues for at least 175 km to the west. A 50-km wide zone of deformation accompanies the main 20-30 km wide fault zone. Figure 13 is a 1:500,000 scale image of subscene 173,45 Q1 with a geologic map overlay that covers the Alaqui suture.

The zone of amphibolite rocks and serpentinites is separated from Nafirdeib rocks to the south by a well defined, through-going fault (Figure 13, Plate 1). The occurrence of these rocks requires thrust or reverse faulting at a convergent boundary. Thus, we interpret the Alaqui suture as a convergent boundary juxtaposing greenschist and amphibolite grade Nafirdeib series on the south with extensive serpentinite and amphibolite (mapped by El Ramly, 1972) to the north.

Concurrent with this study, Stern et al. (1986) also have recognized the Alaqui suture and also have named it the Alaqui suture. During a ground transect through Wadi Alaqui, and by using band 7 TM imagery, Stern et al. mapped ophiolitic rocks and syntectonic granites. Their findings confirm our interpretations of the multi-band TM data. Stern et al., however, believe that the Alaqui suture is the displaced continuation of the Sol Hamed suture.

Our study does not support this interpretation because: (1) on the TM imagery, the Deraheib suture appears to have left lateral and not right lateral displacement, and (2) the Alaqui and Sol Hamed sutures appear to have distinct tectonic styles. Serpentinites are found isolated along the Alaqui suture, but they do not have a consistent ophiolitic lithotectonic stratigraphy as is seen in the Sol Hamed suture. In the main Alaqui suture, faults anastamoze and coalesce around a wide fault zone which contains syntectonic granites and amphibolites. The Sol Hamed suture has a basal thrust that soles regularly facing ophiolite suites with unconformably overlying Nafirdeib island volcanic arc units. En echelon thrusts are present, but not over as wide an area.

6.3.4 The Port Sudan Suture

The Port Sudan suture both cuts and appears to form the southern margin of the Mohammed Qol terrane. It was first referred to by Vail (1985) as the Nakasir suture, although he greatly simplified its nature. Ultramafics occur along its known extent. We see that the Port Sudan

suture is a significant accretionary boundary. By better defining structure and lithology, we have extended the boundaries of the suture and have renamed it. Figure 14 is a photographic image and geologic map overlay of subscene 171,46 Q3 that covers portion of the of the Port Sudan suture that occurs within our study area.

The Port Sudan suture is divided into the Nakasir fault zone and Port Sudan fault zone. These parallel northeasterly fault zones have small occurrences of associated serpentinites and extensive shear zones. Parallel folds and faults deform greenschist and amphibolite facies Nafirdeib series outside the main zones.

The Nakasir fault zone can be followed for at least 100 km. It separates amphibolite-grade Nafirdeib series rocks on the west from batholithic intrusives and amphibolites on the east. This fault has a serpentinite along it (20°33'N,36°30'E) and is developed in complexly deformed Nafirdeib series. It is deformed by later Pan-African structures in this vicinity.

The Port Sudan fault zone intersects the Red Sea coastal plain 20-50 km north of Port Sudan. It is a major northeasterly striking zone of sheared, folded, and altered Nafirdeib sediments. It may form the southeastern border of the Mohammed Qol terrane. A serpentinite occurs along the most intensely faulted front of this suture zone. Amphibolites and a syntectonic granite are also associated with the zone (Gabert et al., 1960; this study). Intensely folded Nafirdeib volcano-sedimentary rocks form a 20-30 km wide zone of deformation parallel to the main shear.

Significant crustal shortening has occurred across these fault zones. Judging by the relative intensities of deformation, the Nakasir fault zone has not experienced as much displacement as the Port Sudan, and may represent the northern limit of the Port Sudan suture within the Mohammad Qol terrane. The Port Sudan fault zone has a wider shear zone and exhibits more intense subparallel deformation. It appears to have been the principal zone of strain during crustal shortening.

Along the southwestern extension of the Port Sudan suture that is beyond the limits of our imagery, Aye et al. (1985) have mapped scattered ultramafics, and show the same general rock types and structural trends continuing for an additional 600 km to the southwest. The Port Sudan suture is cut by two major NNW-striking faults along this extension, both of which extend into our study area.

The Nakasir suture of Vail (1985) separates the "Northern Red Sea Hills" and "Southern Red Sea Hills" terranes. The Mohammed Qol suture aligns across the Red Sea with the Bir Umq suture in the Arabian Shield. Stoeser and Camp (1985) map the Bir Umq as splitting the 800 to 700 m.y. Hijaz island arc terrane. Vail (1985) and Camp (1984) both recognized the continuity of the two sutures across the Red Sea. They believe it was the site of a southeast-dipping subduction zone. This may be so but we do not see evidence of this on the imagery.

6.3.5 Late Pan-African Shear Zones

The Deraheib shear was the main zone of faulting during N-NNE directed shearing, but other parallel fault zones also cut earlier compressional Pan-African structures. The N-NNE shears are found in all terranes.

A 150-km long and 50-75 km wide zone of N-NNE shearing borders the Mohammed Qol terrane extending from 19°40'N, 35°20'E to 20°38'N, 35°30'E. N-NNE shear zones cut the Sol Hamed suture and surrounding volcanics and batholithic rocks (35°57'E, 22°-015'N; 35°37'E 21°45'22°25N). In the Western terrane, N-NNE shears cut WNW striking compressional structures in an area of extensive pelitic rocks (19°35'N, 33°52'E to 34°00'E, 20°15') and Nafirdeib volcanics and pelitic sediments (e.g., 21°05'N, 33°35'E to 21°25'N, 33°35'E and 34°07'E, 20°52'N to 21°38'N, 34°15'E).

Age constraints on these N-NNE shears place them as late orogenic Pan-African (Figure 5). The Deraheib shear cuts the extensive batholithic granites and is cut by small syntectonic granites. It is

therefore apparently late orogenic with an age of 630 to 600 m.y. The same age relationships apply to other, parallel shear structures. Supporting this inferred age are four disturbed whole-rock Rb/Sr isochrons from gneisses and diorite near the Deraheib shear which are approximately 625 m.y. (Stern et al., 1986)

The shear zones are characterized by parallel and anastamozing zones of faulting and fracturing. These are intruded by late dikes or are silicified in places (22°15'N, 35°45;E). Sense of displacement is left lateral on some (e.g., 21°20'N, 34°08'E; 21°45'N, 35°40'E); the sense of displacement of the Deraheib shear is difficult to interpret, but the drag of ophiolitic rocks appears to support left-lateral movement (21°20'N, 35°05'E, Figure 12). This conflicts with the interpretation of Stern et al. (1986) that the sense of movement is right lateral on the Deraheib shear. Their interpretation is based on the assumed continuity of the Sol Hamed and Alaqui sutures.

North-trending, Pan-African, post-compression wrench faulting has not previously been recognized in northeast Africa. Stern et al. (1986) recognized that the Deraheib shear (they call it the Hamisana shear) is a wrench fault, but have inferred the opposite sense of displacement that we have inferred. Shackleton (1986) documented N-S post-collisional shear in the Mozambique mobile belt to the south. We see abundant evidence for a similar system in the northern Red Sea Hills (Plates 1-6).

6.3.5.1 Deraheib Shear. The Deraheib shear cuts both the Sol Hamed and Alaqui sutures. It trends N-S, and is decorated with serpentinites along much of its length. The shear runs north into Red Sea graben faults, and is not traceable south of a Red Sea continental transform fault beneath wind blown sand and alluvium. It is exposed over 350 km. All our observations lead us to believe that the Deraheib shear is a large strike-slip fault. The southern end of the Deraheib shear is shown in subscene 173,46 Q2 (Figure 16, with geologic map overlay).

The zone of shear is wide and pervasive, and the foliation is steep as inferred from the TM images. Field mapping by Stern et al. (1986) confirms that the foliation along the shear is near vertical.

Amphibolites and plutons are not distributed parallel to, or associated with, the fault zone. Serpentinites do not appear to be associated with other ophiolitic rocks, an observation confirmed by Dixon (personal communication, 1986).

6.3.6 Odib Terrane

We identify five NNE-trending belts in the Odib terrane of scene 172,45 (Figure 11). The largest is a belt of batholithic granites 90-100 km wide, approximately the same size as the present exposure of the Sierra Nevada batholith in California.

This belt of batholithic granites is considered to be at or near the axis of a Pan-African arc. It is flanked by two belts of Nafirdeib rocks intruded by small batholithic granites and young granites. To the southeast it is paralleled by a 30-50 km wide fold and thrust belt composed of greenschist facies Nafirdeib bimodal volcanics and reworked volcanics (Figures 10, 11, 15). Calc-alkaline andesitic volcanics predominate; tholeiitic basalts are interbedded with the sedimentary rocks (El Nadi, 1984). Amphibolite-facies Nafirdeib series and batholithic granites of the Mohammed Qol terrane are thrust into tectonic contact with these greenschist-facies Nafirdeib rocks as shown in subscene 172,45 Q4 (Figure 15).

The batholith is flanked to the northeast by the Sol Hamed suture and its associated ophiolites, representing obducted oceanic crust (Figure 11). Unconformably overlying the ophiolite, Nafirdeib volcanics are also found to the northwest of the batholith.

The vergence direction inferred by the Sol Hamed suture and the geometry of associated thrust faults is northwesterly.

The Nafirdeib volcanics (712 m.y.) and batholithic granites (770 to 640 m.y.) in this batholithic belt are very similar geochemically, virtually indistinguishable geochronologically, and considered to be approximately contemporaneous (Neary, 1976; present study). The batholith-volcanic complex probably represents an island arc that developed from early extrusives and associated sediments, to later batholithic plutons intruding a deforming volcano-sedimentary prism. The axis that is exposed is mid- to upper-level of the later arc. Higher levels are exposed to the northeast, where extensive contamination and roof pendants are abundant, and the late, but penecontemporaneous Asoteriba volcanics overlie the batholithic granite (present study; Neary et al., 1976; Cavanaugh, 1979).

The lithotectonic belts southeast of the arc axis represent a Nafirdeib volcanic pile, essentially barren of intrusives, and tectonically juxtaposed against the batholithic arc. Marginal-basin sediments and volcanics are faulted against these to the southeast. Amphibolites of significantly higher metamorphic grade than those in the Mohammed Qol terrane are thrust westward over this belt.

6.3.7 Mohammed Qol Terrane

The Mohammed Qol terrane previously has not been recognized as a distinct tectonic feature. It is found along the coast in the southeastern portion of the study area (Plate 6). It is bounded to the north by thrust faults, to the west by N-S shear faults, to the east by Red Sea graben faults, and to the south by the Port Sudan suture.

The general structural grain is northeasterly, parallel to the Odib island-arc terrane to the north. Predominant Pan-African folding and faulting strikes northeasterly. Rift-related transform faults are abundant and cut all other structures.

The predominant rock types are amphibolite gneiss, greenschist gneiss, and intrusive diorites (Kabesh, 1962; El Nadi, 1984; Gabert et al., 1960). Spectrally, the Nafirdeib series rocks and the intrusives appear altered

and variable. The type section of the Awat series is in this area (20°20'N,36°26'E), and it is seen to unconformably overlie Nafirdeib rocks (Kabesh, 1962). We have mapped the Awat series as late Nafirdeib, but we emphasize that the Nafirdeib series is structurally complex in this area.

The eastern portion of the terrane is largely dioritic. The diorites are variably altered, jointed and intruded by abundant E-W mafic dikes. This belt of diorites intrudes amphibolites and batholithic granites to the west. In some places this contact is a fault contact (e.g., 20°45'N, 36°50'E in Figure 14, Plate 5) (Gabert et al., 1960; Kabesh, 1962; this study).

On the imagery, the rocks in this terrane are distinct from the Odib terrane; amphibolites are abundant, and variably altered granitic and gabbroic intrusives form abundant, distinct plutons rather than extensive batholiths (Figure 13). There are many areas along the axes of folds in which rocks appear to be a hybrid of amphibolitic and batholithic rocks. Some of these rocks we interpret to be syntectonic granites that are foliated parallel to main structural trends. In other areas these rocks may be migmatitic amphibolites (Ba/Namp on Figure 13). These "hybrid" lithologies, in either case, are distinctive of mid-crustal active continental margin conditions. We interpret the Mohammed Qol terrane to represent a deeper level of an island arc than is seen in the Odib terrane. The Nafirdeib series rocks are subordinate in this area and are highly deformed between the more rigid batholithic/amphibolite rock types.

6.3.8 Western Terrane

This portion of the study area has not been mapped on the ground except along its northernmost edge, which is on El Ramly's (1972) map of Egypt (Figures 3, 13, 16). The recognition of this geologic terrane bounded by major shears and fault zones is new. However, its distinction from surrounding terrains is not verified by geochronological data or by field mapping. No radiometric ages are available for this area. We have mapped lithologies based on extrapolation from known areas (Plates 4, 5, 6).

The terrane is bounded on the north by the Alaqui suture and on the east by the Deraheib shear, and is composed largely of Nafirdeib series volcanic and sedimentary rocks. The structural grain is dominantly E-W up to 150 km away from the Alaqui suture. All structure is overprinted closer to the Deraheib shear, and foliation is N-S up to 60 kilometers away from it.

The Western terrane measures at least 375 x 160 kilometers. Batholithic granites are present in the north and pelitic rocks are a more significant fraction of the Nafirdeib series toward the south. Young granites and ring complexes are scattered throughout the terrane.

One of the key differences from other terranes is the paucity of batholithic granites. They are clearly subordinate; intrusive levels of an island arc are not exposed to the same extent. Additionally, the pelitic fraction increases to the south in this terrane, possible indicating the existence of a Pan-African basin.

The structural grain changes strike in the southwestern portion of the area from northerly to northwesterly (Figure 1, Plate 2, 173,46 Q3). Extensive alluvial coverage limits mapping in this area, but the overall structure and gross lithology stand out. This is a large, open, chevron fold hundreds of kilometers across. Its axis trends northeasterly. The bend in the Nile at this location is controlled by this basement structure.

Ring complexes and young granites are scattered throughout the terrane. Two noteworthy occurrences are: (1) a circular granitic intrusion that cuts pre-Deraheib-suture NNW shears (20°45'N, 34°40'E), and (2) a circular syenitic (?) intrusion that cuts a northerly shear (19°57'N, 33°50'E).

6.3.9 Post Pan-African Faulting

6.3.9.1 Northwesterly Faults. Northwesterly faults and lineaments cut all Pan-African structures, and are themselves cut by Red Sea related transforms. These late northwesterly faults are predominantly normal faults, but some show a strike slip component. Total on-strike displacement is small, but the faults and lineaments persist over many tens to hundreds of kilometers.

A particularly prominent fault cuts the Salala and Umm Shibrik ring complexes that were mapped by Gass (1955). It extends nearly 100 km from near the Gebeit mine (21°00'N, 36°17'E) NNW to the north of Umm Shibrik (21°40'N, 36°00'E). This is an east-side down normal fault. A possible en-echelon continuation extends nearly 100 km from 21°40'N, 36°05'E to 22°24'N, 35°33'E. The southern portion is a lineament with no mappable displacement at this scale. The northern portion is a fault with apparent right-lateral displacement. Parallel faults cut Nubian sandstone (e.g., 20°58'N, 35°58'E), while others are covered by sandstone (area of 21°04'N, 36°03'E).

This faulting is post-Pan-African and pre-Red Sea rifting but difficult to date more specifically. It may be related to East African rifting that preceded Red Sea rifting.

6.3.9.2 Red Sea Rifting. Miocene rifting has been documented in Sudan, Ethiopia, and throughout East Africa. Parallel to the Red Sea are graben faults; transform faults are normal to these. We see abundant jointing and small scale faulting in the northern Red Sea Hills that cross-cut all structure and lithology.

The presence of continental transform faults related to the Red Sea was documented in Sudan by Ahmed (1982). Ahmed conducted a 1:1,000,000 scale lineament study with Band 7 MSS imagery, concluding that the Red Sea structures often reactivate pre-Cambrian zones of weakness. Rectilinear features trend dominantly ENE and NNW.

On the imagery, we also find that late linear features which could be attributed to Cenozoic rifting trend dominantly ENE and NNW. The ENE strike-slip faults dominate NNW-striking, en-echelon graben faults and are found along the coast (Plate 5). They are uncommon more than 20-30 km inland. ENE strike-slip faults also are concentrated toward the coast, but extend much farther inland, where frequency decreases. A 50-75 km wide strip along the coast has the greatest concentrations of rift-related faulting. Some areas show concentrations of short, sub-parallel faults which may correspond to continental extension of marine transforms.

The most prominent continental transform fault intersects the coast at 21°07'N, just north of Mohammed Qol (Figure 19, Plates 5, 6). This transform has right-lateral displacement and aligns with marine Red Sea transforms that were mapped by Hall et al. (1977) and Guennoc and Thisse (1982). A strong parallel magnetic anomaly is associated with the marine transform. Between 18° and 21°N, Hall et al (1977) mapped three major transforms intersecting the Sudanese coast. An easily identified magnetic anomaly intersects the coast at 20°N, where we have mapped abundant through-going transform faults.

Our interpretation shows that marine transforms related to Red Sea rifting extend into the continent, displacing rocks as far as 400 km inland along the Mohammed Qol transform (Plates 2, 4, 5; Figure 1). An interesting aspect of the continental extension of the faults is their deflection. Transform faults mapped by other investigatiors strike NE in the Red Sea and those mapped in this study and elsewhere in the Nubian shield by Ahmed (1982) strike ENE on the continent. The same deflection is seen on lineament maps of Saudi Arabia (Guennoc, 1982).

6.4 PLATE TECTONIC MODEL

6.4.1 Tectonic Development of the Northern Red Sea Hills

The oldest major structures in the area are convergent boundaries represented by the Port Sudan, Sol Hamed and Alaqui sutures (Plates 6, 3, 5, 1). These are cut by the Deraheib and parallel shear zones. The Western, Odib, and Mohammed Qol terranes are surrounded by major shear zones and are distinct lithologically.

There is insufficient available information to judge the relative ages of the Port Sudan, Alaqui and Sol Hamed sutures. Preliminary radiometric dates on a syntectonic granite reported by Stern et al. (1986) imply that the Alaqui suture is 690 m.y. Radiometric ages and geologic relations indicate 740 to 710 m.y. for the Sol Hamed suture (Stern et al., 1986; present study). The Port Sudan suture is known only to be younger than the 720 m.y. age on the nearby Nafirdeib volcanics. This is in agreement with the assessment of Stoeser and Camp (1985) of the Bir Umq suture in Saudi Arabia being post 715 m.y.

The Sol Hamed and Alaqui sutures are the approximate locations of Pan-African plate margins, although we do not believe that they represent a continuous subduction zone as suggested by Stern et al. (1986). Pan-African island-arc volcanics and arc-related sediments of the Western and Odib terranes were deposited on oceanic crust. The Mohammed Qol arc terrane developed approximately contemporaneously. Batholithic syntectonic granites intruded the volcano-sedimentary piles. Convergence along the various arcs continued from approximately 800 m.y. to 630 m.y.

Volcanism and plutonism were superimposed over all terranes during syn- and post-suturing arc activity. The position of the subduction zones related to the Alaqui and Sol Hamed sutures is unknown. The distribution of lithotectonic belts in the Odib terrane (Figure 11) indicates that the trench was to the north and that subduction was directed toward the southeast. The Phanerozoic model shown in Figure 17 places the trench at the Sol Hamed suture.

6.4.2 Phanerozoic Models Which Fit Proterozoic Observations

Figure 17A shows a typical Phanerozoic island-arc configuration modified from Almond (1978), who compared this model directly to the less-known island arcs in the Nubian Shield. This model fits the packet of five belts in the Odib terrane well (Figure 11). The Sol Hamed suture represents the paleo-subduction zone; the batholithic island-arc-

intruding volcanics comprise the next lithotectonic unit; the back-arc basin sediments and volcanics follow. Figure 17B shows a sequence of obduction of the arc along a suture (which would contain ophiolites). In this scenario, the fold and thrust belt is developed in the back-arc basin during collision; imbricate thrusts and folding deform the ophiolite and overlying volcano-sedimentary pile. Note that dominant vergence of all structures in the collision zone is to the west, and the subduction is to the southeast, in agreement with the stress regime inferred by Camp (1984) for the Yanbu suture in Saudi Arabia.

East of this island-arc packet is the Mohammed Qol terrane, which appears as a 100-150 km wide belt of greenschist to amphibolite gneisses and syntectonic granites on the imagery. The Nafirdeib series rocks are present only as what we interpret to be highly deformed, rare roof pendants. The dominant structural grain is still northeast, but middle levels of an arc system are exposed. Syntectonic, deformed granites dominate over batholiths. Batholithic granites along the coast are dominantly dioritic (Kabesh, 1962). The Mohammed Qol terrane is identified here as a mid-level island arc. This agrees well, in terms of lithologies and expected structures, with the convergent model in Figure 17.

6.4.3 Tectonic Models for the Nubian-Arabian Shield

Current tectonic models hold that the Nubian Shield of the Red Sea Hills of Sudan, together with the Arabian Shield of southwestern Saudi Arabia, are the northward extension of the African Proterozoic continental margin, represented by the Mozambique Mobile Zone of Holmes (1951) (Figure 5). Burke and Dewey (1972) suggest that the mobile zone in southern and eastern Africa is a broad zone of deposition and deformation representing the collision and suturing of two continents. Farther north in the Nubian-Arabian Shield, the character of rocks in the continental margin changes; island-arc type intermediate volcanic rocks predominate, ophiolite belts are present, and sialic continental basement appears to be absent (Greenwood et al., 1980; Gass, 1979; Schmidt et al., 1979).

alternative hypothesis proposed by Garson and Shalaby (1976) and Delfour (1981) suggests that rifting of an earlier cratonic margin may have occurred, and that subsequent accretion included the collision of microcontinents as well as trapped oceanic crust and island-arc complexes.

Tectonic studies in Saudi Arabia indicate that island-arc accretion occurred from west to east with the easternmost Afif terrane having continental affinity (Stoeser and Camp, 1985). Some of the sutures between accreted terranes strike northeast and should cross the Red Sea into eastern Sudan (Vail, 1985, 1983; Stoeser and Camp, 1985; Camp, 1984; Shackleton, 1986). The directions of plate convergences and the number of accretionary and orogenic events is not well known. Lateral transport and accretion of exotic terranes has not been evaluated.

Many recent workers favor the idea that several island arcs, as many as ten (Gass, 1982), comprise the Proterozoic Arabian-Nubian Shield (Almond, 1978; Shackleton, 1986; Stoeser and Camp, 1985). These concepts were developed first on the Arabian side of the shield where mapping is more complete and radiometric dating provides a clearer picture of the geochronology. Recognition of individual island-arc packets is complicated on both sides because several arcs with differing polarity and ages have been superimposed.

We see widespread evidence of island-arc activity and convergent deformation lasting from 800 to 630 m.y. followed by left-lateral wrench faulting from 630 to 600 m.y. (Figure 5). The accretionary events took place during the time preceding wrench faulting. At least two distinct batholithic island-arc terranes identified in this study accreted during this time: the Odib and Mohammed Qol terranes. Calc-alkaline and tholeiitic Nafirdeib volcanics attest to the immaturity of oceanic island-arc and back-arc-basin lithologies. The distribution of these tectonic settings is evident in the Odib terrane, but not in other areas.

Drawing on the sparse radiometric data, we see weak evidence for northwestward accretion of terranes. The Alaqui suture is somewhat younger than the Sol Hamed suture; it is further west. The available radiometric ages for the Nafirdeib series are tightly clustered at 720 to 700 m.y. over a wide area of the northern Red Sea Hills of Sudan, and do not give clues to dinsinguish separate arc ages. The syntectonic granite ages likewise do not imply distinctly different ages for the arcs.

Continental fragments apparently are not present in the northern Red Sea Hills. All areas of higher-grade metamorphism can be explained by proximity to batholiths. Crustal growth was by incorporation of oceanic-type crust and oceanic arcs.

The Nubian Shield appears to have grown rapidly by accretion of oceanic arcs and crust. Island-arc activity and accretion took place throughout the area between 800 and 630 m.y. as a distinct event in the evolution of the Nubian-Arabian Shield.

SCALE: 1:4,000,000

BECHTEL
SAN FRANCISCO

TECTONIC MAP OF THE NORTHERN RED SEA HILLS, SUDAN

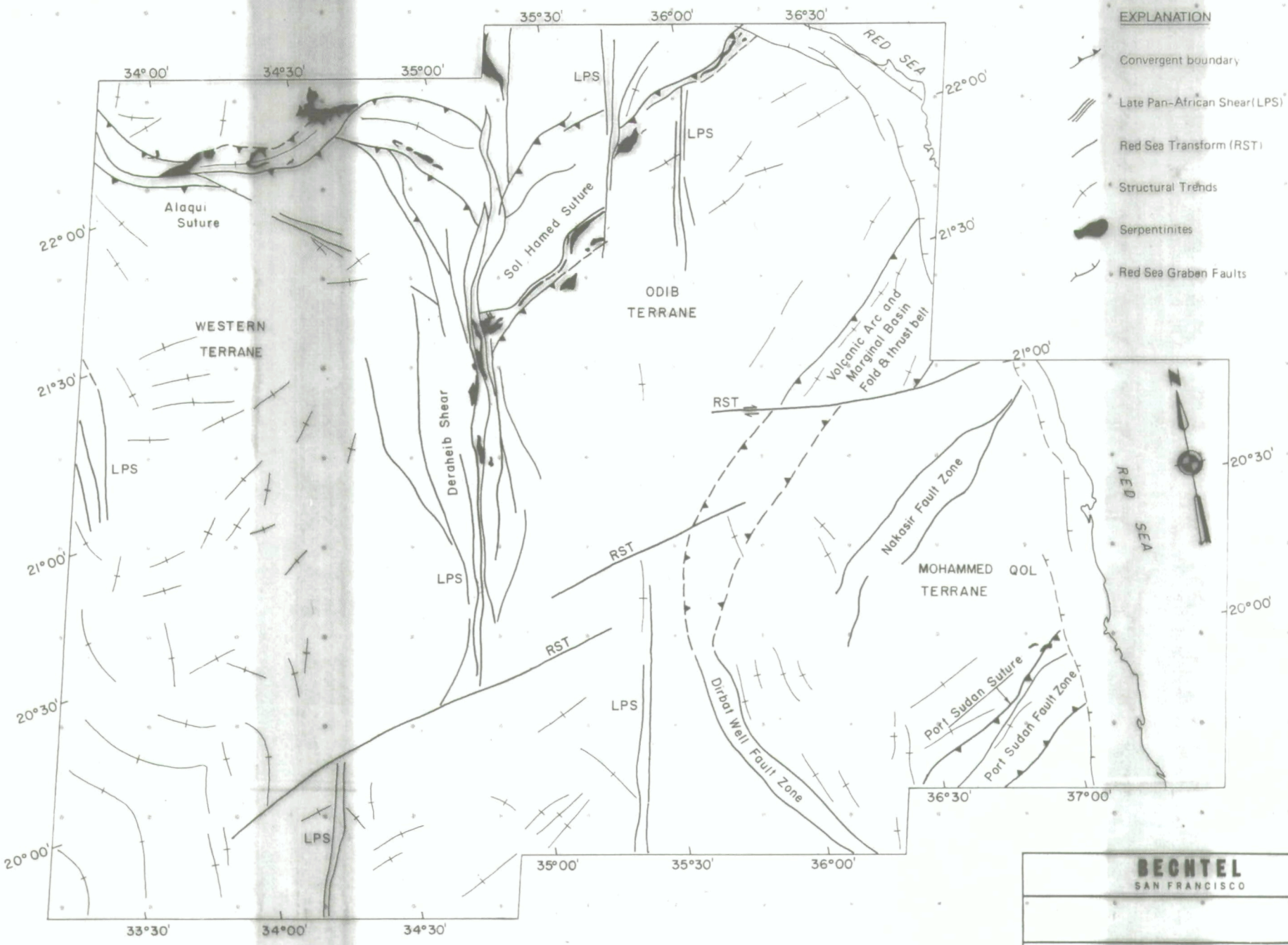

SCALE: 1:4,000,000

BECHTEL
SAN FRANCISCO

TECTONIC MAP OF THE NORTHERN RED SEA HILLS, SUDAN

JOB No.	DRAWING No.	REV.

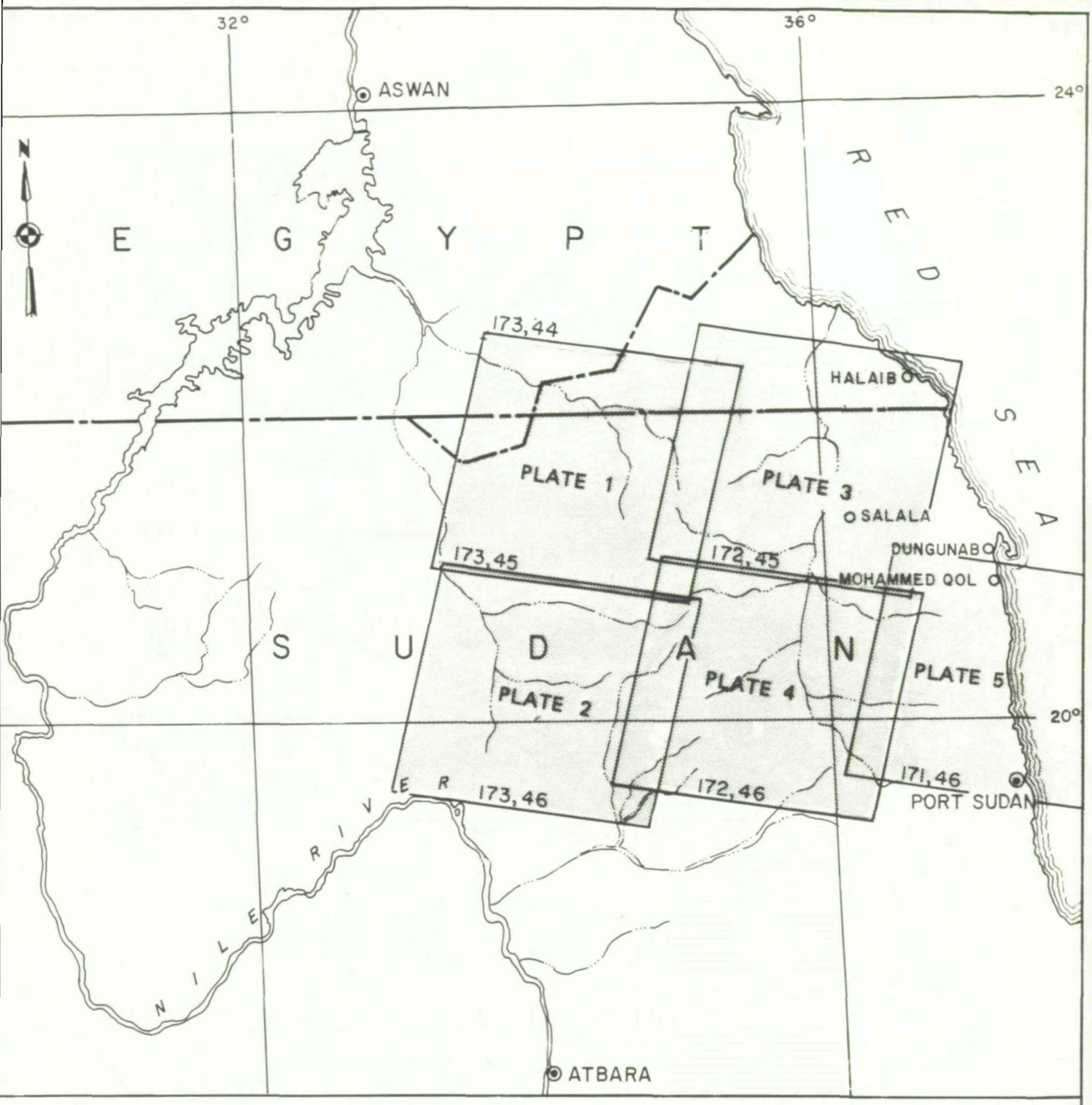

0 50 100 150 200 250

SCALE IN KILOMETERS

BECHTEL
SAN FRANCISCO

RED SEA HILLS

LOCATION MAP
TM LANDSAT SCENES

JOB No.	DRAWING No.	REV.
17835	FIGURE 2	

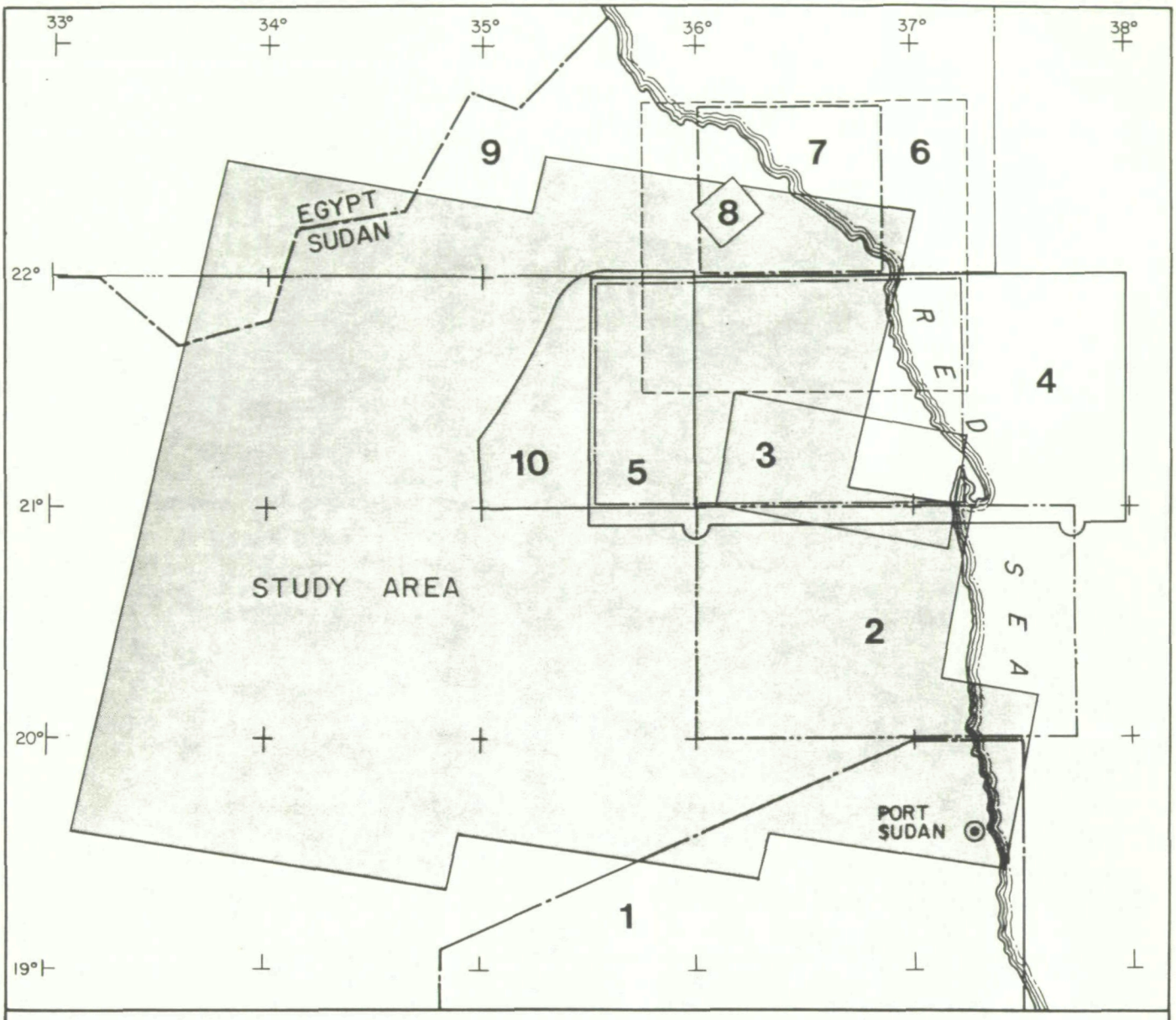

EXPLANATION

1. Aye,et al.(1985)1:3,700,000
2. Kabesh(1963 1962)!1:250,000
3. El Nadi(1984)1:250,000
4. Cavanagh(1979)(studied granites)
5. Gass(1955)1:250,000
6. Hussein(1977)1:300,000)
7. Hussein(1977)1:150,000
8. Hussein(1977)1:40,000
9. Geologic Map of Egypt (1981)1:2,000,000
10. Gabert et al.(1960)

Figure 3 Location of Previous Field Studies

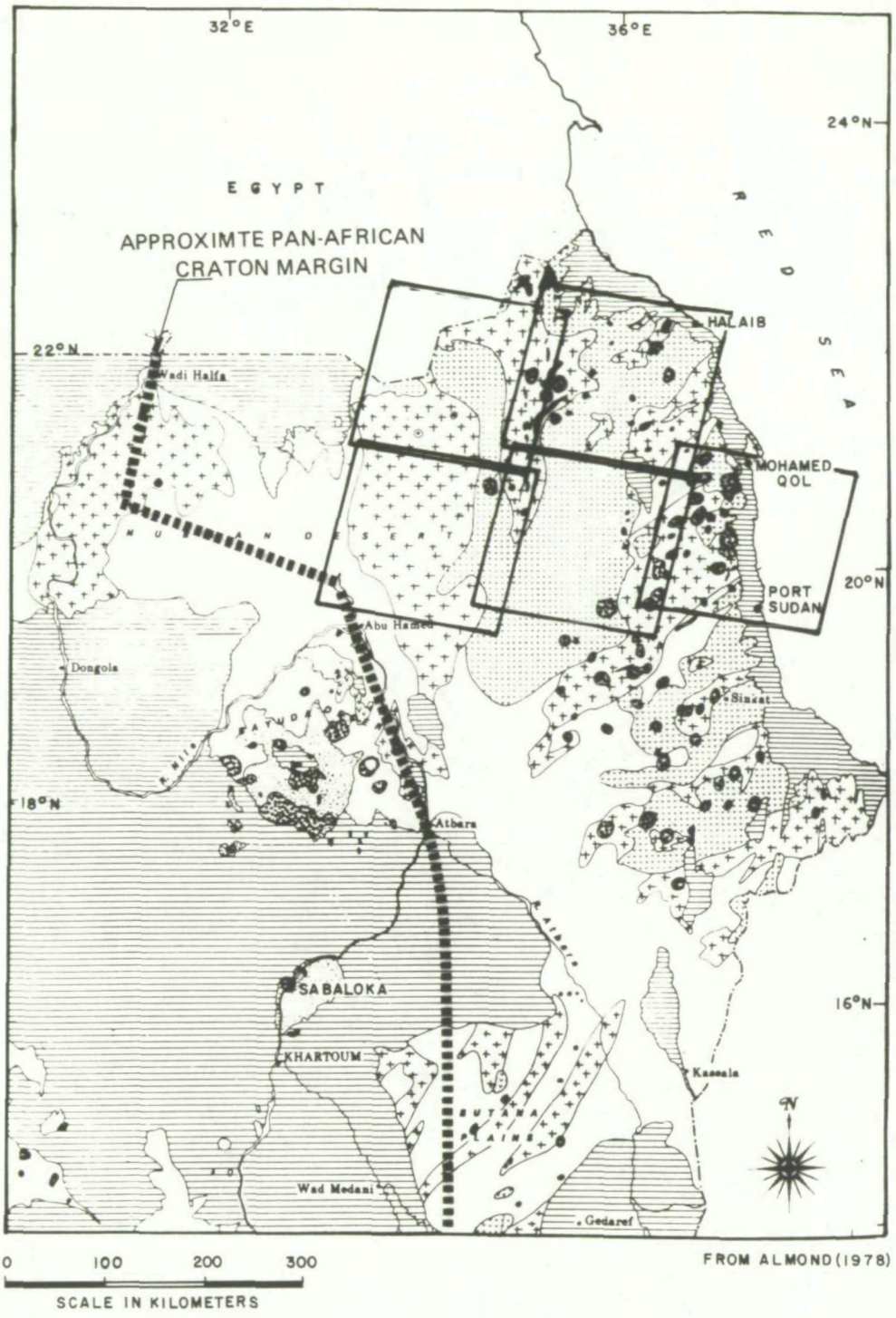

Figure 4 Generalized geologic map of northeastern Sudan. Plusses are low grade metamorphic rocks,horizontal rule is cover series,small v's are batholithic granites,dots are high grade metamorphic rocks,circular features are young ring complexes,black units are ophiolites. The continental margin complex is east of the dashed line marking the edge of the Nile craton(from El Ramly,1972 and Brown,1972).

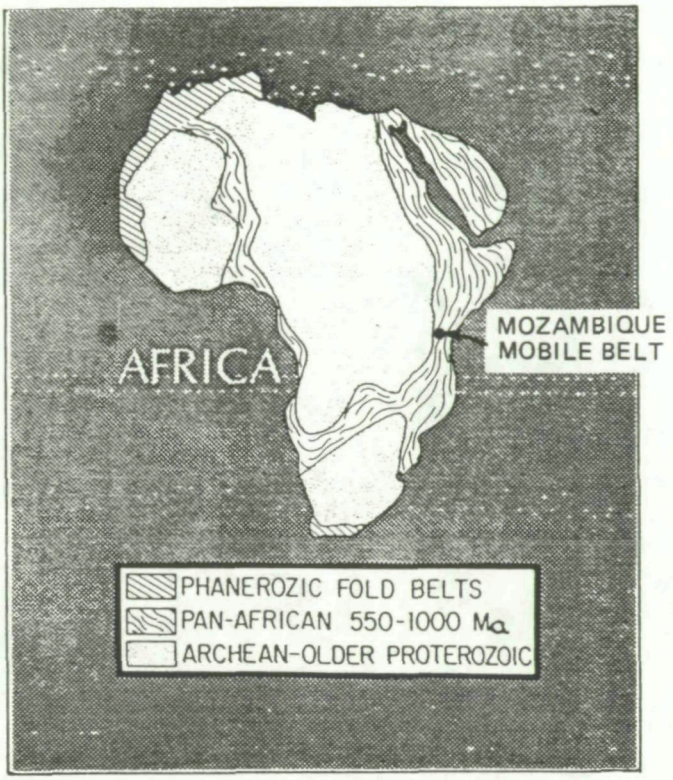

Figure 5 Distribution of Pan-African orogenic rocks and and older cratons(From Stern,1981)

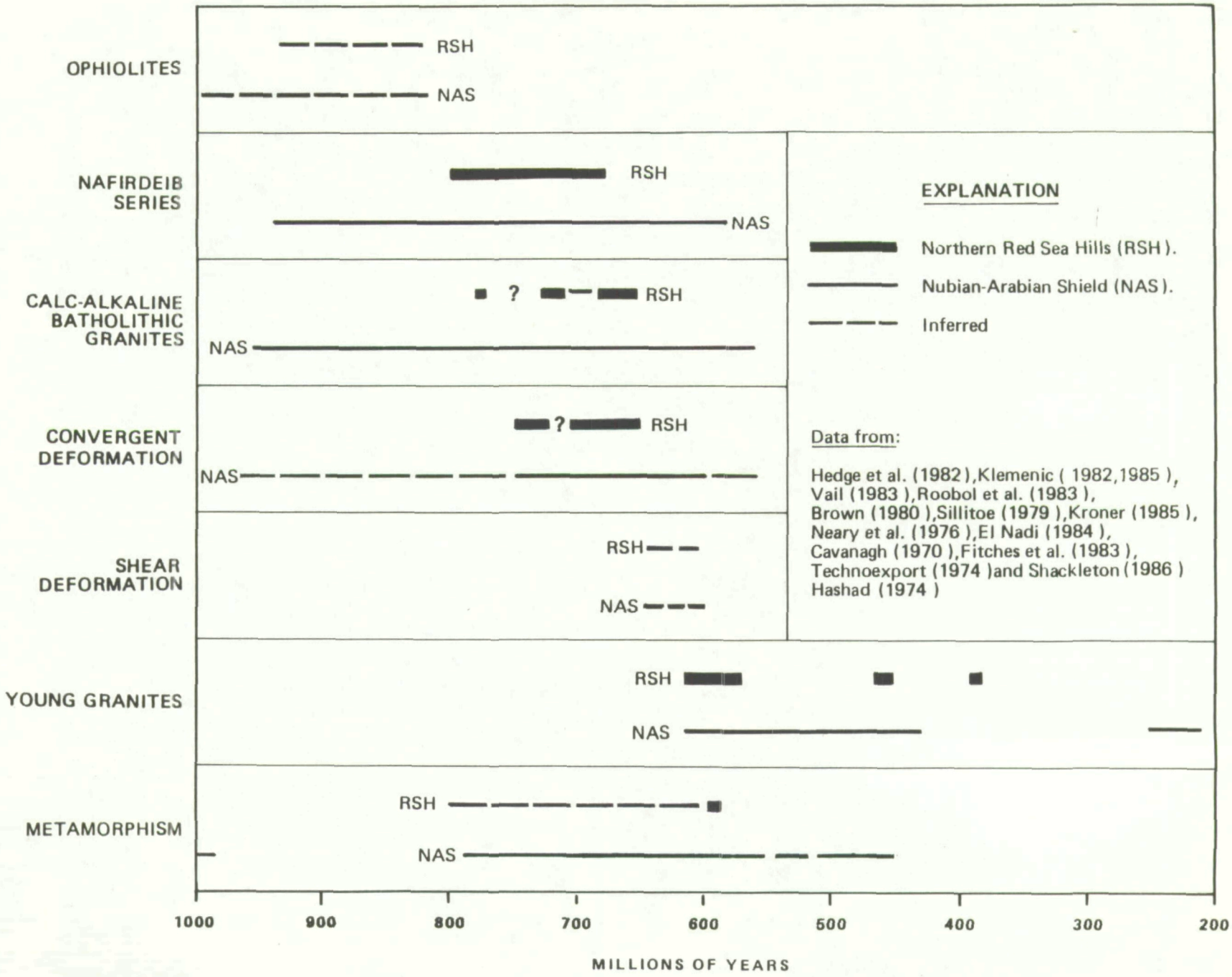

Figure 6: SUMMARY OF PAN-AFRICAN GEOCHRONOLOGY

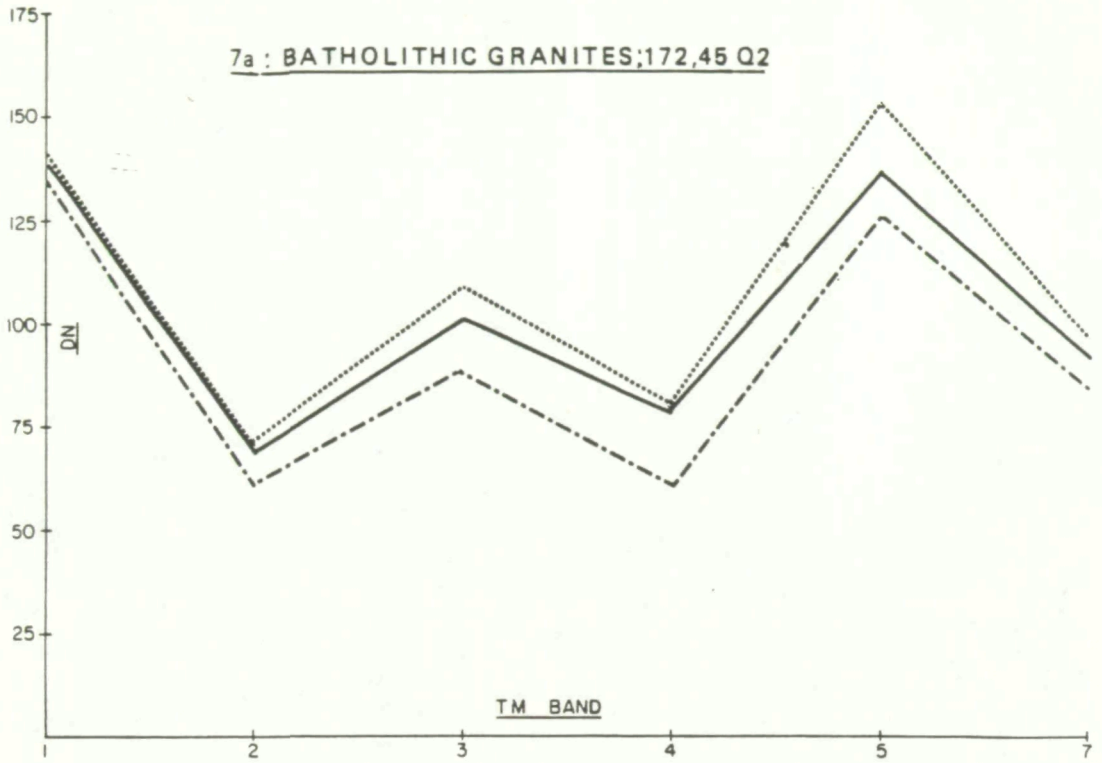

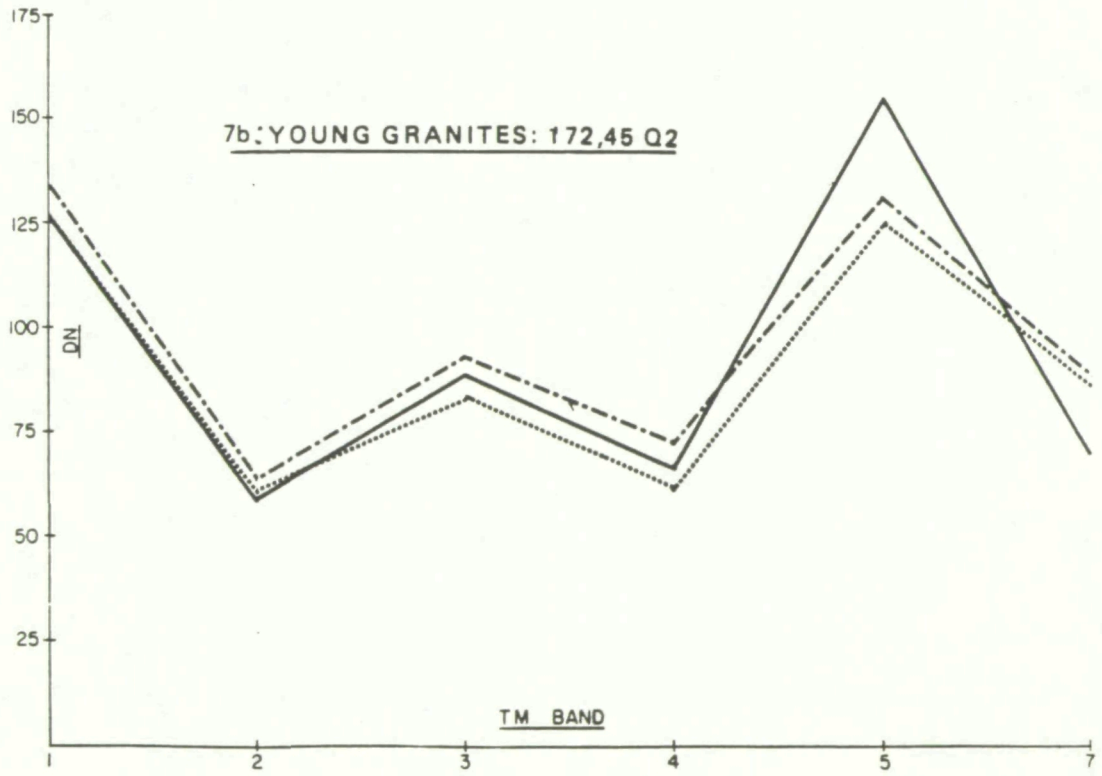

Figure 7 Sample digital number plots(not corrected for atmospheric scattering) of various lithologies

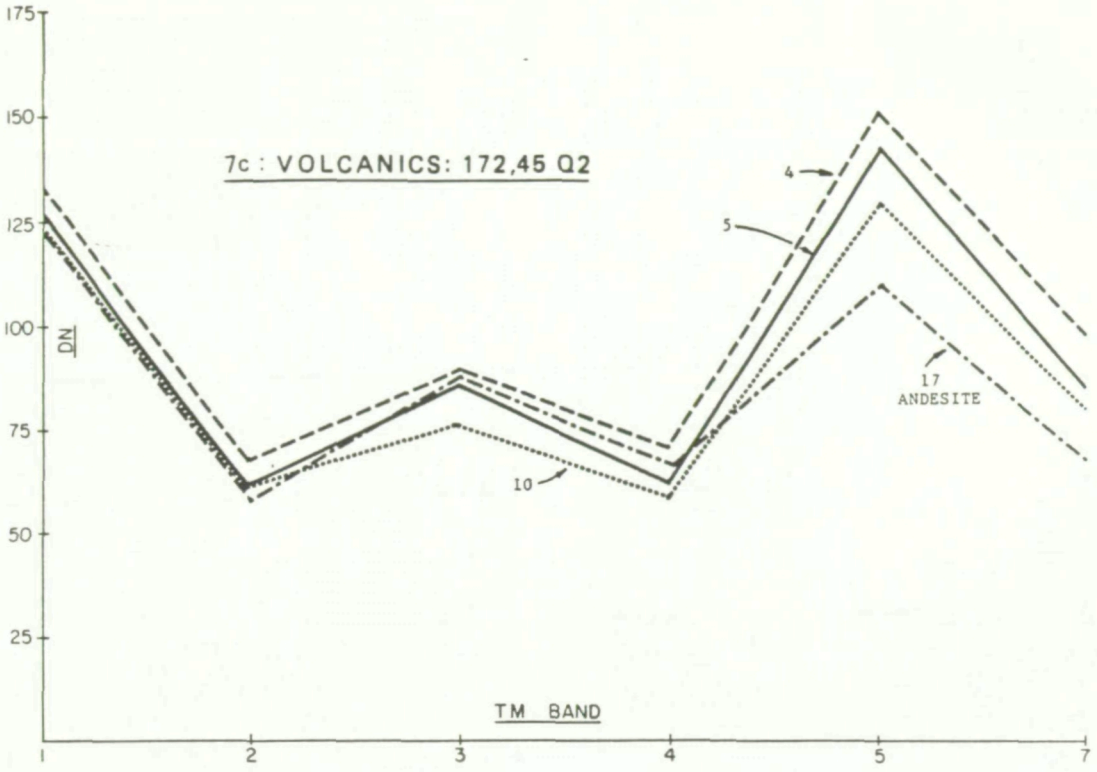
7c : VOLCANICS: 172,45 Q2
DN
TM BAND
4
5
10
17
ANDESITE
175
150
125
100
75
50
25
1
2
3
4
5
7

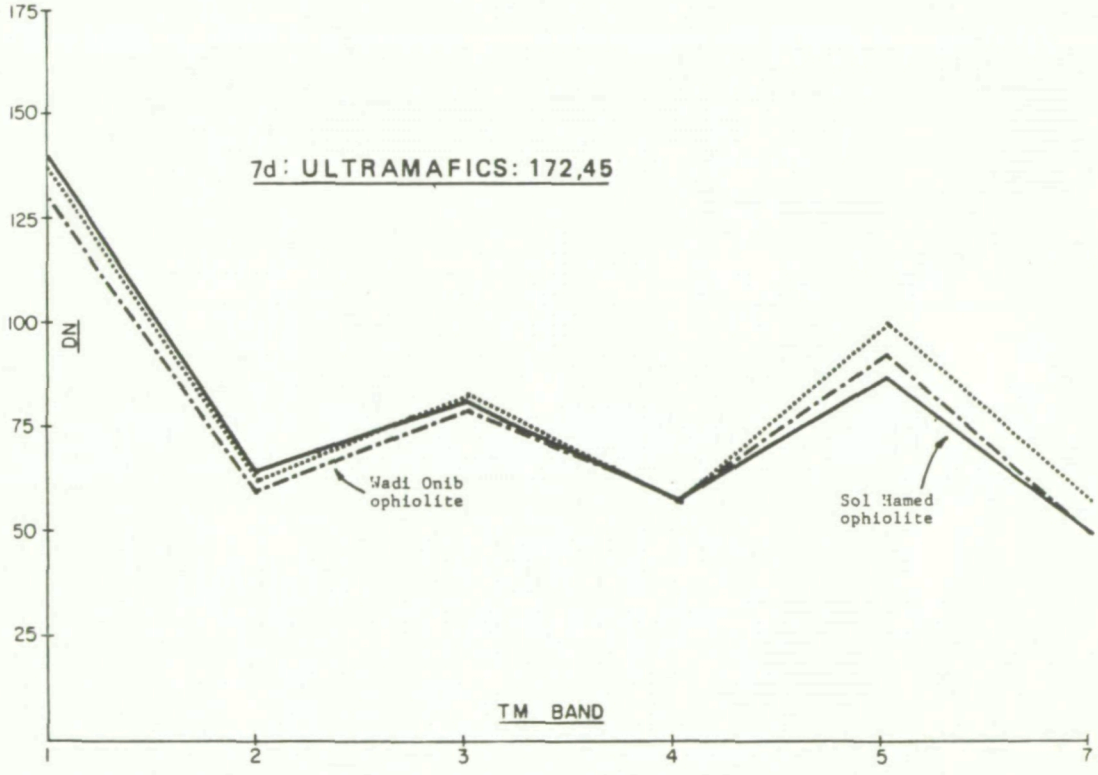
7d : ULTRAMAFICS: 172,45
DN
TM BAND
Wadi Onib
ophiolite
Sol Hamed
ophiolite
175
150
125
100
75
50
25
1
2
3
4
5
7

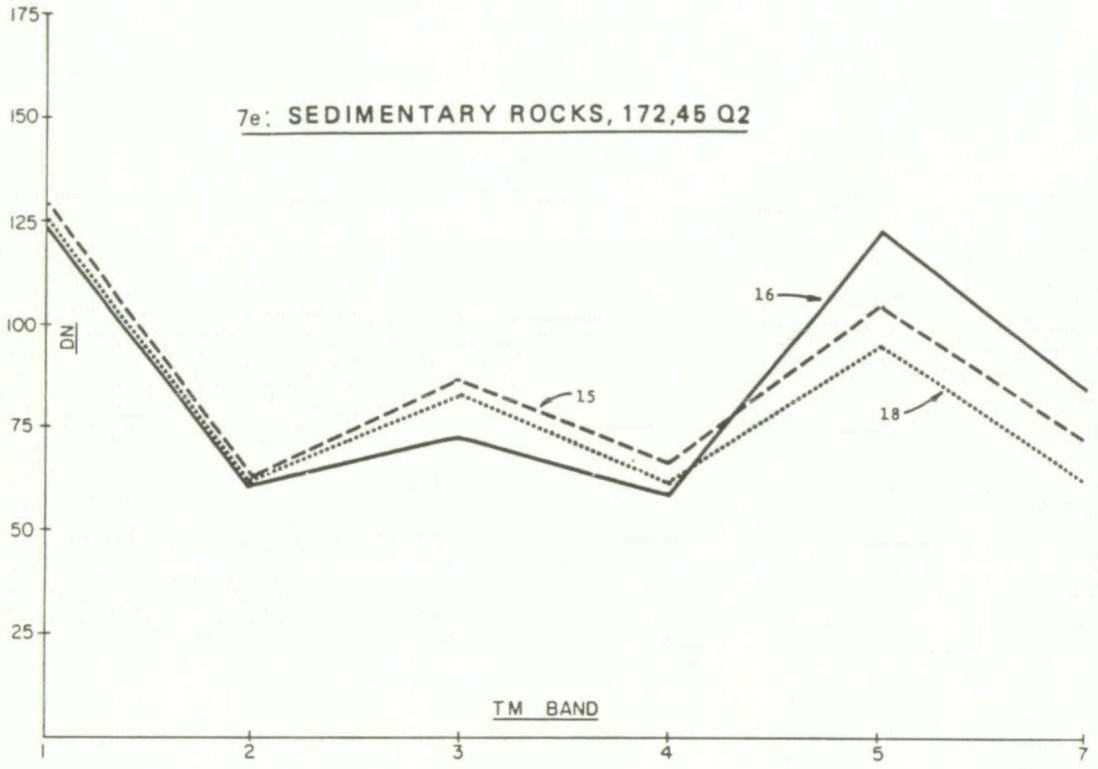
7e: SEDIMENTARY ROCKS, 172,45 Q2
175
150
125
100
75
50
25
DN
16
15
18
TM BAND
1
2
3
4
5
7

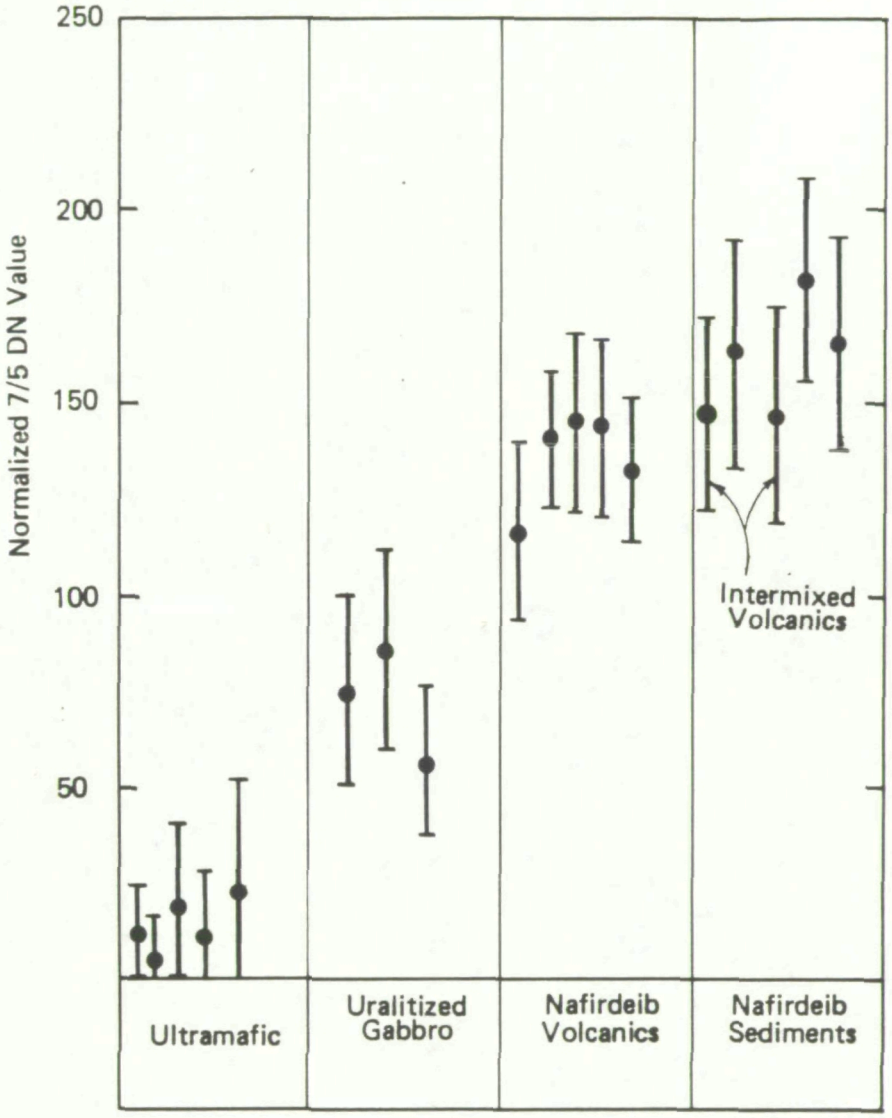

Figure 8 Sample 7/5 values from identically enhanced single ratio images illustrating split of ultramafics from other lithologies. Bars are one standard from the mean.

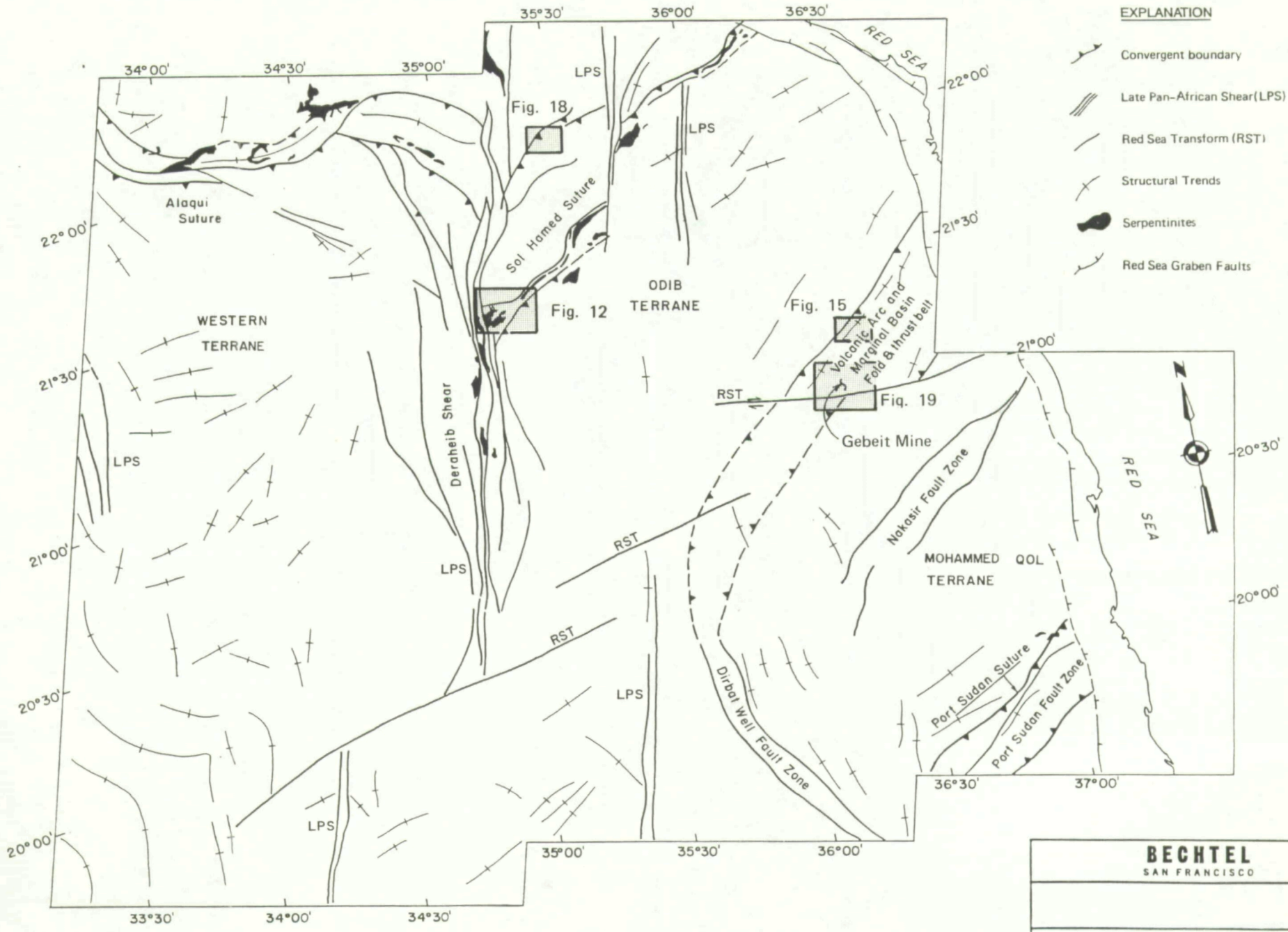

SCALE: 1:4,000,000

BECHTEL
SAN FRANCISCO

LOCATION OF SUBSCENE GEOLOGIC MAPS

JOB No.	DRAWING No.	REV.
	Figure 9	

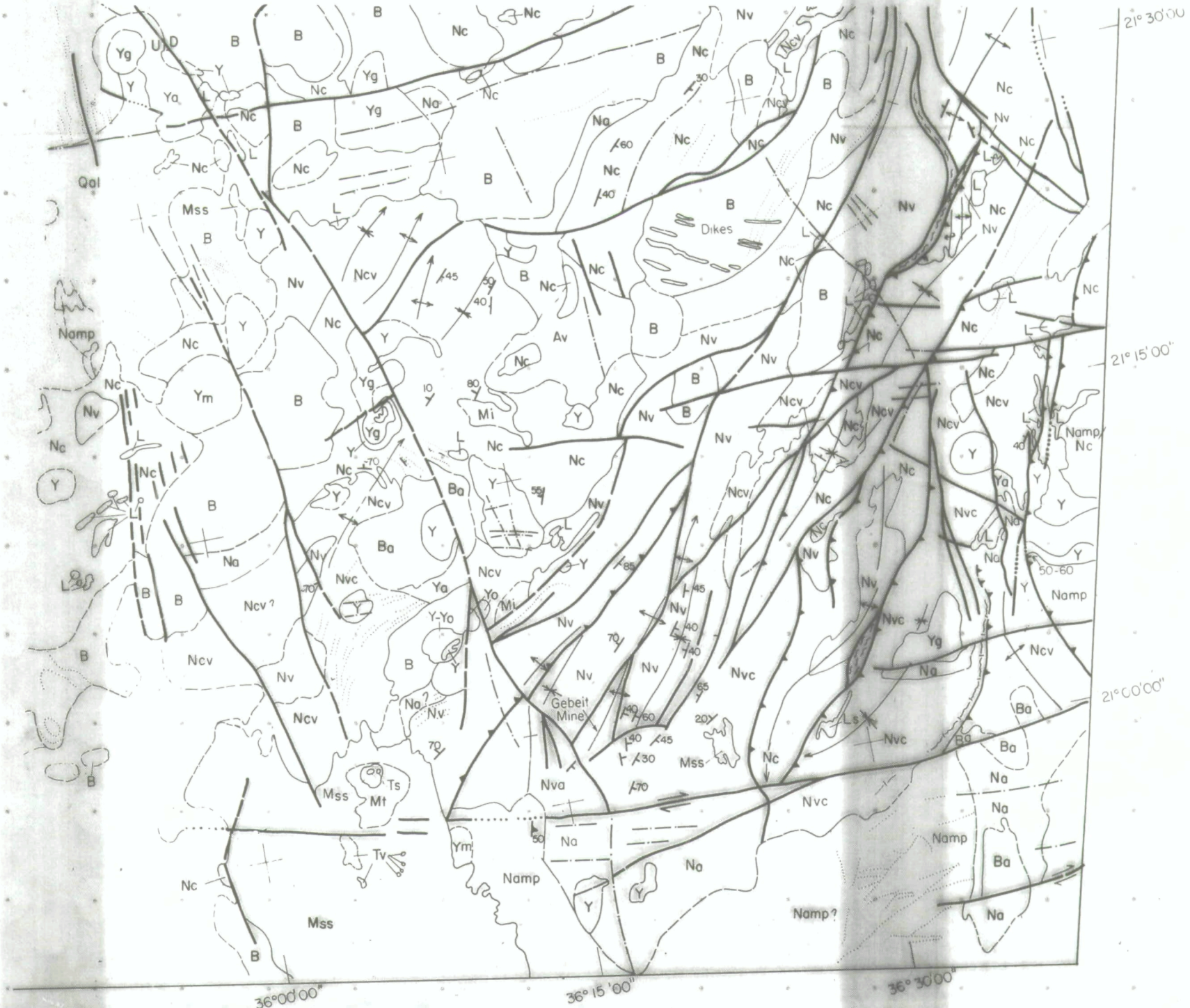
21° 30'00"
21° 15'00"
21° 00'00"
36° 00'00"
36° 15'00"
36° 30'00"
Dikes
Gebeit Mine
Qal
Namp
Mss
Ncv
Nv
Nc
Nvc
Nva
Na
Ba
Yg
Ya
Y
Ym
Mi
Av
Ts
Mt
Tv
Ls
Y-Yo
Yo
Ncv?
Na?
Namp?
Namp/Nc
50-60

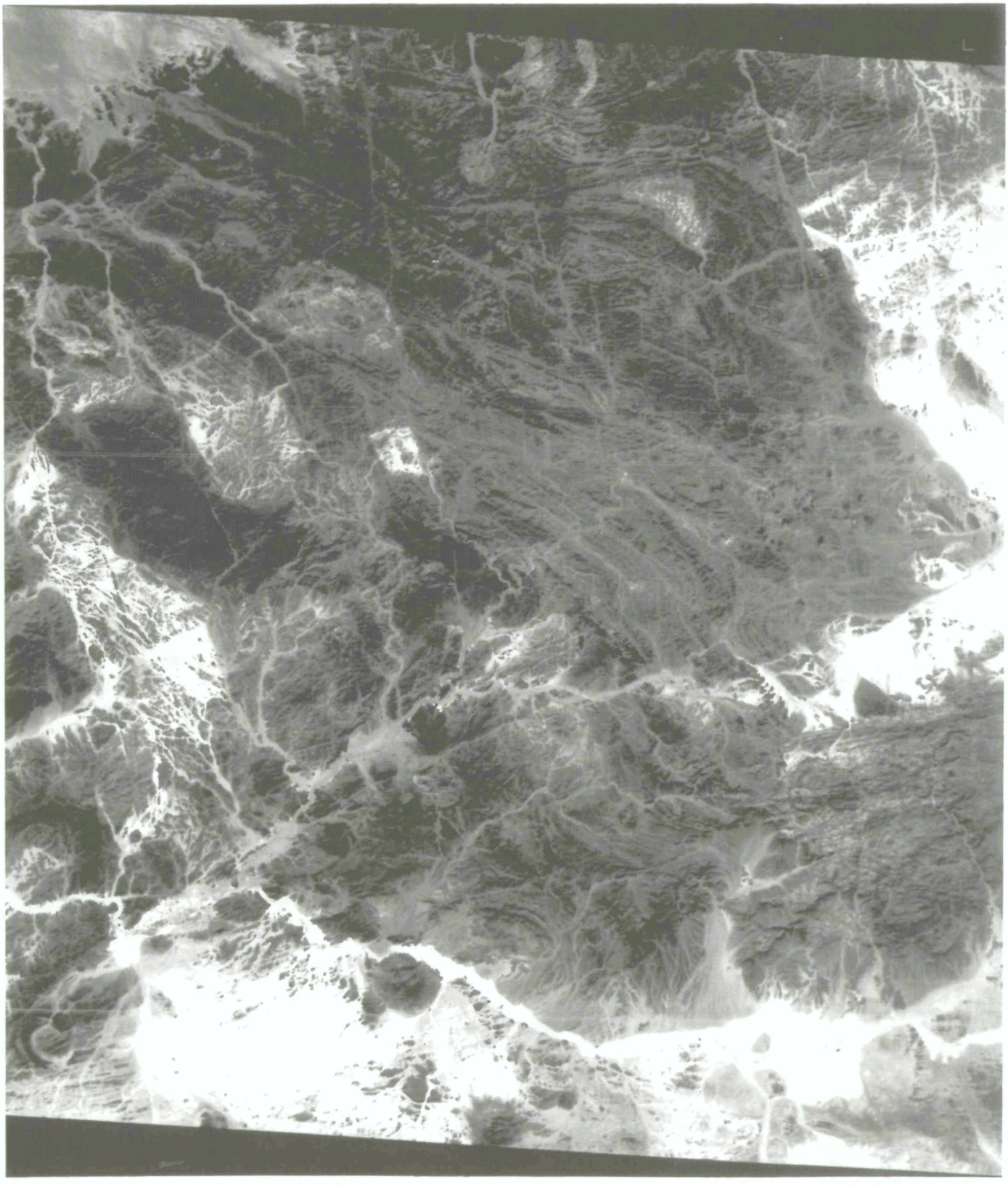

FIGURE 10 GEOLOGIC MAP OVERLAY AND 7,4,2 IMAGE; ODIB TERRANE, THE EASTERN EDGE OF THE BATHOLITH THROUGH THE MARGINAL BASIN, SCENE 172,45 Q4 (1:500,000).

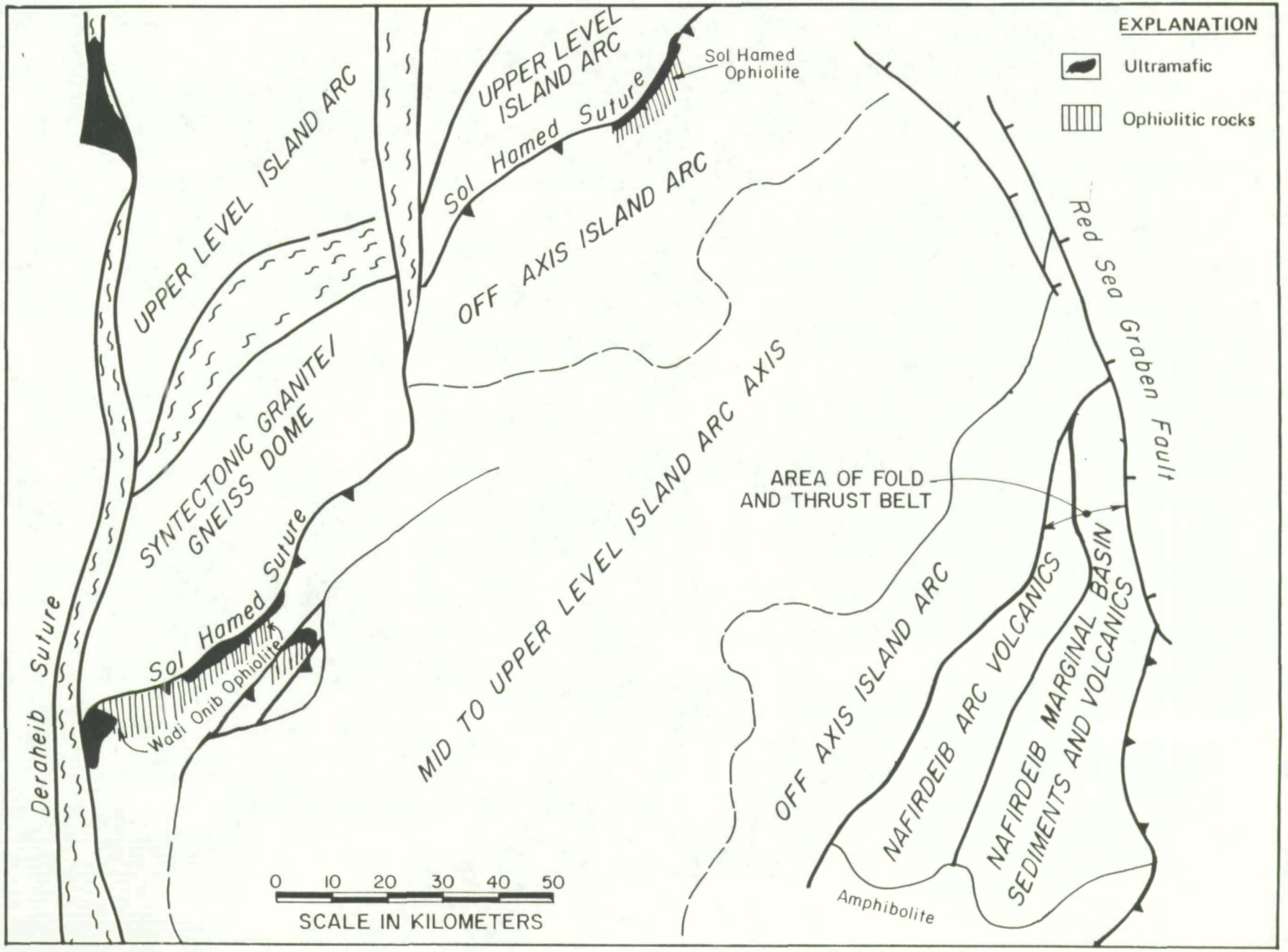

Figure II: LITHOLOGIC BELTS OF THE ODIB TERRANE, SCENE 172,45

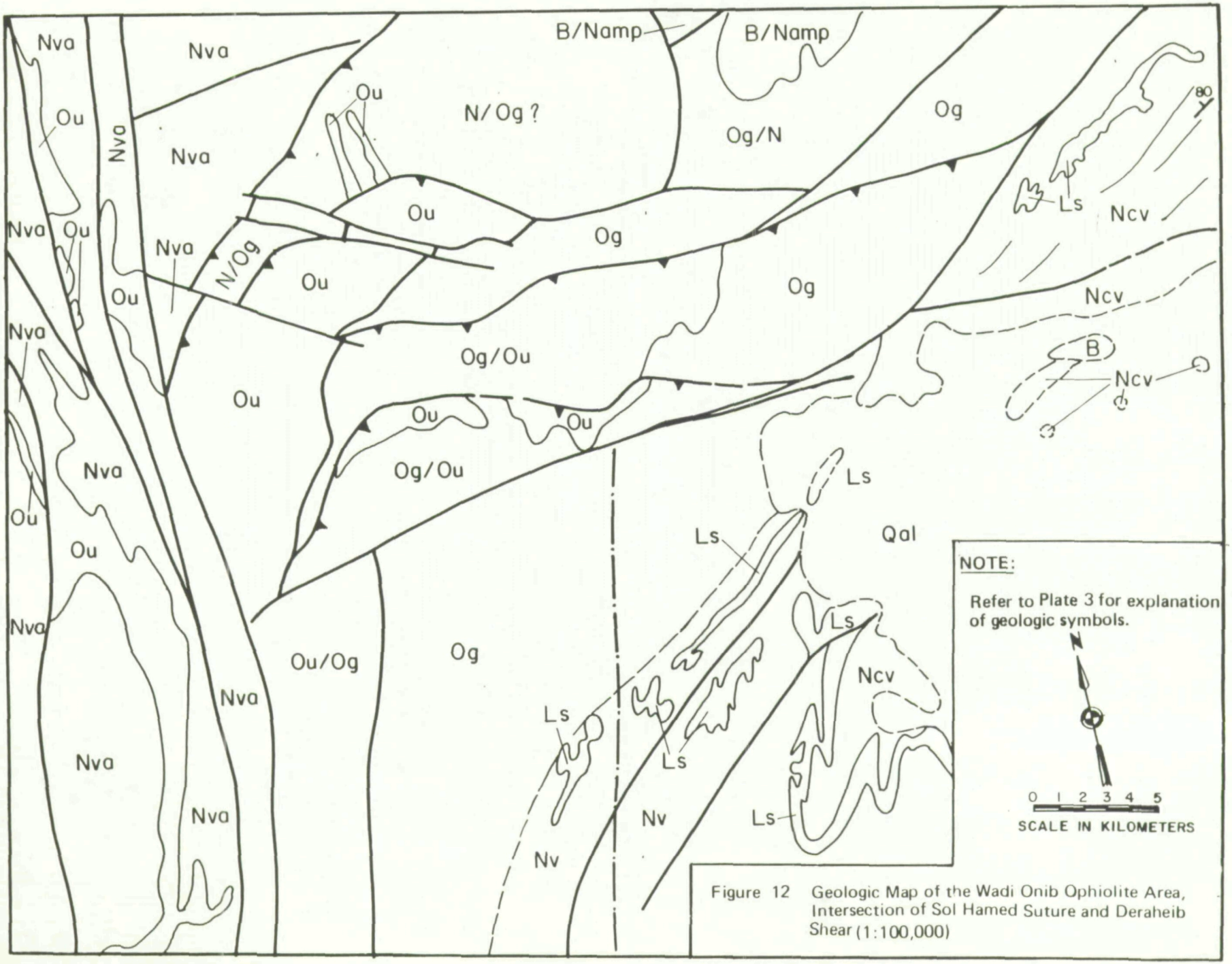

Figure 12 Geologic Map of the Wadi Onib Ophiolite Area, Intersection of Sol Hamed Suture and Deraheib Shear (1:100,000)

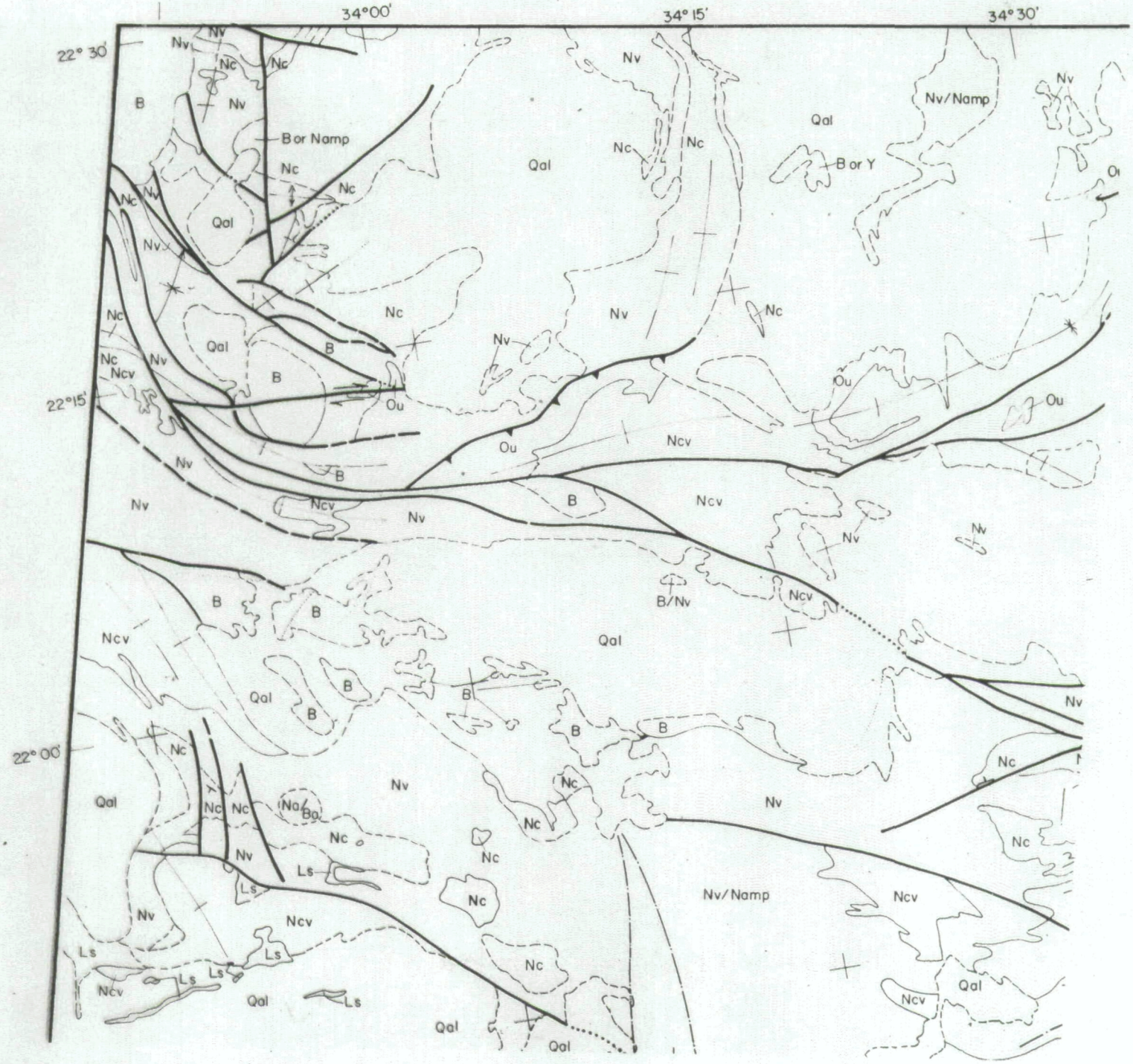
34°00'
34°15'
34°30'
22° 30'
22°15'
22°00'
Nv
Nc
B
B or Namp
Qal
Ncv
Ou
Nv/Namp
B or Y
B/Nv
Na
Ba
Ls

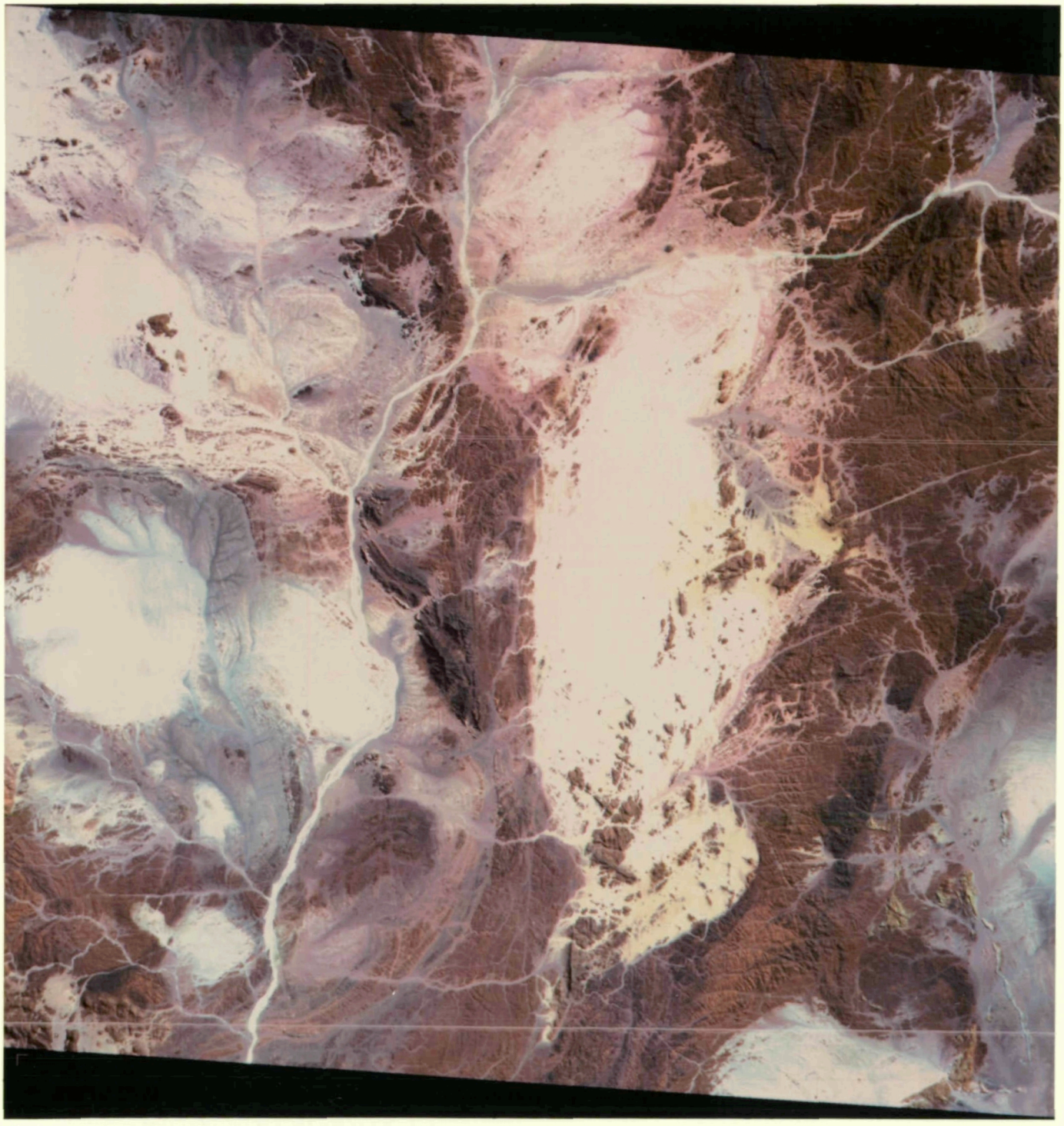

FIGURE 13: GEOLOGIC MAP AND 7,4,2 IMAGE: THE ALAQUI SUTURE ON THE NORTH MARGIN OF THE WESTERN TERRANE, 173,45 Q1 (1:500,000)

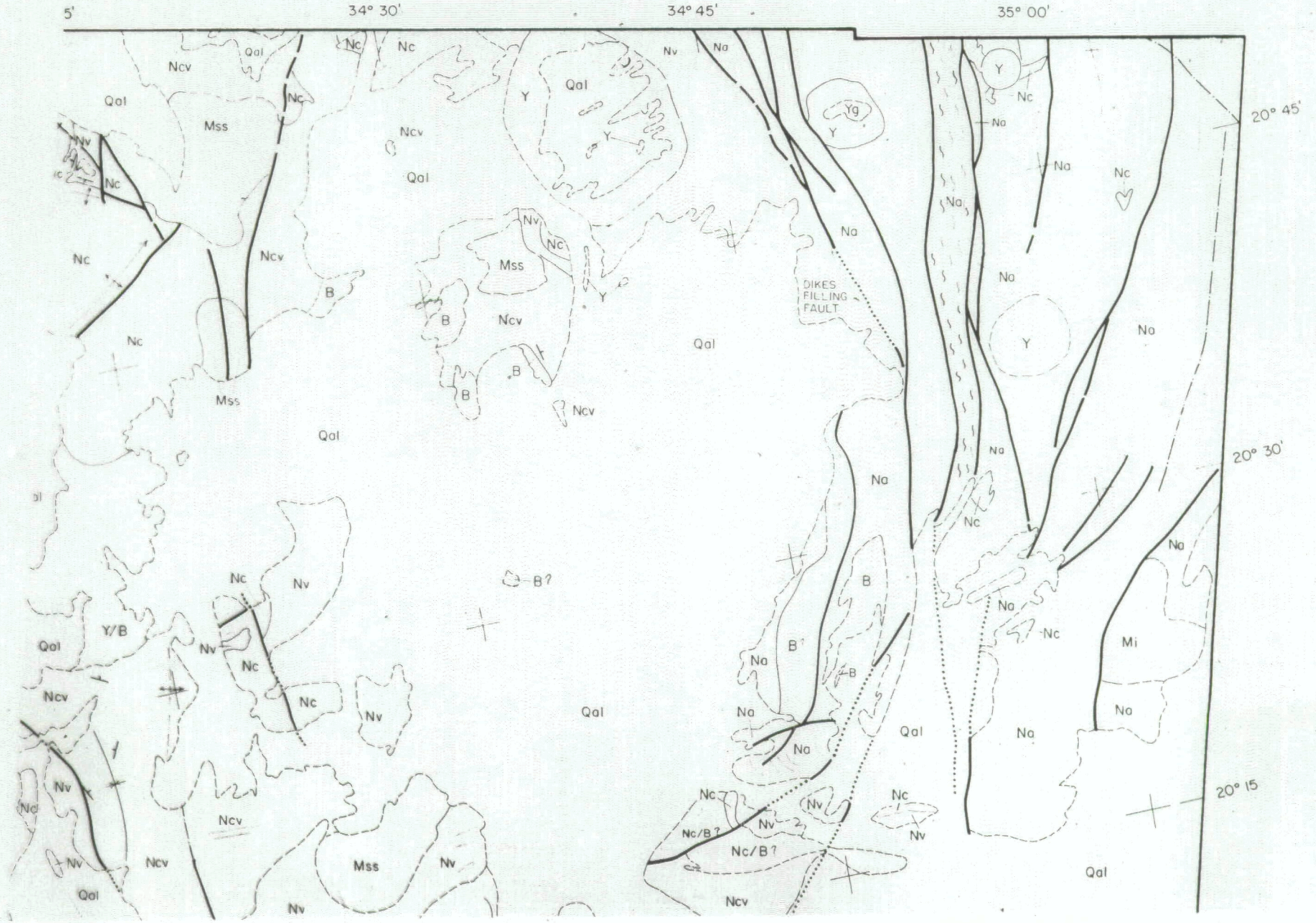
5'
34° 30'
34° 45'
35° 00'
20° 45'
20° 30'
20° 15'
Qal
Ncv
Nc
Nv
Mss
Y
Yg
B
Na
Mi
Y/B
B?
Nc/B?
DIKES
FILLING
FAULT

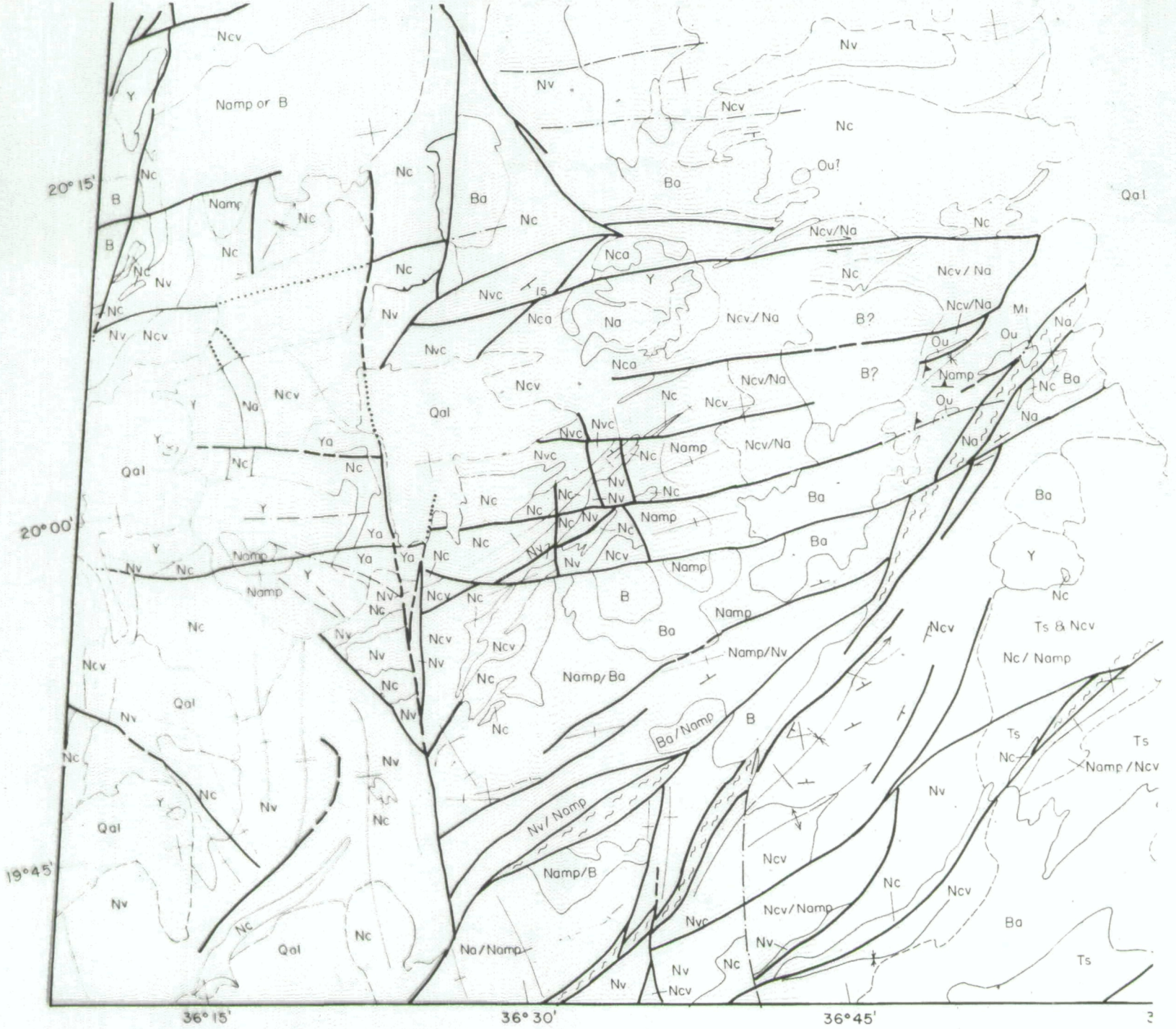
20° 15'
20° 00'
19° 45'
36° 15'
36° 30'
36° 45'
Ncv
Namp or B
Y
B
Nc
Namp
Nv
Ncv
Ba
Nvc
Nca
Na
Ncv/Na
B?
Ou?
Qal
Mi
Ou
Ya
Namp/Nv
Namp/Ba
Ba/Namp
Nv/Namp
Namp/B
Na/Namp
Ncv/Namp
Ts & Ncv
Nc/Namp
Namp/Ncv
Ts

FIGURE 14: GEOLOGIC MAP AND 7,4,2 IMAGE: THE PORT SUDAN AND NAKASIR FAULT ZONES IN THE MOHAMMED QOL TERRANE, 171,46 Q3.

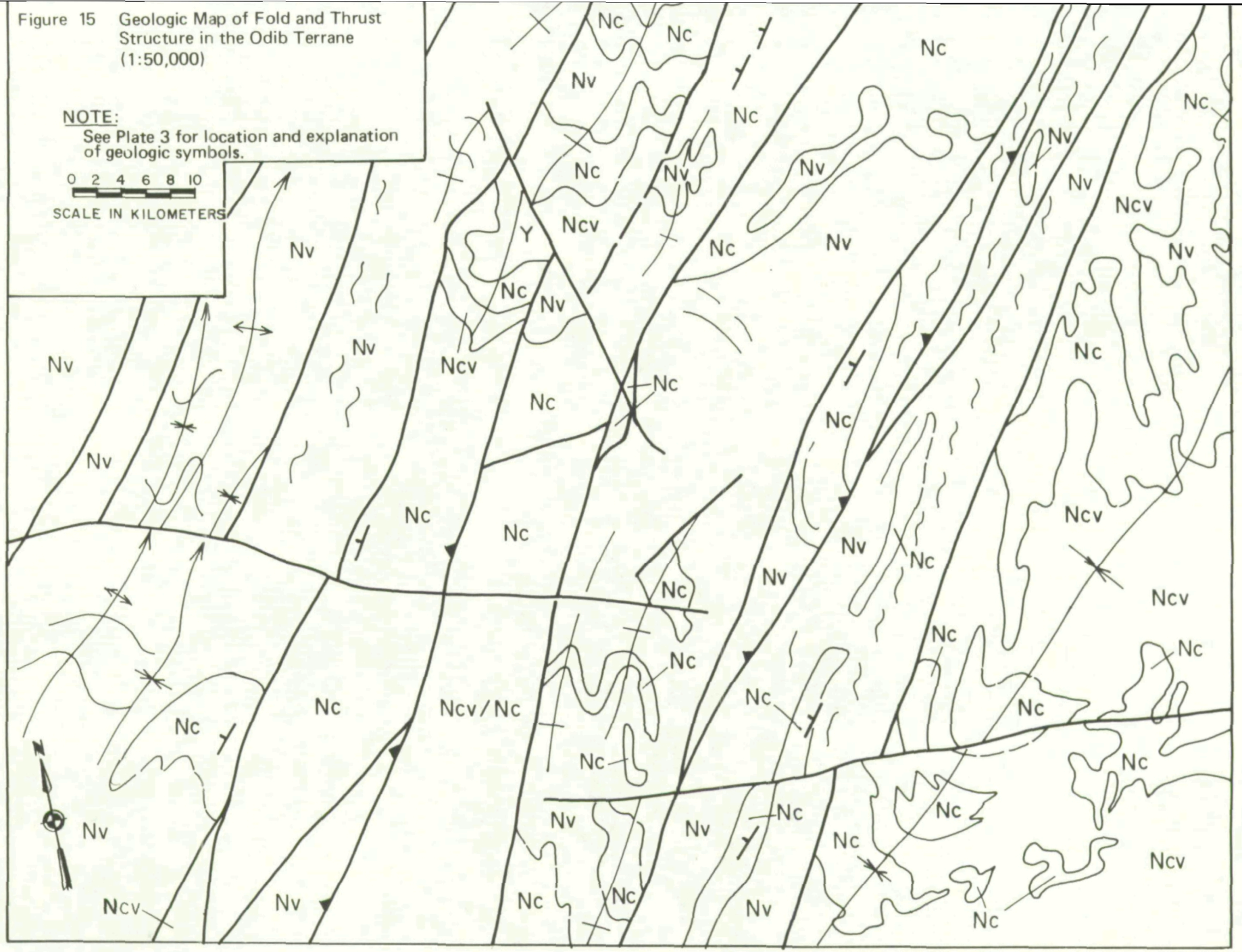

Figure 15 Geologic Map of Fold and Thrust Structure in the Odib Terrane (1:50,000)

FIGURE 16: GEOLOGIC MAP AND 7,4,2 IMAGE: SOUTHERN PORTION OF THE DERAHEIB SHEAR AND A PROMINENT YOUNG GRANITE IN THE WESTERN TERRANE, 173,46 Q2 (1:500,000).

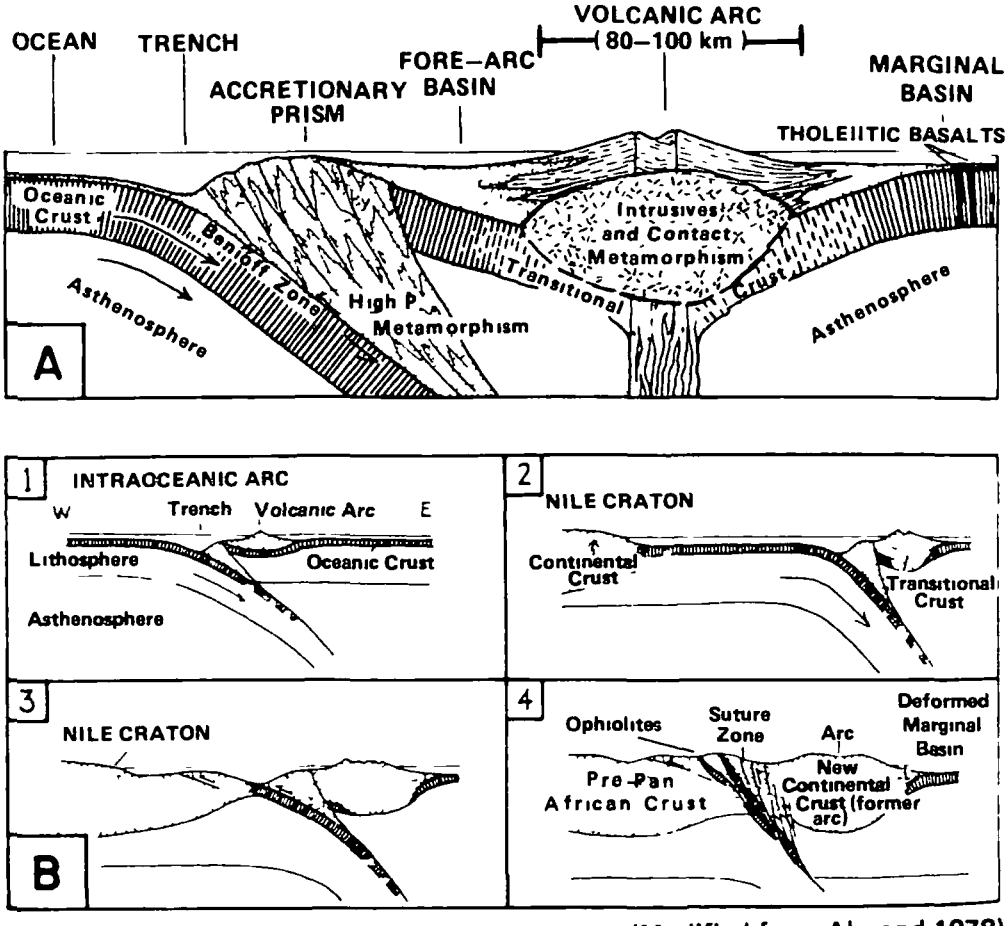

(Modified from Almond,1978)

A Schematic section across a typical Phanerozoic island arc,showing the main lithotectonic units. This distribution fits that seen in the Odib Terrane of the Red Sea Hills,Figure .

B (1,2) Development of an intra-oceanic arc. Collision and emplacement of ophiolites intermixed with arc volcanics and sediments (3,4). If subduction then began from left to right,the Nafirdaib arc would be overprinted by the deformation and plutonism from the newer arc.

Figure 17 Plate Tectonic Model of Pan-African Arc Accretion

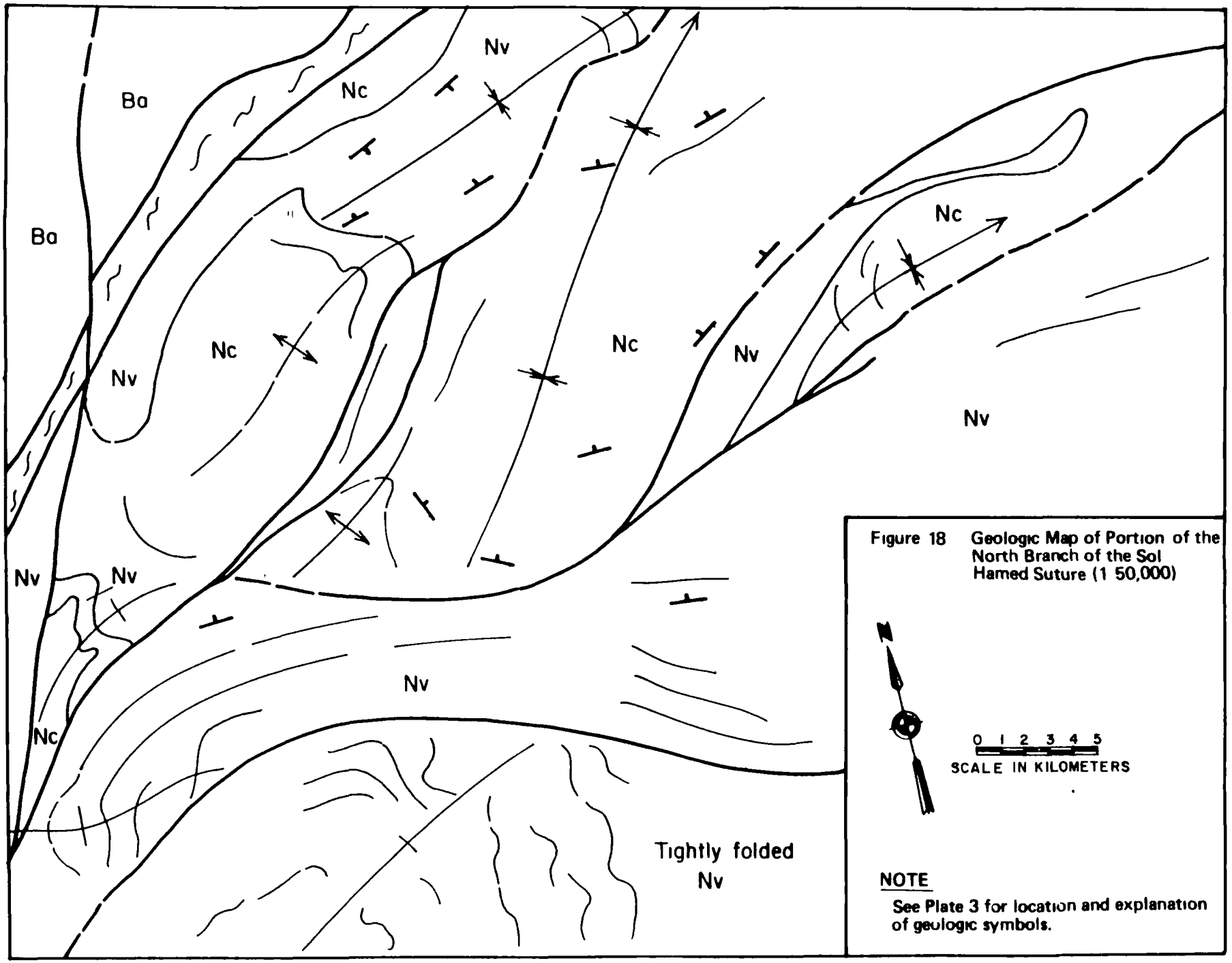

Figure 18 Geologic Map of Portion of the North Branch of the Sol Hamed Suture (1 50,000)

NOTE

See Plate 3 for location and explanation of geologic symbols.

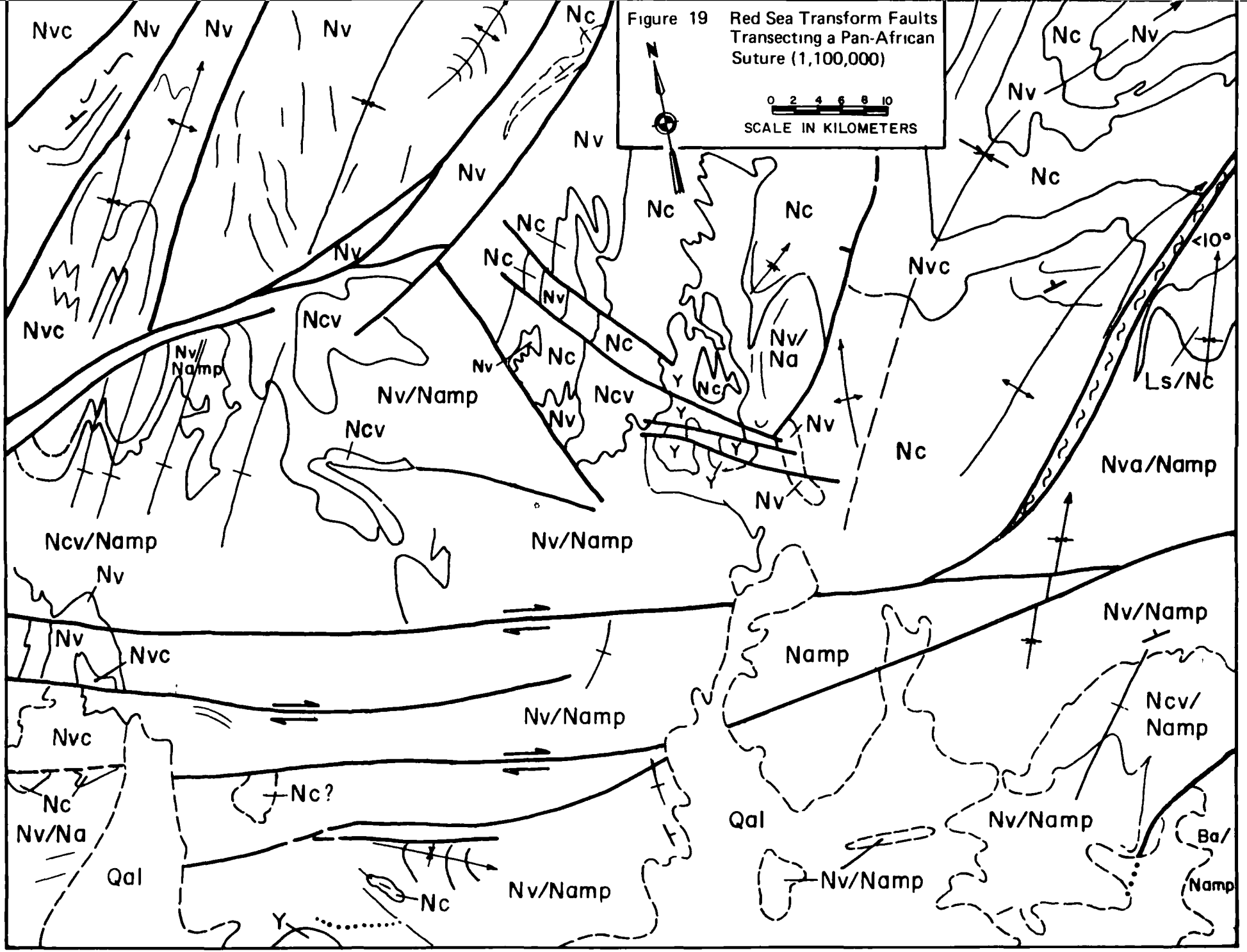
Figure 19 Red Sea Transform Faults Transecting a Pan-African Suture (1,100,000)
N
0 2 4 6 8 10
SCALE IN KILOMETERS
Nvc
Nv
Nc
Ncv
Nv/Namp
Ncv/Namp
Nv/Na
Nc?
Qal
Namp
Nva/Namp
Ls/Nc
Ba/
<10°

Section 8

REFERENCES

A

Abrams, M. J., Ashley, R. P., Rowan, L. C., Goetz, A. F. H., and Kahle, A. B., 1977. Mapping of hydrothermal alteration in the Cuprite mining district, Nevada, using aircraft scanner images for the spectral region 0.46 to 236 um, Geology, Vol. 5, p. 713-718.

Ahmed,, F., 1983. Sudan's Mineral Deposits, Mining Magazine, Vol. 148, No. 1, p. 31-35.

Ahmed, F., 1982. Implications of the Precambrian Lineaments on the Red Sea Tectonics Based on Landsat Study of Northeast Sudan, Global Tectonics and Metallogeny, Vol. 1, No. 4, p. 326-335.

Almond, D.C., 1982. The Concepts of 'Pan-African Episode Mozambique Belt' in Relation to the Geology of East and Northeast Africa, Precambrian Res., Vol. 16, No. 4, p. A4.

Almond, D.C., 1979. Younger Granite Complexes of Sudan, in Al-Shanti, A.M.S. (ed.), Evolution and Mineralisation of the Arabian-Nubian Shield, Vol. 1, King Abdul Aziz Univ., Inst. Appl. Geol. Bull. 3, Pergamon Press, Oxford-New York, p. 151-164.

Almond, D. C., 1978. New Ideas on the Geological History of the Basement Complex of North-East Sudan, Sudan Notes and Records, Vol. LIX, p. 106.

Al-Shanti, A.M.S., and Roobol, M.J., 1979. Some thoughts on Metallogenesis and Evolution of the Arabian - Nubian Shield Inst. of Applied Geology (I.A.G. Bulletin #3) King Abdul Aziz Univ., Jeddah, Kingdom of Saudi Arabia, Evolution and Mineralisation of the Arabian-Nubian Shield, p. 87-96.

Aye, F., Cheze, Y., and El Hindi, M.A., 1985. Discovery of a Major Massive Sulphide Province in Northeastern Sudan, in Prospecting in Areas of Desert Terrain, London, The Institution of Mining and Metallurgy, p. 43-48.

B

Bechtel, 1983A. Applications of Remote Sensing Techniques to Mineral Exploration in the Republic of the Sudan, 48 p, unpublished report.

Bechtel, 1983B. A Comparative Study Between Minealization in Western Saudi Arabia and Northeastern Sudan, 45 p, unpublished report.

Bentor, Y. K., 1985, The Coastal Evolution of the Arabo-Nubian Massif with Special Reference to the Sinai Peninsula, Precambrian Research, Vol. 28, p. 1-74.

Blodget, H. W. and Brown, G. F., 1982. Geological Mapping by Use of Computer-enhanced Imagery in Western Saudi Arabia: U.S. Geologic Survey Professional Paper 1153, 10 p.

Blodget, H. W., Gunther, F. J., and Podwysocki, M. H., 1978. Discrimination of Rock Classes and Alteration Products in Southwestern Saudi Arabia with Computer-Enhanced Landsat Data, NASA Technical Paper 1327, 34 p.

Burke, K. and Dewey, J. F., 1972, Orogeny in Africa, in African Geology, eds. Dessauvagie, T. F. and Whitemar, A. J., Ibadar University Press, pp. 583-608.

C

Camp, V. E., 1984. Island Arcs and Their Role in the Evolution of the Western Arabian Shield, Geol. Soc. Am. Bull., Vol. 95, No. 8, p. 913-921.

Cavanaugh, B. J., 1979. Rb/Sr Geochronology of Some Pre-Nubian Igneous Complexes of Central and Northeastern Sudan, Unpublished Ph.D. thesis, University of Leeds.

Chavez, P.S., Jr., Guptill, S.C., and Bowell, J.A., 1984. Image Processing Techniques fo Thematic Mapper Data, Proc. Amer. Soc. of Photogrammetry Conf., Wash., D.C.

D

Dawoud, A.S., 1982. Mozambiquan and Pan-African Events in Part of the Nubian Shield, North Nile Province, Sudan, Univ. Khartoum, Khartoum, SUDAN.

D

Delfour, J., 1981. Geologic, Tectonic and Metallogenic Evolution of the Northern Part of the Precambrian Arabian Shield: BRGM (France) Section II, Geologie des Gites Mineraux, Number 2, p. 1-20.

E

El-Nadi, A. H., 1984. The Geology of the Late Precambrian Metavolcanics, Red Sea Hills, Northeast Sudan, University of Nottingham, PhD. Thesis, 245 p.

El Ramly, M. F., 1972. A New Geological Map of the Basement Rocks in the Eastern and Southwestern Deserts of Egypt, Geol. Survey Egypt Annals, Vol. 2, p. 1-18, Scale 1:1000,000.

Embleton, J. C. B., Hughes, D. J., Klemenic, P. M., Poole, S. and Vail, J. R., 1982. A New Approach to The Stratigraphy and Tectonic Evolution of the Red Sea Hills, Sudan, Precambrian Research, Vol. 16, No. 4, p. A19 (Abs.).

F

Fitches, W. R., Graham, R. M., Hussein, I. M., Ries, A. C., Shackleton, R. M., and Price, R. C., 1983. The Late Proterozoic Ophiolite of Sol Hamed, N.E. Sudan, Precambrian Research, Vol. 19, p. 385-411.

Fleck, R. J., Coleman, R. G., Cornwall, H. R., Greenwood, W. R., Hadley, D. G., Schmidt, D. L., Prinz, W. C. and Ratte, J. C., 1976. Geochronology of the Arabian Shield, Western Saudi Arabia: K-Ar Results, Geological Soc. Amer. Bulletin, Vol. 87, p. 9-21.

G

Gabert, V. G., Ruxton, B. P. and Venzlaff, H., 1960. Uber Untersuchungen in Kristallin der Nordlichen Red Sea Hills in Sudan, Geologisches Jahrbuch, Band 77, p. 241-270.

Garson, M. S., and Shalaby, I. M., 1976. Precambrian-Lower Paleozoic Plate Tectonics and Metallogenesis in the Red Sea Region, Geol. Assoc. of Canada, Special Paper No. 14, p. 573-595.

G

Gass, I.G., 1982. Upper Proterozoic (Pan-African) Calc-Alkaline Magmatism in North-Eastern Africa and Arabia, in Thorpe, R.S., ed., Andesites, Orogenic Andesites and Related Rocks, Chichester, John Wiley and Sons, p. 591-609.

Gass, I. G. , 1955, The geology of the Dunganas area, Angelo-Egyptian Sudan, unpublished M. S. thesis, Universidy of Leeds, 112 pp.

Gass, I. G., 1979. Evolutionary Model for the Pan-African Crystalline Basement, in Al-Shanti, A.M.S., (ed.), Evolution and Mineralisation of the Arabian-Nubian Shelf, Vol. 1, King Abdul Aziz Univ., Inst. Appl. Geol. Bull. 3, Permagon Press, Oxford and New York, p. 11-20.

Greenberg, J. K., 1981. Characteristics and Origin of Egyptian Younger Granites, Summary, Geol. Soc. of Amer. Bull., Part I, Vol. 92, p. 224-232.

Greiling, R., Kroner, A., and El Ramly, M. F., 1984. Structural Interference Patterns and Their Origin in the Pan-African Basement of the Southeastern Desert of Egypt, in Kroner, A., Grielins, R., editors, Precambrian Tectonics Illustrated, Federal Republic of Germany, E. Schweizer bartlsche Verlags-buchhandl, p. 401-412.

Greenwood, W. R., Anderson, R. E., Fleck, R. J., and Roberts, R. J., 1980. Precambrian Geologic History and Plate Tectonic Evolution of the Arabian Shield, DGMR Mineral Resources Bulletin 24, 35 p.

Guennoc, P. and Thisse, Y., 1982, Genese de l'ouverture de la Mer Rouge et des mineralisations des fosses axiales, Documents du B.R.G.M. no. 51, France.

H

Hall, S. A., Anderson, R. E. and Girdler, R. W., 1977, Total intensity magnetic anomaly map of the Red Sea and adjacent coastal areas, a description and preliminary interpretation, in Red Sea Research 1970-1975, Saudi Arabian, Dir. Gen. Miner. Res. Bull. 22, p. F1-F15.

H

Harris, N.B.W., 1982. The Petrogenesis of Alkaline Intrusives from Arabia and Northeast Africa and Their Implications for Within-plate Magmatism, Tectonophysics, Vol. 83, p. 243-258.

Hashad, A. J., 1979, Present Status of Geochronological data on the Egyptian basement complex, in Evolution and Mineralization of the Nubian-Arabian Shield, Vol. 3, p. 31-46.

Hashad, A. H., 1978, Present status of geochronological data on the Egyptian basement complex, in Evolution and Minerilization of the Arabian-Nubain Shield, editor A. M. Al-Shanti, Vol. 3.

Hepworth, J. V., 1979. Does the Mozambique Orogenic Belt Continue into Saudi Arabia?, in Al-Shanti, A. M. S. (ed.), Evolution and Mineralisation of the Arabian-Nubian Shield, Vol. 1, King Abdul Aziz Univ., Inst. Appl. Geol. Bull. 3, Pergamon Press Oxford - New York, p. 39-51.

Hollister, L. S., and Crawford, M. L., 1986. Melt-Enhanced Deformation; A Major Tectonic Process, Geology, Vol. 14, No. 7, p. 558-561.

Holmes, A., 1951, A sequence of Pre-Cambrian orogenic belts in south and central Africa. Rep. 18th session Int'l. Geol. Congr., G. B., 1948, Part 14, pp 254-269.

Hord, R.M., 1982. Digital Processing of Remotely Sensed Data. Academic Press.

Hussein, I.M., Kroner, A., and St. Dorr, 1982. Wadi Onib: A Dismembered Pan-African Ophiolite in the Red Sea Hills of the Sudan, Precambrian Research, Vol. 16, p. 452.

Hussein, J. M., 1977, Geology of the Halaib area of the northern Red Sea Hills. Sudan, with special reference to the Sol Hamed basic complex, unpublished Ph.D. thesis, Portsmouth Polytechnic, 175 pp.

K

Kabesh, M. L., 1962. The Geology of Muhammad Qol Sheet: Sudan Geological Survey Department, Memoir No. 3.

Kabesh and Afia (1959). The Wollastonite Deposit of Dirbat Well, Bull. Geol. Surv. Sudan, No. 5. 32 pp.

Klemenic, P. M., 1983, Two anorogenic intrusive complexes of the Red Sea Hills, Sudan. Rep. Act. Dept. Geol., Portsmouth Polytechnic, 8, pp. 15-19.

Klemenic, P. M., 1982, Progress report on the isotope geology and geochemistry of the Kadaweib-Shabateim area, north-east Red Sea Hills, Sudan. Rep. Act. Dept. Geol. Portsmouth Polytechnic, 9, pp. 14-19.

Kroner, A., 1985. Ophiolites and the Evolution of Tectonic Boundaries in the Late Proterozoic Arabian - Nubian Shield of Northeast Africa and Arabia. Precambrian Research, Vol. 27, p. 277-300.

Kroner, A., 1979. Pan-African Mobile Belts as Evidence for a Transitional Tectonic Regime from Intraplate Orogeny to Plate Margin Orogeny, Inst. of Appl. Geology Bull. No. 3, King Abdul Aziz Univ., Jeddah, Kingdom of Saudia Arabia, Evolution and Mineralization of the Arabian-Nubian Shield, p. 21-37.

M

Merembeck, B.F., Borden, F.Y., Podwysocki, M.H., Applegate, D.N., 1976. Application of Canonical Analysis to Multispectral Scanner Data., Proc. 14th Ann. Symposium on Computer Applications in the Mineral industries, Pennsylvania, September 1976.

N

Neary, C. R. 1978. Evolution and Mineralization of the Arabian - Nubian Shields, Mining Mag., Vol. 143, No. 7, p. 47-48.

Neary, C. R., Gass, I. G., and Cavanaugh, B. J., 1976. Granitic Association of Northeastern Sudan, Geol. Society of America Bull., Vol. 87, p. 1501-1512.

P

Podwysocki, M. H., Gunther F.J., and Blodget, H.W., 1977. Discrimination of Rock and Soil Types by Digital Analysis of Landsat Data, NASA TM X-71290, 37 p.

R

Ries, A.C., Shackleton, R.M., Graham, R.M., and Fitches, W. R., 1983. Pan-African Structures, Ophiolites and Melanges in the Eastern Desert of Egypt: A Traverse at 26°N, Journal Geol. Soc. London, Vol. 140, p. 75-95.

Ruxton, B. P., 1956. The Major Rock Groups of the Northern Red Sea Hills, Sudan, Geology Mag., Vol. 93, No. 4, p. 314-331.

S

Schmidt, D. L., Hadley, D. G., and Stoeser, D. B., 1979. Late Protezoroic Crustal History of the Arabian Shield, Southern Najd Province, Kingdom of Saudi Arabia: in "Evolution and Mineralization of the Arabian-Nubian Shield", Inst. App. Geology Bulletin 3, Vol. 2, p. 41-58.

Serencsits, C. McC., Faul, H., Foland, K.A., Hussein, A.A., and Lutz, T.M., 1981. Alkaline Ring Complexes in Egypt: Their Ages and Relationship in Time, Journal of Geophysical Research, Vol. 86, No. B4, p. 3009-3013.

Shackleton, R. M., Ries, A. C., Graham, R. H., and Fitches, W. R., 1980. Late Precambrian Ophiolitic Melange in the Eastern Desert of Egypt, Nature, Vol. 285, p. 472-474.

Shackleton, R. M., 1986. Precambrian Collision Tectonics in Africa, in Coward, M. P., and Ries, A. C., (eds), Collision Tectonics, Geological Society Special Publication No. 19, p. 329-349.

Sheffield, C., 1985. Selecting Band Combinations from Multispectral Data, Photogrammetric Engineering and Remote Sensing, Vol. 51, No. 6, p. 681-687.

Sillitoe, R. M., 1979. Metallogenic Consequences of Late Precambrian Suturing in Arabia, Egypt, Sudan and Iran, Instit. of Appl. Geol. (I.A.G. Bulletin #3); King Abdul Aziz Univ., Jeddah, Kingdom of Saudi Arabia, Evolution and Mineralization of the Arabian-Nubian Shield. p. 110-120.

S

Stern, R. J., Dixon, T. H., Golombek, M. P., Kroner, A., Manton, WI., Walter, M., and Hussein, J. M., 1986, The Hamisana Shear Zone: a major late Precambrian structure in the Red Sea Hills of Sudan, in 1986 GSA Abstracts with Programs, 99th Annual meeting, San Antonio, TX., p 763.

Stern, R. J., 1981, Petrogenesis and tectonic setting of late Precambrian ensimatic volcanic rocks, central eastern desert of Egypt, Precambian Research, v. 16, p. 195-230.

Stoeser, D. B., and Camp, V. E., 1985. Pan-African Microplate Accretion of the Arabian Shield, Geol. Soc. of America Bulletin, Vol. 96, p. 817-826.

T

Taylor, M.M., 1974. Principal Components Color Display of ERTS Imagery, Third Earth Resources Technology Satellite Symp., Washington, D.C., Section B.

Turner, F. J., 1981, Metamorphic Petrology - mineralogical, field and tectonic aspects, McGraw Hill, 524 p.

V

Vail, J. R., 1985. Pan-African (late Precambrian) Tectonic Terrains and the Reconstruction of the Arabian-Nubian Shield, Geology, Vol. 13, p. 839-842.

Vail, J. R., 1984. The Nature of the Basement Complex of the Nubian Shield in North-east Africa: Addendum, Journal of African Earth Sciences, Vol. 2, No. 4, p. 389-390.

Vail, J. R., 1983. Pan-African Crustal Accretion in North-east Africa, Journal of African Earth Sciences, Vol. 1, No. 3/4, pp. 285-294.

Vail, J. R., 1979. Outline of Geology and Mineralization of the Nubian Shield East of the Nile Valley, Sudan: in Al-Shanti, A.M.S. (ed.), Evolution and Mineralization of the Arabian-Nubian Shield, Vol. 1, King Abdul Aziz Univ., Inst. Appl. Geol. Bull. 3, Pergamon Press, Oxford - New York, p. 97-107.

V

Vail, J. R., 1978. Outline of the Geology and Mineral Deposits of the Democratic Republic of the Sudan and Adjacent Areas, Overseas Geology and Mineral Resources, No. 49, Inst. of Geolog. Sciences, London.

W

Whiteman, A. J., 1971. The Geology of the Sudan Republic, Oxford, Clarendon Press, XIV, 290 p.

Section 9

BIBLIOGRAPHY

A

Abdel-Khalek, M.L., 1979. Tectonic Evolution of the Basement Rocks in the Southern and Central Eastern Desert of Egypt, Inst. of Appl. Geology Bull. No. 3, King Abdul Aziz Univ., Jeddah, Kingdom of Saudi Arabia, Evolution and Mineralization of the Arabian Nubian Shield, p. 53-62.

Ahmed, A.A.M., 1979. General Outline of the Geology and Mineral Occurrences of the Red Sea Hills, Democratic Republic of Sudan, Ministry of Energy and Mining, Geological and Mineral Resources Department, Bull. No. 30, 69 p.

Ahmed,, F., 1983. Sudan's Mineral Deposits, Mining Magazine, Vol. 148, No. 1, p. 31-35.

Ahmed, F., 1982. Implications of the Precambrian Lineaments on the Red Sea Tectonics Based on Landsat Study of Northeast Sudan, Global Tectonics and Metallogeny, Vol. 1, No. 4, p. 326-335.

Almond, D.C., 1982. The Concepts of 'Pan-African Episode Mozambique Belt' in Relation to the Geology of East and Northeast Africa, Precambrian Res., Vol. 16, No. 4, p. A4.

Almond, D.C., 1979. Younger Granite Complexes of Sudan, in Al-Shanti, A.M.S. (ed.), Evolution and Mineralisation of the Arabian-Nubian Shield, Vol. 1, King Abdul Aziz Univ., Inst. Appl. Geol. Bull. 3, Pergamon Press, Oxford-New York, p. 151-164.

Almond, D. C., 1978. New Ideas on the Geological History of the Basement Complex of North-East Sudan, Sudan Notes and Records, Vol. LIX, p. 106.

Almond, D.C., Ahmed, F., and Dawoud, A.S., 1982. Tectonic, Metamorphic and Magmatic Styles in the Northern Red Sea Hills of Sudan, Precambrian Res., Vol. 16, No. 4, p. A4-A5.

Al-Shanti, A.M.S., and Roobol, M.J., 1979. Some thoughts on Metallogenesis and Evolution of the Arabian - Nubian Shield Inst. of Applied Geology (I.A.G. Bulletin #3) King Abdul Aziz Univ., Jeddah, Kingdom of Saudi Arabia, Evolution and Mineralisation of the Arabian-Nubian Shield, p. 87-96.

Anon., 1972. Guide to Mineral Investment in the Sudan, Rep. Geol. Survey Sudan, 44 p., Unpublished

Arnold, Guy, 1984. Sudan: Middle East Review, p. 255-259.

A

Aye, F., Cheze, Y., and El Hindi, M.A., 1985. Discovery of a Major Massive Sulphide Province in Northeastern Sudan, in Prospecting in Areas of Desert Terrain, London, The Institution of Mining and Metallurgy, p. 43-48.

B

Balkhanov, V.V., and Razvalyayev, A.V., 1979. The Origin of the Manganese Deposits of the Western Shore of the Red Sea. (In Association With Rifting), Internat. Geology Rev., Vol. 23, No. 2, p. 162-166.

Barr, D., Holdsworth, R. E., and Roberts, A. M., 1986. Caledonian Ductile Thrusting in a Precambrian Metamorphic Complex: The Moine of Northwestern Scotland, Geological Society of America Bulletin, Vol. 97, No. 6, p. 754-764.

Bechtel, 1983A. Applications of Remote Sensing Techniques to Mineral Exploration in the Republic of the Sudan, 48 p, unpublished report.

Bechtel, 1983B. A Comparative Study Between Minealization in Western Saudi Arabia and Northeastern Sudan, 45 p, unpublished report.

Bentor, Y. K., 1985, The Coastal Evolution of the Arabo-Nubian Massif with Special Reference to the Sinai Peninsula, Precambrian Research, Vol. 28, p. 1-74.

Blodget, H. W., 1977. Lithology Mapping of Crystalline Shield Test Sites in Western Saudi Arabia Using Computer-Manipulated Multispectral Satellite Data: Unpublished Ph.D. Thesis, George Washington University.

Blodget, H. W., Andre, C.G., and Marcell, R. F., 1985. Enhanced Rock Discrimination Using Landsat-5 Thematic Mapper (TM) Data, 1985 ACSM-ASPRS Fall Convention Technical Paper, Indianapolis.

Blodget, H. W. and Brown, G. F., 1982. Geological Mapping by Use of Computer-enhanced Imagery in Western Saudi Arabia: U.S. Geologic Survey Professional Paper 1153, 10 p.

Blodget, H. W., Gunther, F. J., and Podwysocki, M. H., 1978. Discrimination of Rock Classes and Alteration Products in Southwestern Saudi Arabia with Computer-Enhanced Landsat Data, NASA Technical Paper 1327, 34 p.

B

Brown, G. C., 1980. Calc-alkaline Magma Genesis: The Pan-African Contribution to Crustal Growth, in Al Shanti, A.M.S. (ed.), Evolution and Mineralisation of the Arabian-Nubian Shield, I.A.G. Bulletin 3, 3, p. 19-29.

Brown, G. F., and Jackson, R.O. 1979. An Overview of the Geology of Western Arabia, Instit. of Appl. Geology. Bull. No. 3, King Abdul Aziz Univ. Jeddah, Kingdom of Saudi Arabia, Evolution and Mineralization of the Arabian-Nubian Shield p. 3-10.

Brown, G.F., and Jackson, R.O., 1979. Geologic Map of the Asir Quadrangle, Kingdom of Saudi Arabia, U.S. Geological Survey Map I-217A, Scale 1:500,000.

Brown, G. F., Jackson, R.O., Bogue, R. G., and Elbert, E. L. Jr., 1963. Geologic Map of the Northwestern Hijaz Quadrangle, Kingdom of Saudi Arabia, U.S. Geological Survey Miscellaneous Geologic Investigations Map I-204A, Scale 1:500,000.

Brown, G. F., 1970. Eastern Margin of the Red Sea and the Coastal Structures in Saudi Arabia, Royal Society of London Philosophical Transactions, A, Vol. 267, p. 75-87.

Burke, K. and Dewey, J. F., 1972, Orogeny in Africa, in African Geology, eds. Dessauvagie, T. F. and Whitemar, A. J., Ibadar University Press, pp. 583-608.

C

Camp, V. E., 1984. Island Arcs and Their Role in the Evolution of the Western Arabian Shield, Geol. Soc. Am. Bull., Vol. 95, No. 8, p. 913-921.

Cavanaugh, B. J., 1979. Rb/Sr Geochronology of Some Pre-Nubian Igneous Complexes of Central and Northeastern Sudan, Unpublished Ph.D. thesis, University of Leeds.

Chavez, P.S., Jr., Guptill, S.C., and Bowell, J.A., 1984. Image Processing Techniques fo Thematic Mapper Data, Proc. Amer. Soc. of Photogrammetry Conf., Wash., D.C.

Chevremont, P., and Johan, Z., 1981. Complexe Intrusif Stratifie de Wadi Kamal-Wadi Murattiyah (Arabie Saoudite), Son Evolution Magmatique et Metallogenique: BRGM (France), Section II, Geologie des Gites Mineraux, Number 2, p. 21-40.

C

Cobbing, E. J., 1978, The Andean Geosyncline in Peru, and its Distinction from Alpine Geosynclines; Journal Geological Society London, Vol. 135, p. 207-218.

Connor, K. 1982. The Mineral Industry of Sudan: Minerals Yearbook, p. 845-850.

Conway, C. M., Elliott, J. E. and Stoesser, D., 1979. Mineral Belt Studies: U.S. Geological Survey, Prof. Paper 1150, 332 p.

Cortial, P., Lefevre, J. C. and Salih, H. M., 1986. Gold Deposits Related to the Volcano Sedimentary Sequence of Ariab, Sudan, In Prospecting In Areas of Desert Terrain, London, The Institution of Mining and Metallurgy, p. 155-159.

Coulomb, J. J., Felenc, J., and Testard, J., 1981. Volcanism et Mineralisations a Zn-Cu de la Ceinture d'Al Amar (Royaume d'Arabie Saoudite): BRGM (France), Section II, Geologie des Gites Mineraux, Number 2, p. 41-72.

D

Davies, F. B., 1984. Strain Analysis of Wrench Faults and Collision Tectonics of the Arabian-Nubian Shield, Journal Geol., Vol. 92, No. 1, P. 37-53.

Dawoud, A.S., 1982. Mozambiquan and Pan-African Events in Part of the Nubian Shield, North Nile Province, Sudan, Univ. Khartoum, Khartoum, SUDAN.

Dayuerman, H. J. and others, 1982. Late Proterozoic Evolution of Afro-Arabian Crust from Ocean Arc to Craton, Discussion and Reply, Geol. Soc. Am. Bull., Vol. 93, No. 2, p. 174-178.

Delfour, J., 1981. Geologic, Tectonic and Metallogenic Evolution of the Northern Part of the Precambrian Arabian Shield: BRGM (France) Section II, Geologie des Gites Mineraux, Number 2, p. 1-20.

Delfour, J., 1976. Comparative Study of Mineralization in the Nubian and Arabian Shields, DGMR Mineral Resources Bulletin 15, 22 p.

Dodge, F.C.W., and Rossman, D.L., 1975. Mineralization in the Wadi Qatan Area, Kingdom of Saudi Arabia, U.S. Geological Survey Saudi Arabian Project Report 190, 71 p.

D

Drysdall, A. R., Ramsay, C. R., and Stoeser, D. B., eds., 1986. Felsic Plutonic Rocks and Associated Mineralization of the Kingdom of Saudi Arabia, Journal of African Earth Sciences, Special Volume, Vol. 4.

E

El Boushi, I. M., 1972. Geology of the Gebeit Gold Mine, Democratic Republic of Sudan, Economic Geology, Vol. 67, No. 4, p. 481-486.

El-Gaby, S., 1985. On the Relation Between Tectonics and Ore Mineral Occurrences in the Basement Complex of the Eastern Desert of Egypt, International Conference on Basement Tectonics, 1985, Sante Fe, New Mexico, Proceedings, 26 p.

El Ghawaby, M. A., 1981, Role of Structural Deformation in Controlling Copper Occurrences in Abu Swayel Region, Egypt. International Basement Tectonics Association Publication No. 4, p. 165-172.

EL-Nadi, A. H., 1984. The Geology of the Late Precambrian Metavolcanics, Red Sea Hills, Northeast Sudan, University of Nottingham, PhD. Thesis, 245 p.

El Ramly, M. F., 1972. A New Geological Map of the Basement Rocks in the Eastern and Southwestern Deserts of Egypt, Geol. Survey Egypt Annals, Vol. 2, p. 1-18, Scale 1:1000,000.

El Shazly, E. M., Hashad, A. H., Sayyah, T. A., and Bassyuni, F. A., 1973. Geochronology of Abu Swayel Area, South Eastern Desert, Egypt, Journal of Geology Vol. 17, No. 1, p. 1-18.

El Shazly, E. M., El Sokkay, A. A., and Aly M. M., 1982. Development of Granitics and Associated Granitoids in Egypt According to Alternative Orogenic and Plate Tectonic Models, Precambrian Res., Vol. 16, No. 4, p. A56.

Embleton, J. C. B., Hughes, D. J., Klemenic, P. M., Poole, S. and Vail, J. R., 1982. A New Approach to The Stratigraphy and Tectonic Evolution of the Red Sea Hills, Sudan, Precambrian Research, Vol. 16, No. 4, p. A19 (Abs.).

E

Engel, A. E. J., Dixon T. H., and Stern, R. J., 1980. Late Precambrian Evolution of Afro-Arabian Crust from Ocean Arc to Craton, Geological Soc. of Am. Bull. Part I, Vol. 91, p. 699-706.

F

Fitches, W. R., Graham, R. M., Hussein, I. M., Ries, A. C., Shackleton, R. M., and Price, R. C., 1983. The Late Proterozoic Ophiolite of Sol Hamed, N.E. SUDAN, Precambrian Research, Vol. 19, p. 385-411.

Fleck, R. J., Coleman, R. G., Cornwall, H. R., Greenwood, W. R., Hadley, D. G., Schmidt, D. L., Prinz, W. C. and Ratte, J. C., 1976. Geochronology of the Arabian Shield, Western Saudi Arabia: K-Ar Results, Geological Soc. Amer. Bulletin, Vol. 87, p. 9-21.

Fleck, R. J. and others, 1981. Geochronology and Isotope Studies, U.S. Geological Surv., Prof. Paper 1275, 291 p.

G

Gabert, V. G., Ruxton, B. P. and Venzlaff, H., 1960. Uber Untersuchungen in Kristallin der Nordlichen Red Sea Hills in Sudan, Geologisches Jahrbuch, Band 77, p. 241-270.

Garson, M. S., and Miroslav, K. R. S., 1976. Geophysical and Geological Evidence of the Relationship of Red Sea Transverse Tectonics to Ancient Fractures, Geological Society of America, Bulletin, Vol. 87, p. 169-181.

Garson, M. S., and Shalaby, I. M., 1976. Precambrian-Lower Paleozoic Plate Tectonics and Metallogenesis in the Red Sea Region, Geol. Assoc. of Canada, Special Paper No. 14, p. 573-595.

Gaskell, J. L., 1985. Reappraisal of Gebeit Gold Mine, Northeast Sudan: A Case History, in Prospecting in Areas of Desert Terrain, The Institution of Mining and Metallurgy, p. 49-58.

Gass, I.G., 1982. Upper Proterozoic (Pan-African) Calc-Alkaline Magmatism in North-Eastern Africa and Arabia, in Thorpe, R.S., ed., Andesites, Orogenic Andesites and Related Rocks, Chichester, John Wiley and Sons, p. 591-609.

G

Gass, I. G. , 1955, The geology of the Dunganas area, Angelo-Egyptian Sudan, unpublished M. S. thesis, Universidy of Leeds, 112 pp.

Gass, I. G., 1979. Evolutionary Model for the Pan-African Crystalline Basement, in Al-Shanti, A.M.S., (ed.), Evolution and Mineralisation of the Arabian-Nubian Shelf, Vol. 1, King Abdul Aziz Univ., Inst. Appl. Geol. Bull. 3, Permagon Press, Oxford and New York, p. 11-20.

Greenberg, J. K., 1981. Characteristics and Origin of Egyptian Younger Granites, Summary, Geol. Soc. of Amer. Bull., Part I, Vol. 92, p. 224-232.

Greiling, R., Kroner, A., and El Ramly, M. F., 1984. Structural Interference Patterns and Their Origin in the Pan-African Basement of the Southeastern Desert of Egypt, in Kroner, A., Grielins, R., editors, Precambrian Tectonics Illustrated, Federal Republic of Germany, E. Schweizer bartlsche Verlags-buchhandl, p. 401-412.

Greenwood, W. R., Anderson, R. E., Fleck, R. J., and Roberts, R. J., 1980. Precambrian Geologic History and Plate Tectonic Evolution of the Arabian Shield, DGMR Mineral Resources Bulletin 24, 35 p.

Greenwood, W. R. and Brown, G. F., 1973. Petrology and Chemical Analyses of Selected Plutonic Rocks from the Arabian Shield, Kingdom of Saudi Arabia: DGMR Mineral Resources Bulletin 9, 9 p.

Greenwood, W. R., Hadley, D. G., Anderson, R. E., Fleck, R. J., and Schmidt, D. L., 1976. Late Proterozoic Cratonization in Southwestern Saudi Arabia: Royal Society London Philos. Trans., A,, Vol. 280, p. 517-527.

H

Harris, N.B.W., 1982. The Petrogenesis of Alkaline Intrusives from Arabia and Northeast Africa and Their Implications for Within-plate Magmatism, Tectonophysics, Vol. 83, p. 243-258.

Harris, N. B., Hawkeswoth, C. J. and Ries, A. C., 1984. Crustal Evolution in Northeast and East Africa from Modal Nb Ages, Nature, Vol. 309, p. 773-776.

H

Hashad, A. H., 1978, Present status of geochronological data on the Egyptian basement complex, in Evolution and Minerilization of the Arabian-Nubain Shield, editor A. M. Al-Shanti, Vol. 3.

Hepworth, J. V., 1979. Does the Mozambique Orogenic Belt Continue into Saudi Arabia?, in Al-Shanti, A. M. S. (ed.), Evolution and Mineralisation of the Arabian-Nubian Shield, Vol. 1, King Abdul Aziz Univ., Inst. Appl. Geol. Bull. 3, Pergamon Press Oxford - New York, p. 39-51.

Hollister, L. S., and Crawford, M. L., 1986. Melt-Enhanced Deformation; A Major Tectonic Process, Geology, Vol. 14, No. 7, p. 558-561.

Holmes, A., 1951, A sequence of Pre-Cambrian orogenic belts in south and central Africa. Rep. 18th session Int'l. Geol. Congr., G. B., 1948, Part 14, pp 254-269.

Hord, R.M., 1982. Digital Processing of Remotely Sensed Data. Academic Press.

Hussein, I.M., Kroner, A., and St. Dorr, 1982. Wadi Onib: A Dismembered Pan-African Ophiolite in the Red Sea Hills of the Sudan, Precambrian Research, Vol. 16, p. 452.

Hussein, J. M., 1977, Geology of the Halaib area of the northern Red Sea Hills. Sudan, with special reference to the Sol Hamed basic complex, unpublished Ph.D. thesis, Portsmouth Polytechnic, 175 pp.

I

Ishag, A. H., 1980. A Guide to Mineral Investment In The Sudan: Democratic Republic of Sudan, Ministry of Energy and Mining, Geological and Mineral Resources Department, Bull. No. 31, 25 p.

J

Jackaman, B. 1972. Genetic and Environmental Factors Controlling the Formation of the Massive Suplhide Deposits of Wadi Bidah and Wadi Wassat, Saudi Arabia, Tech. Report TR-1972-1, Director General of Mineral Resources, Ministry of Petroleum and Mineral Resources, 243 p.

K

Kabesh, M. L., 1964. Classification of the Mineral Deposits of the Sudan, Jour. Geology U. A. R., Vol. 8. No. 2, p. 53-66.

Kabesh, M. L., 1961. The Geology and Economic Minerals and Rocks of the Ingessana Hills, Republic of the Sudan, Republic of the Sudan, Ministry of Mineral Resources, Geological Survey Department, Bull. No. 11, 61 p.

Kabesh, M. L., 1962. The Geology of Muhammad Qol Sheet: Sudan Geological Survey Department, Memoir No. 3.

Kabesh and Afia (1959). The Wollastonite Deposit of Dirbat Well, Bull. Geol. Surv. Sudan, No. 5. 32 pp.

Kabesh, M. L., Afia, M. S., and Widatalla, A. L., 1958. Fodikwan Iron Deposits, Dungunab District, North Eastern Red Sea Hills, Sudan Survey Department., Bull. No. 4, 29 p.

Kazmin, V., 1978. Geology of the Ethopian Basement and Possible Relation Between the Mozambique and Red Sea Belts: Egypt. Journal Geology, Vol. 22, No. 1.

Kroner, A., and Jahn, B. M., 1985. Precambrian Crustal Evolution, Precambrian Res., Vol. 27, p. 277-300.

Kroner, A., 1985. Ophiolites and the Evolution of Tectonic Boundaries in the Late Proterozoic Arabian - Nubian Shield of Northeast Africa and Arabia. Precambrian Research, Vol. 27, p. 277-300.

Kroner, A., 1979. Pan-African Mobile Belts as Evidence for a Transitional Tectonic Regime from Intraplate Orogeny to Plate Margin Orogeny, Inst. of Appl. Geology Bull. No. 3, King Abdul Aziz Univ., Jeddah, Kingdom of Saudia Arabia, Evolution and Mineralization of the Arabian-Nubian Shield, p. 21-37.

L

Lillesand, T. M. and Kiefer, R. W., 1979. Remote Sensing and Image Interpretation, John Wiley and Sons, New York, 612 p.

Lyon, R. J. P., 1981. Status of Remote Sensing Technology in Exploration, Stanford Remote Sensing Laboratory Tech. Rpt. 81-11, 12 p.

M

Merembeck, B.F., Borden, F.Y., Podwysocki, M.H., Applegate, D.N., 1976. Application of Canonical Analysis to Multispectral Scanner Data., Proc. 14th Ann. Symposium on Computer Applications in the Mineral industries, Pennsylvania, September 1976.

Moore, J. M., 1982. Structure, Stratigraphy, and Mineralization in the Southern Arabian Shield: A Study in Satellite - Image Interpretations, Precambrian Res., Vol. 16, No. 4, p. A53-A54.

N

Nagy, R. M., Ghuma M., and Rogers, J. J. W., 1976. A Crustal Suture and Lineament in North Africa, Tectonophysics, Vol. 31, No. 3-4, p. T67-T72.

Neary, C. R. 1978. Evolution and Mineralization of the Arabian - Nubian Shields, Mining Mag., Vol. 143, No. 7, p. 47-48.

Neary, C. R., Gass, I. G., and Cavanaugh, B. J., 1976. Granitic Association of Northeastern Sudan, Geol. Society of America Bull., Vol. 87, p. 1501-1512.

O

Overstreet, W.C. and Rossman, D.L., 1970. Reconnaissance Geology of the Wadi Wassat Quadrangle, Kingdom of Saudi Arabia, U.S. Geological Survey Saudi Arabian Project Report 117, 69 p.

P

Podwysocki, M. H., Gunther F.J., and Blodget, H.W., 1977. Discrimination of Rock and Soil Types by Digital Analysis of Landsat Data, NASA TM X-71290, 37 p.

Powell, C. M., 1984. Terminal Fold-Belt Deformation: Relationship of Mid-Carboniferous Mega Kinks in the Tasman Fold Belt to Coeval Thrusts in Cratonic Australia, Geology Vol. 12, p. 546-549.

R

Ressetar, R., and Monrad, J. R., 1983. Chemical Composition and Tectonic Setting of the Dokhan Volcanic Formation, Eastern Desert, Egypt, Journal of African Earth Sciences, Vol. 1, No. 2, p. 103-112.

R

Reymer, A. P. S., 1984. Metamorphism and Tectonics of a Pan-African Terrain in Southeastern Sinai; A Reply, Precambrian Res., Vol. 24, No. 2, p. 189-197.

Reymer, A. P. S., 1983. Metamorphism and Tectonics of a Pan-African Terrain in Southeastern Sinai. Precambrian Research, Vol. 19, p. 225-238.

Ries, A.C., Shackleton, R.M., Graham, R.M., and Fitches, W. R., 1983. Pan-African Structures, Ophiolites and Melanges in the Eastern Desert of Egypt: A Traverse at 26°N, Journal Geol. Soc. London, Vol. 140, p. 75-95.

Routhier, P., and Delfour, J., 1980. Geology of Massive Sulfide Deposits Associated with Acid Volcanism and its Application to the Search for Such Deposits in the Precambrian of Saudi Arabia, DGMR Mineral Resources Bulletin 18, 61 p.

Rowan, L. C., Wetlaufer, P. H., Goetz, A. F. H., Billingsley, F. C., and Stewart, J. H., 1976. Discrimination of Rock Types and Detection of Hydrothermally Altered Areas in South-Central Nevada by the Use of Computer-Enhanced ERTS Images, U. S. Geol. Survey Prof. Paper 883, 35 p.

Ruxton, B. P., 1956. The Major Rock Groups of the Northern Red Sea Hills, Sudan, Geology Mag., Vol. 93, No. 4, p. 314-331.

S

Sabert, A. M. 1981. Tectonics of the Northern Red Sea Hills, Proc. of the 4th Intl. Conf. on Basement Tectonics, p. 201-208.

Sabir, H., 1981. Metallogenic and Textural Features of Sulfide Mineralization at Jabal Sayid, Saudi Arabia: BRGM (France) Section II, Geologie des Gites Mineraux, Number 2, p. 103-111.

Said, R., 1962. The Geology of Egypt, Elsevier Publishing Co., Amsterdam.

Salama, R.B., 1985. Buried Troughs, Grabens and Rifts in Sudan, Journal of African Earth Sciences, Vol. 3, No. 3, P. 381-390.

S

Schmidt, D. L., Hadley, D. G., and Stoeser, D. B., 1979. Late Protezoroic Crustal History of the Arabian Shield, Southern Najd Province, Kingdom of Saudi Arabia: in "Evolution and Mineralization of the Arabian-Nubian Shield", Inst. App. Geology Bulletin 3, Vol. 2, p. 41-58.

Serencsits, C. McC., Faul, H., Foland, K.A., Hussein, A.A., and Lutz, T.M., 1981. Alkaline Ring Complexes in Egypt: Their Ages and Relationship in Time, Journal of Geophysical Research, Vol. 86, No. B4, p. 3009-3013.

Sestini, J., 1965. Cenozoic Stratigraphy and Depositional History, Red Sea Coast, Sudan, Bull. of Amer. Assoc. of Pet. Geol., Vol. 49, No. 9, p. 1453-1472.

Shackleton, R. M., Ries, A. C., Graham, R. H., and Fitches, W. R., 1980. Late Precambrian Ophiolitic Melange in the Eastern Desert of Egypt, Nature, Vol. 285, p. 472-474.

Shackleton, R. M., 1986. Precambrian Collision Tectonics in Africa, in Coward, M. P., and Ries, A. C., (eds), Collision Tectonics, Geological Society Special Publication No. 19, p. 329-349.

Shaddad, M. Z., 1978. Sudan: Mining Annual Review, p. 514-515.

Sheffield, C., 1985. Selecting Band Combinations from Multispectral Data, Photogrammetric Engineering and Remote Sensing, Vol. 51, No. 6, p. 681-687.

Shekarchi, E., 1978-79. The Mineral Industry of Sudan, Minerals Yearbook, Vol. 3, p. 867-872.

Shimron, A. E., 1984. Evolution of the Kid Group, Southeast Sinai Peninsula: Thrusts, Melanges, and Implications for Accretionary Tectonics During the Late Proterozoic of the Arabian-Nubian Shield, Geology, Vol. 12, p. 242-247.

Sillitoe, R. M., 1979. Metallogenic Consequences of Late Precambrian Suturing in Arabia, Egypt, Sudan and Iran, Instit. of Appl. Geol. (I.A.G. Bulletin #3); King Abdul Aziz Univ., Jeddah, Kingdom of Saudi Arabia, Evolution and Mineralization of the Arabian-Nubian Shield. p. 110-120.

S

Soliman, M. M., 1981. Mineral Exploration in Egypt, Proc. of the 4th Intl. Conf. on Basement Tectonics, Oslo, Norway, p. 157-163.

Stacey, J. S., and Hedge, C. E., 1984. Geochronologic and Isotope Evidence for Early Proterozoic Crust in the Eastern Arabian Shield, Geology, Vol. 12, p. 310-313.

Stacey, J. S., and Stoeser, D. B., 1983. Distribution of Oceanic and Continental Leads in the Arabian-Nubian Shield, Contrib. to Mineralogy and Petrology Vol. 84, p. 91-105.

Stern, R. J., Dixon, T. H., Golombek, M. P., Kroner, A., Manton, WI., Walter, M., and Hussein, J. M., 1986, The Hamisana Shear Zone: a major late Precambrian structure in the Red Sea Hills of Sudan, in 1986 GSA Abstracts with Programs, 99th Annual meeting, San Antonio, TX., p 763.

Stern, R. J., and Hedge C. E., 1985. Geochronologic and Isotopic Constraints on Late Precambrian Crustal Evolution in the Eastern Desert of Egypt, Am. Jour. Sci., Vol. 285, No. 2, p. 97-127.

Stern, R. J., Gottfield, D., and Hedge, C.E., 1984. Late Precambrian Rifting and Crustal Evolution in the Northeastern Desert of Egypt, Geology, Vol. 12, p. 168-172.

Stern, R. J., 1982. Petrogenesis and Tectonic Setting of Late Precambrian Ensimatic Volcanic Rocks, Central Eastern Desert of Egypt, Precambrian Research, Vol. 16, p. 195-230.

Stern, R. J., 1981, Petrogenesis and tectonic setting of late Precambrian ensimatic volcanic rocks, central eastern desert of Egypt, Precambian Research, v. 16, p. 195-230.

Stoeser, D. B., and Camp, V. E., 1985. Pan-African Microplate Accretion of the Arabian Shield, Geol. Soc. of America Bulletin, Vol. 96, p. 817-826.

Stoeser, D. B., Stacey, J.S., Greenwood, W.R., and Fisher, L.B., 1984. U/Pb Zircon Geochronology of the Southern Part of the Nabitah Mobile Belt and Pan-African Continental Collision in the Saudi Arabian Shield, U.S. Geol. Surv., Open-File Report, 92 p.

S

Stoeser, D. B., and Stacey, J. S., 1983. Granitoid Plutonic Rocks of the Arabian Shield, U.S. Geol. Surv., Prof. Paper 1375, 287 p.

Sturchio, N. C., 1983. Geologic Evolution of Precambrian Basement of Eastern Desert of Egypt, AAPG Bulletin, Vol. 67, No. 3, p. 554.

Sturchio, N. C., Sultan, M., and Batiza, R., 1983. Geology and Origin of Meatig Dane, Egypt: A Precambrian Metamorphic Core Complex?, Geology, Vol. 11., p. 72-76.

T

Taylor, M.M., 1974. Principal Components Color Display of ERTS Imagery, Third Earth Resources Technology Satellite Symp., Washington, D.C., Section B.

Technoexport, 1974. Results of K-Ar Absolute Age Determination. Report by Ministry of Geology of the U.S.S.R. for the Sudan Government, Report of the Geological Survey of Sudan, Unpublished.

V

Vail, J. R., 1985. Pan-African (late Precambrian) Tectonic Terrains and the Reconstruction of the Arabian-Nubian Shield, Geology, Vol. 13, p. 839-842.

Vail, J. R., 1984. The Nature of the Basement Complex of the Nubian Shield in North-east Africa: Addendum, Journal of African Earth Sciences, Vol. 2, No. 4, p. 389-390.

Vail, J. R., 1983. Pan-African Crustal Accretion in North-east Africa, Journal of African Earth Sciences, Vol. 1, No. 3/4, pp. 285-294.

Vail, J. R., 1979. Outline of Geology and Mineralization of the Nubian Shield East of the Nile Valley, Sudan: in Al-Shanti, A.M.S. (ed.), Evolution and Mineralization of the Arabian-Nubian Shield, Vol. 1, King Abdul Aziz Univ., Inst. Appl. Geol. Bull. 3, Pergamon Press, Oxford - New York, p. 97-107.

Vail, J. R., 1978. Outline of the Geology and Mineral Deposits of the Democratic Republic of the Sudan and Adjacent Areas, Overseas Geology and Mineral Resources, No. 49, Inst. of Geolog. Sciences, London.

W

Warden, A. J., 1982. The Northeast Branch of the Mozambique Belt, Precambran Res., Vol. 16, No. 4, p. A41-A42.

Weissenborn, A. E., and Earhart, R.L., 1968. Appraisal of the Wadi Wassat and Wadi Abhat Pyrite Deposits, Asir Quadrangle, Kingdom of Saudi Arabia, U.S. Geological Survey Saudi Arabian Project Tech. Letter 101, 21 p.

Whiteman, A. J., 1971. The Geology of the Sudan Republic, Oxford, Clarendon Press, XIV, 290 p.

Woodward, L. A., 1984. Basement Control of Tertiary Intrusions and Associated Mineral Deposits Along Tijeras - Canoncito Fault System, New Mexico, Geology, Vol. 12, p. 531-533.

SCALING RULES

SIZE E

This drawing and the design it covers are the property of BECHTEL. They are merely loaned and on the borrower's express agreement that they will not be reproduced, copied, loaned, exhibited, nor used except in the limited way and private use permitted by any written consent given by the lender to the borrower.

34°00' 34°15' 34°30' 34°45' 35°00'

22°30' 22°15' 22°00' 21°45' 21°30' 21°15' 21°00'

33°30' 33°45' 34°00' 34°15' 34°30' 34°45'

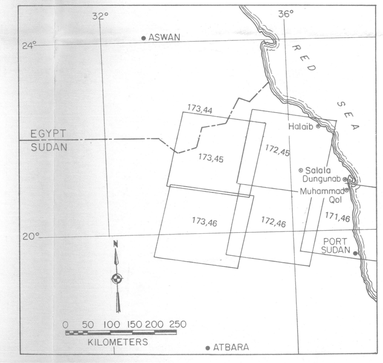

LOCATION OF LANDSAT SCENE 173,45

0 10 20 30 40

SCALE IN KILOMETERS

No.	DATE	REVISIONS	BY	CHKD	DESIGN SUPV	ENGR	PROJ ENGR	APPR
△								
△								

BECHTEL
SAN FRANCISCO

GEOLOGIC MAP OF TM LANDSAT SCENE 173,45 NORTHERN RED SEA HILLS

JOB No.	DRAWING No.	REV.
17835	PLATE 1	

34 x 44 "E" SIZE

33° 30' 33° 45' 34° 00' 34° 15' 34° 30' 34° 45' 35° 00'

21° 00' 20° 45' 20° 30' 20° 15' 20° 00' 19° 45' 19° 30'

DIKES FILLING FAULT

NOTE:

Latitude-longitude grid is extrapolated from surrounding quadrants and less exact than on other maps.

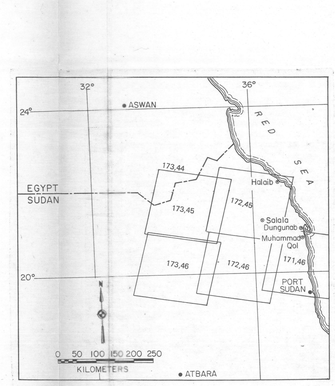

LOCATION OF LANDSAT SCENE 173,46

0 5 10 20 30 40

SCALE IN KILOMETERS

No.	DATE	REVISIONS	BY	CHKD	DESIGN SUPV	ENGR	PROJ ENGR	APPR

BECHTEL
SAN FRANCISCO

GEOLOGIC MAP OF TM LANDSAT SCENE 173,46 NORTHERN RED SEA HILLS

JOB No.	DRAWING No.	REV.
	PLATE 2	

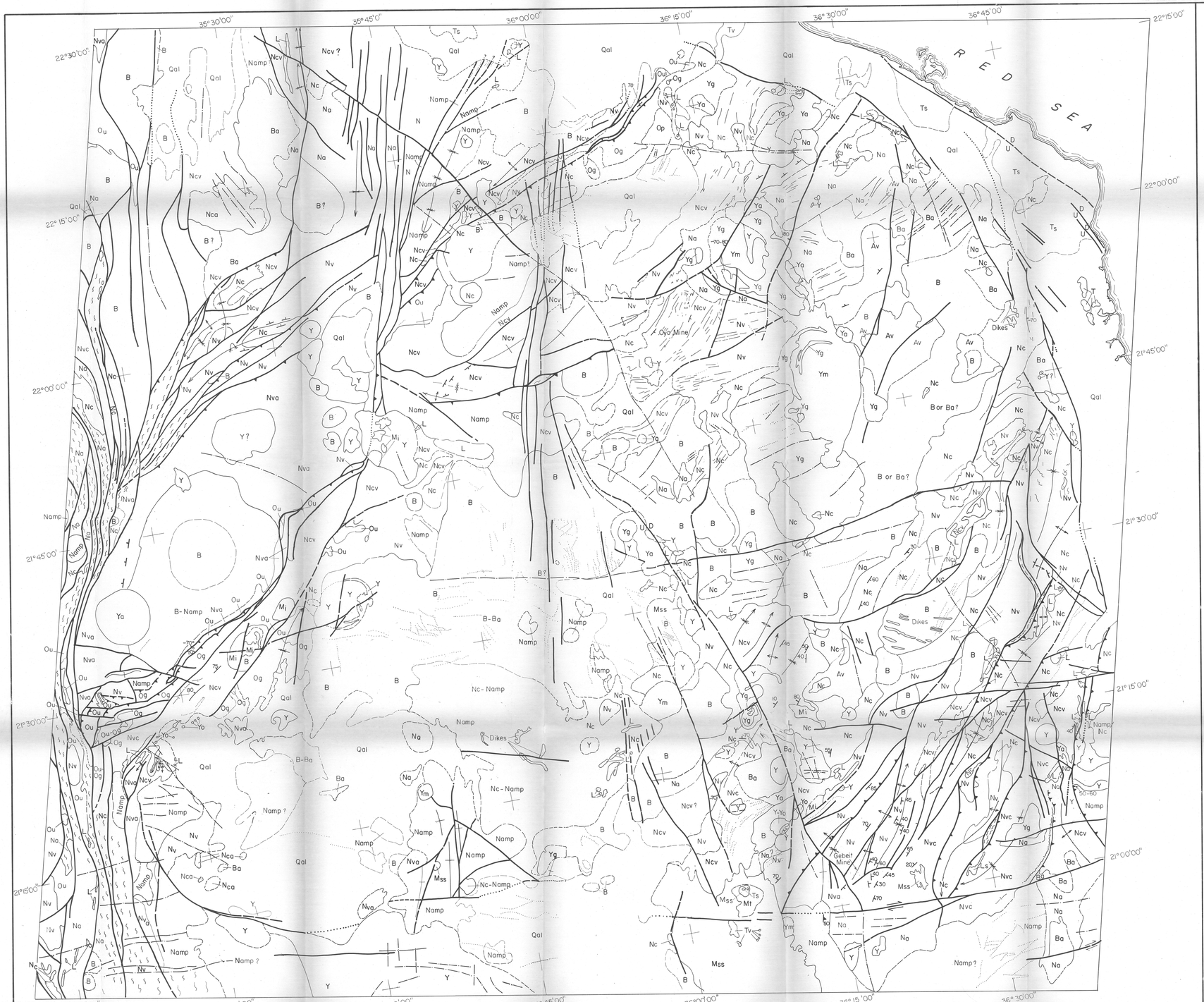

EXPLANATION

QUATERNARY

- Qal — Alluvium

TERTIARY

- Tv — Tertiary volcanics—basalt and trachyte dikes and flows
- Ts — Tertiary marine and terrestial sediments

CRETACEOUS

- Mss — Nubian sandstone and related sediments

PALEOZOIC TO TERTIARY

YOUNGER GRANITE SERIES

- Yo — Undifferentiated
- Yg — Granitic
- Ym — Mafic intrusive—gabbroic, some layered.
- Ya — Altered young intrusive

BATHOLITHIC GRANITES

- B — Batholithic granite
- Ba — Altered batholithic granite

PROTEROZOIC

NAFIRDEIB SERIES

- Av — Asoteriba Volcanics
- Mi — Mafic—ultramafic intrusive, some layered
- Nc-Ncv — Nafirdeib sediments—Greenschist facies greywackes, silts, minor limestone (L). Ncv—minor volcanics
- Nv-Nvc — Nafirdeib volcanics—Greenschist facies calc-alkaline basalts and andesites, with tuffs, agglomerates and volcaniclastics. Nvc—Minor sediments
- Na — More extensively metamorphosed and/or metasomatized Nafirdeib
- Namp — Amphibolite facies Nafirdeib

SOL HAMED SERIES

- Op — Pillow lavas and breccias
- Og — Sheeted dikes and gabbros, brecciated with serpentinite matrix.
- Ou — Ultramafic—dunites, wehrlites and lherzolites; serpentinized and carbonated.

- 70 — Strike and dip of joint surface, from literature.
- 30 — Strike and dip of beds or volcanic units, taken from literature source.
- Strike and dip of beds or volcanic units inferred from imagery.
- Lithologic contact—dashed where approximately located, dotted where concealed.
- Strike of beds and units (within lithologic contacts).
- N70W — Fault—dashed where approximately located, dotted where concealed. Dip inferred from imagery.
- Joints and lineaments.
- Thrust fault—barbs on upper plate.
- Strike Slip fault showing relative movement.
- Normal fault showing upthrown (U) and downthrown (D) sides.
- Anticline showing trace of axial plane, bearing and plunge of axis.
- Syncline showing trace of axial plane, bearing and plunge of axis.
- Horizontal anticline and syncline.
- Fold axis, dips unknown.
- Overturned plunging anticline, showing direction of plunge and overturning.
- Overturned syncline, showing direction of plunge end overturning.

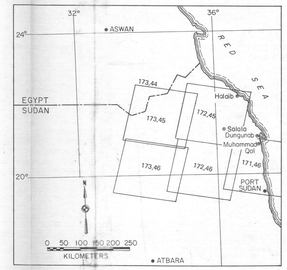

LOCATION OF LANDSAT SCENE 172,45

0 10 20 30 40

SCALE IN KILOMETERS

No.	DATE	REVISIONS	BY	CHKD	DESIGN SUPV	ENGR	PROJ ENGR	APPR

BECHTEL
SAN FRANCISCO

PRELIMINARY GEOLOGIC MAP OF TM LANDSAT SCENE 172,45 NORTHERN RED SEA HILLS

JOB No.	DRAWING No.	REV.
	PLATE 3	

NOTE:

Latitude-longitude grid is extrapolated from surrounding quadrants and less exact than on other maps.

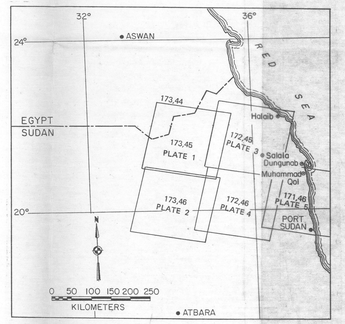

LOCATION OF LANDSAT SCENE FROM TM 142,46

0 5 10 20 30 40

SCALE IN KILOMETERS

No.	DATE	REVISIONS	BY	CHKD	DESIGN SUPV	ENGR	PROJ ENGR	APPR
△								
△								

BECHTEL
SAN FRANCISCO

GEOLOGIC MAP OF TM LANDSAT SCENE 172,46 NORTHERN RED SEA HILLS

JOB No.	DRAWING No.	REV.
	PLATE 4	

SCENE 172.45

RED SEA

PORT SUDAN

21°00'
20°45'
20°30'
20°15'
20°00'
19°45'
19°30'
36°15'
36°30'
36°45'
37°00'
37°15'

LOCATION OF LANDSAT SCENE 171,46

0 5 10 20 30 40
SCALE IN KILOMETERS

No.	DATE	REVISIONS	BY	CHKD	DESIGN SUPV	ENGR	PROJ ENGR	APPR
△								
△								

BECHTEL
SAN FRANCISCO

GEOLOGIC MAP OF TM LANDSAT SCENE 171,46 NORTHERN RED SEA HILLS

JOB No.	DRAWING No.	REV.
	PLATE 5	

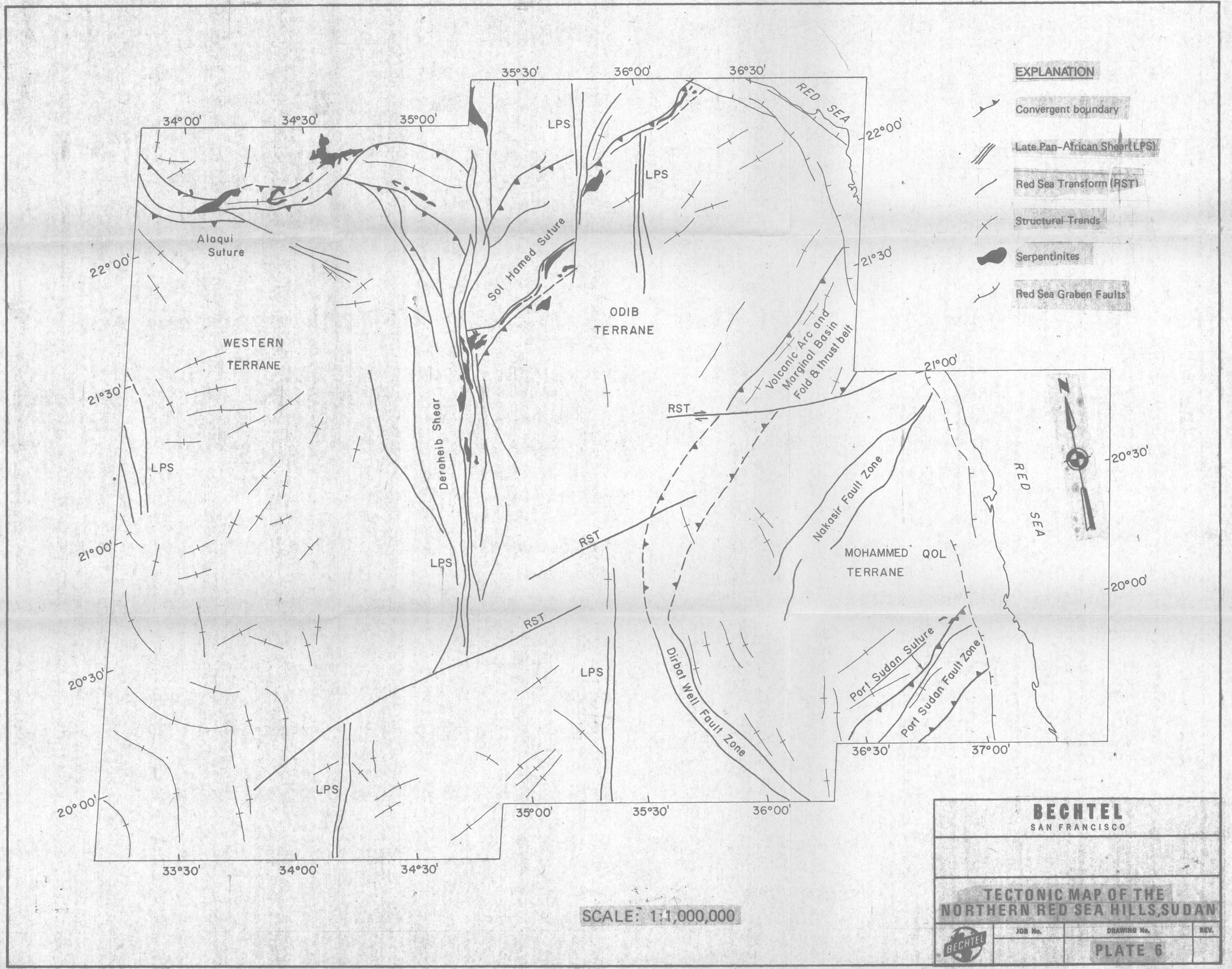

BECHTEL
SAN FRANCISCO

TECTONIC MAP OF THE NORTHERN RED SEA HILLS, SUDAN

JOB No.	DRAWING No.	REV.
	PLATE 6	